DISSERTATION

AVAILABLE WATER EFFECTS ON WATER STRESS INDICES FOR IRRIGATED CORN GROWN IN SANDY SOILS

Submitted by

Cagatay Tanriverdi

Bioresource and Agricultural Engineering Program

Department of Civil Engineering

In partial fulfillment of the requirements

for the degree of Doctor of Philosophy

Colorado State University

Fort Collins, CO

Fall, 2003

COLORADO STATE UNIVERSITY

October 21, 2003

WE HEREBY RECOMMEND THAT THE **DISSERTATION** PREPARED UNDER OUR SUPERVISION BY CAGATAY TANRIVERDI, ENTITLED AVAILABLE WATER EFFECTS ON WATER STRESS INDICES FOR IRRIGATED CORN GROWN IN SANDY SOILS, BE ACCEPTED AS FULFILLING IN PART REQUIREMENTS FOR THE DEGREE OF DOCTOR OF PHILOSOPHY

Committee on Graduate Work

Co-Adviser

Co-Adviser

Department Head

ABSTRACT OF **DISSERTATION**

AVAILABLE WATER EFFECTS ON WATER STRESS INDICES FOR IRRIGATED CORN GROWN IN SANDY SOILS

Water stress indices were investigated in this study to improve irrigation management for corn. These indices were used to improve irrigation management by determining irrigation timing and soil water deficit (SWD) on sandy soil using ground-based remote sensing (GBRS) system. The remote sensed data were acquired from the nadir (down-looking) view for canopy reflectance and surface temperature (T_s) measurements as well as an oblique (80^o) view. Canopy reflectance measurements were used to calculate vegetation indices to estimate vegetation cover.

Experimental data were collected in a corn (Zea mays L.) field, Wiggins, Colorado during the 2002 growing season. The study was conducted on two experimental corn sites. The first site consisted of six non-replicated plots where the water stress indices were developed. One of the six plots was bare soil and the remaining five plots were drip-irrigated. The second site consisted of half of a center pivot irrigated cornfield where the developed water stress indices were tested.

Water stress indices investigated in this study were crop water stress index (CWSI) and water deficit index (WDI). Results of collected experimental data indicated that the WDI was superior to the CWSI since it enables users to determine the amount of

irrigation water to be applied to the soil by estimating the SWD at each irrigation besides the irrigation timing that the CWSI is able to determine. Estimating SWD using GBRS data is an innovative technique. SWD provides the necessary information to the irrigator with less fieldwork, and is useful in saving money, time and labor. It can be used with remotely-sensed data measurements, which is a very important feature, especially for large agricultural areas. Results also indicated that the soil-adjusted vegetation index (SAVI) was the best index to represent vegetation cover. If available, oblique (80^{o}) view data should be used to measure T_s to reduce the soil background effect since experimental data of nadir and oblique views were compared to establish baselines of water stress indices.

Cagatay Tanriverdi
Bioresource and Agricultural Engineering Program
Department of Civil Engineering
Colorado State University
Fort Collins, CO 80523
Fall 2003

ACKNOWLEDGEMENTS

I would like to start with special thanks to my co-adviser, Dr. Walter Bausch, for his help in the office, in the field and even at his home, as well as his guidance during this study. I am also thankful to Dr. Terence Podmore, Dr. Luis Garcia, Dr. Grant Cardon and Dr. Ramchand Oad for their help, time and advice. I would like to thank Dr. Kenan Diker for his help and his guidance. Ted Bernard, Engineering Technician of USDA ARS deserves special thanks for his help in collecting necessary data. I would like to thank Chris Farland and other USDA ARS people for their friendship and help in the field and office.

I would like to thank Esma Tanriverdi for her proofreading, encouragement and patience all the time during my Ph.D. program. Thanks also go to my parents, for their help at the home taking care of us very well. I also would like to express my thanks to my parents in law whose encouragement and patience made this research possible. I would like to thank my best friends, Numan Altinkopru and Eshabil Kirici, for their support and encouragement.

DEDICATION

To:

My wife

Esma Tanriverdi.

TABLE OF CONTENTS

LIST OF TABLES

LIST OF FIGURES

Chapter 4
Figures

CHAPTER 1

INTRODUCTION

The major limiting factor in crop productivity is water (Howell and Musick, 1984; Jones, 1999). Consequently, crop water needs must be satisfied (Penuelas et al., 1992) in order to make correct management decisions (Wanjura and Upchurch, 2002). Hence, water is expected to be a major topic of discussion in continued national and international efforts to determine precisely what problems will occur as a result of water scarcities and accelerating water contamination. Currently, on a global basis, 73% of all fresh water used is for irrigation, another 21% is accounted for by the industrial sector, and the remaining 6% is used for domestic purposes (Gonzalez, 1998).

Boyer, 1982 reported that "Commercial production yields of major crops average 33% or less of record yields." Among the various factors that can reduce crop yield, plant water stress caused by an insufficient supply of water is a common major limiting factor. Even in areas of high rainfall, crop water stress is a problem that occurs from time to time (Wanjura and Upchurch, 2000). Gonzalez (1998) warned that water would undoubtedly become a very serious resource issue during the twenty-first century.

Issues of water supply and quality are impacting developed countries as well as less-developed ones. Increasing food demands and declining water availability threaten food security in Asia, where about 60% of the world's population lives (Bouman and Tuong, 2001). Some countries, such as Japan, recognize the gravity of water issues and

are developing strategies to guarantee long-term supplies of good quality water. In countries for which water is in naturally short supply, such as the Middle East, water may become synonymous with power. If sustained development and maintenance of a satisfactory quality of life is to be realized, it will be essential to ensure a reliable supply of good quality water (Gonzalez, 1998).

Crop irrigation is an essential and effective strategy for enhancing agricultural production and productivity, so much so that during the past decade, increased food production has been attributed primarily to the expansion of irrigated areas. Although at present only about 20% of the world's agricultural land is irrigated, it is estimated that this percentage accounts for 40% of global agricultural production. Thus, the development of a better, more diversified crop pattern, as well as the growth of high-value crops, is irrigation dependent, providing the basis for and facilitating general socio-economic improvement in the agricultural community (Ambast et al., 2002).

Without proper management, irrigated agriculture can be detrimental to the environment and can endanger sustainability. Irrigated agriculture is in growing competition for low-cost, high-quality water. One of the ways to conserve high-quality water is increasing water use efficiency in agriculture. In many rain-fed regions of the world, a small fraction of the total water available for crop production is transpired and water use efficiency is low (Gregory et al., 2000).

According to Steele et al. (2000), irrigation scheduling has increased the yield of corn by 5%, while decreasing the water applied by 30% in the Northern Great Plains. Without efficient water management, it will be impossible to make any significant

improvement in consolidating and accelerating various globalization and sustainable development processes, or to ensure the quality of life of the people of a region.

Many researchers have used statistical analysis to get a better idea of the functional relationship of crop yield to other spatial factors. At the same time, crop production is both a function of spatial and temporal variability; indeed, in some cases climate variability may be more important than spatial variability. In fact, in some years the impact of spatial variability on crop yield may be negligible (Mulla and Schepers, 1997). The difference in crop yield between poor and excellent climatic years may be one order of magnitude (Huggins and Alderfer, 1995).

Soil and water management practices deal with the processes of evapotranspiration by modifying the available energy, the exchange rate between the soil and the atmosphere, or the available water in the soil profile (Hatfield et al., 2001). Management of irrigation systems for efficient use of applied water requires an understanding of the many physical, biological and economic factors involved in crop production. During the last twenty years, considerable progress has been made in the development of crop growth models based on an increased understanding of soil-plant-atmospheric processes.

However, the literature indicates that during the last two decades the effectiveness of irrigation schemes, especially in large areas, has not met expectations. Seckler et al. (1988) elaborate on the extent of this underperformance, offering the alarming conclusion that although the average irrigation scheme costs twice as much, it actually delivers no more than half the benefits specified in plans. However, despite increasing awareness of the need for improving the performance of irrigation systems by proper management

techniques, properly and regularly monitored and evaluated irrigation projects in which the results of such monitoring and evaluation are used to improve the management of irrigation projects are virtually non-existent (Biswas, 1990).

Up to the mid-1980s, the primary reason that prevented the evaluation of irrigation systems' performances in quantifiable units was the lack of performance indicators. Subsequently, various researchers (Malhotra et al., 1984; Abernethy, 1986; Clemmens and Bos, 1990) proposed a number of performance indicators. However, although monitoring and evaluation have received much lip service during the present decade, they have seldom been carried out properly and effectively. One of the main reasons is that the conventional methods of data collection through field observation are difficult, time-consuming and cannot be carried out simultaneously, particularly in large irrigated commands. Moreover, monitoring at frequent intervals is not possible (Ambast et al., 2002).

Reviews on the potentials and limitations of remote sensing applications in the field of water resource management have been presented by Engman and Gurney (1991), Thiruvengdachari (1993) and Bastiaanssen et al (2000). It is, however, possible to collect information concerning large areas at frequent intervals through satellite remote sensing techniques. In the past decade, the capability of satellite remote sensing to monitor agricultural and hydrological conditions of a land surface has improved greatly (Ambast et al., 2002).

Satellites are able to measure fixed bandwidths of reflected and emitted radiance in the electromagnetic spectrum. Generating the radiance at the surface requires an atmospheric correction procedure, while a geometric correction is necessary to ensure

that image coordinates agree with the topographical coordinates at selected pixels (the smallest element of a picture). To carry out a meaningful evaluation, information concerning spectral radiance can be used together with field data (Ambast et al., 2002).

The following areas of irrigation water management using remote sensing techniques have been addressed: (1) assessment of storage in reservoirs, (2) estimates of irrigated crop acreage, (3) identification of irrigated crops, (4) estimates of crop condition and yield, (5) estimate of crop water requirements and soil moisture availability, (6) assessment of water-logging and soil salinity, and (7) evaluation of irrigation system performance (Ambast et al., 2002).

In the present study, using remote sensed data, baselines of the crop water stress index (CWSI) and the water deficit index (WDI) were established from drip-irrigated corn plots. Thus, CWSI provides irrigation timing by monitoring plant water status. By evaluating plant water status with WDI, soil water deficit was estimated for irrigated corn in northeastern Colorado. Since the study represents water deficit dependency on WDI values, remote sensing data are an important tool for estimating the amount of irrigation water prior to irrigation, thus serving as a guide for irrigators, especially in large areas.

The overall objective of this study was to assess the potential of the crop water stress index (CWSI) and water deficit index (WDI) to improve irrigation management by determining irrigation timing and amount of irrigation water to apply on a sandy soil using ground-based remote sensing (GBRS).

Specific study objectives were:

- Use ground-based RS to establish the lower and upper vapor pressure deficit (VPD) baselines of CWSI and the four corners of the vegetation index / temperature (VIT) trapezoid of WDI.
- Measure the effect of the difference between surface and air temperature levels at various growth stages on the amount of irrigation water applied and crop yield.
- Compare the estimated vegetation cover from reflectance data using ground-based RS with measured vegetation cover to determine WDI.
- Determine volumetric water content (VWC) using time domain reflectometry (TDR) in soil containing various levels of sand to calculate soil water deficit to correlate with WDI.
- Analyze the CWSI and WDI to determine the relationships between them and soil texture, soil moisture, and yield.

CHAPTER 2

LITERATURE REVIEW

2.1 Introduction

Considerable research has been conducted to calculate Crop Water Stress Index (CWSI) and Water Deficit Index (WDI) in order to analyze their relationship to irrigation management, which may affect plant growth and crop production as well. As mentioned in Chapter 1, one of the most important inputs in agricultural production is irrigation. If properly managed, irrigation plays a critical role in increasing crop production. In northeastern Colorado, where the study site was located, center pivot irrigation is generally used without scientific irrigation management, which may affect crop production in various percentage of sandy soil. CWSI is the most useful index for developing the timing of irrigations (Alves and Pereira, 2000), although it does not indicate how much to irrigate (Colaizzi et al., 2003b). The previous researches were not able to determine the amount of irrigation water using calculated WDI values, however, the present study carried out amount of irrigation water at the study site.

2.2 Thermal Infrared (IR) Sensor

Plant growth is frequently limited by two primary environmental parameters: water availability and temperature. However, due to differing response times and the problem of quantifying water deficit (i.e., severity vs. duration), plant responses to water deficit have been difficult to model (Kanemasu et al., 1985). Increased plant canopy

temperature in comparison to a well-watered crop during the daytime when absorbed solar radiation is high is the earliest symptom that can be externally detected of a limiting soil water level (Wanjura and Upchurch, 2000).

Plant stress is a term used to describe factors that affect the normal functioning of a plant. However, a common cause of plant stress is an insufficient supply of water in the soil, which results in the plant transpiring at a rate less than the evaporative demand of the atmosphere (Reginato, 1982).

It is important that techniques for measuring plant water stress should provide non-destructive, rapid, reliable plant water status estimates. During the 1960s, infrared technology advanced rapidly, and instruments that could be used for agricultural purposes (e,g,, to measure crop canopy temperature) became commercially available, leading to the availability of lightweight, portable, hand-held, battery operated infrared thermometers (IRT) during the past decades.

Water stress of plant was indicated by measuring plant canopy temperature. This was carried out by using infrared thermometers without physical contact with plants (Ehrler et al., 1978).

Infrared thermometers can rapidly measure canopy temperatures over large areas, and with the development of portable and reliable infrared thermometers, canopy temperature became an easily measured parameter (Hatfield et al., 1985). Since their development, commercial versions of infrared sensors have been increasingly used to determine canopy temperatures and schedule irrigations (Stockle and Dugas, 1992). During the 1980s, the use of IRT became more routine in irrigation scheduling when Idso et al. (1981a) developed and demonstrated an empirical method for using the crop water

stress index (CWSI). Funchs and Tanner, 1966; Fuchs et al., 1967; Gardner and Shock, 1989; Hatfield, 1990); and Gardner et al., 1992a, discussed the theory of IRT operation, while Jackson and Idso, 1969, dealt with temperature effects in infrared thermometry.

In arid climates, infrared thermometry has been widely used to detect plant stress (as indicated by stomatal closure). In cooler, more humid climates, it has been found to be less reliable for irrigation scheduling (Jones, 1999). The calculated CWSIs were not related to soil-moisture measurements. Such discrepancies in IR thermometry-based water-stress indices may be due to increased errors in the calculation of minimum CWSI at low VPDs, as well as to the fluctuating solar radiation and evapotranspiration which are prevalent in humid, temperate climates (Andrews et al., 1992).

2.3 Crop Water Stress Index (CWSI)

Water management in modern agriculture requires the determination of the crop water requirement and time of irrigation. The CWSI is a technique that utilizes vapor pressure deficit (VPD) and measurements of the crop surface temperature by an infrared thermometer to determine the crop water status.

The majority of conventional methods detect crop water stress remotely through the measurement of the surface temperature of the crop. The relationship between surface temperature and water stress is based on the statement that as a crop transpires, the evaporated water cools the leaves below the air temperature. Leaf temperature increases as the crop becomes water-stressed and transpiration decreases. While other factors should be considered in order to attain accurate measurements of stress levels, leaf temperature is the most important. A crop's surface temperature can be measured remotely through the use of infrared thermometers or thermal scanners (Jackson, 1982).

Water deficiencies in plant tissues that impair plant growth processes result in crop water stress, generally occurring as a result of drought in dry land production, or improperly timed or inefficient water application in irrigated production (Howell et al., 1984a).

Many methods have been proposed to use plant indicators of plant water deficit to schedule irrigations. Among these is leaf temperature. To quantify crop water stress, Hiler and Clark (1971) and Hiler et al. (1974) proposed a "stress day index". This concept employs a plant-based water deficit measure (e.g., leaf water potential, canopy-air temperature differential, stem diameter, etc.), together with a crop-based factor related to crop species and its yield sensitivity to imposed water deficit (Howell et al., 1984a).

Although Hiler and Clark (1971) proposed leaf temperature as one possible indicator of plant stress, Hiler and Howell (1983) found that leaf water potential was a better indicator of plant water deficit. Stegman et al. (1976) modified the stress day index to account for air temperature and soil moisture. Ehrler (1973), however, found leaf temperature to be a sensitive indicator of plant water deficit in cotton, provided that due consideration was given to the effect of ambient air vapor pressure. Idso et al. (1977) proposed canopy-air temperature differences as a stress indicator. To develop an environmentally responsive indicator of plant stress, Idso et al. (1981a) later incorporated vapor pressure deficit with the canopy-air difference.

The indicator of plant stress was termed "crop water stress index." Jackson et al. (1981) demonstrated its theoretical validity, while Idso et al. (1981b), Idso et al. (1982) and Reginato (1983) showed its empirical validity. More recently, Jackson (1982) summarized the state-of-the-art of canopy temperature measurement in evaluating crop water stress.

The crop water stress index has proven to be useful in assessing many physiological plant responses to water stress via remote measurements of foliage temperature (Idso et al., 1981b, c, 1982; Pinter and Reginato, 1982). Of interest in this respect are assessments of leaf stomatal conditions and net photosynthesis rates, since these parameters are associated with water loss by transpiration and production of dry matter, basic plant functions that farm management practices are designed to influence to produce the most yields for the least financial expenditure (Idso et al., 1984).

The crop water stress index was proposed as an important tool for irrigation timing (Pinter and Reginato 1981; Hatfield 1982; Reginato 1983; Howell et al. 1984a; Howell et al. 1984b; Reginato and Howe 1985; Braunworth and Mack 1989; Garrot et al. 1990; Mateos et al. 1991; Stockle and Dugas 1992; Stegman and Soderlund 1992; Jones 1999; Alves and Pereira 2000; Irmak et al. 2000; Wanjura and Upchurch 2000; Alderfasi and Nielsen 2001; Colaizzi et al. 2003b). As proposed by Clawson and Blad (1982), canopy temperature variability can also be used as a basis for scheduling irrigation.

Under natural conditions of evaporation, the state of a given mass of air can be described by its temperature and vapor pressure (VP). The crop water stress index (CWSI) is an indicator of the relative transpiration rate occurring from a plant at the time of measurement using a measure of plant temperature and the vapor pressure deficit (VPD), which is a measurement of air dryness.

Jackson et al. (1981) presents the theory behind the energy balance that separates net radiation from the sun into sensible heat that heats the air and latent heat that is used for transpiration. As the crop undergoes water stress, the stomata close, transpiration decreases and leaf temperature increases. When a plant is transpiring fully, the leaf

temperature is 1 to 4 degrees cooler than the air temperature and the CWSI approaches 0. As transpiration decreases, the leaf temperature rises and can be 4 to 6 degrees warmer than the air temperature. When the plant is no longer transpiring, the CWSI is 1. The difference between crop surface and air temperatures may depend on soil texture, meteorological parameters and vegetation types (Skeen, 1996).

CWSI requires vapor pressure deficit (VPD) and temperature data of the crop canopy and air. Figure 2.1 shows a sample of VPD baselines for soybeans. VPD is a necessary calculation to determine VPD baselines to establish CWSI plot.

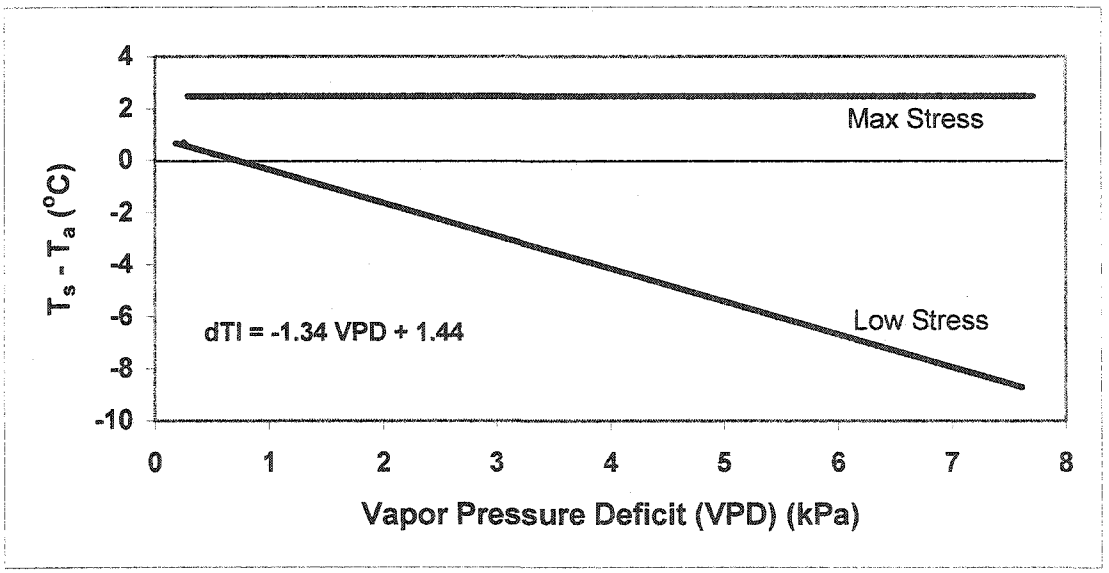

Figure 2.1. An example of VPD upper and lower baselines for soybeans (USWCL, 2001).

In this study, it was used to calculate the lower limit of canopy minus air temperature (dT_l).

$$dT_l = \text{Intercept} + \text{Slope (VPD)}, \quad (2.1)$$

$$dT_u = \text{Intercept} + \text{Slope } (VP_{sat}\{T_a\} - VP_{sat}\{T_a + \text{Intercept}\}), \quad (2.2)$$

from Figure 2.1.

These calculated factors are used in the CWSI formula,

$$CWSI = \frac{(dT - dT_l)}{(dT_u - dT_l)}, \qquad (2.3)$$

where

dT = the current difference in canopy and air temperature °C.

dT_l = the baseline difference in canopy and air temperature of a well-watered, transpiring plant, °C.

dT_u = the baseline difference in canopy and air temperature of a fully-stressed, non-transpiring plant, °C.

Canopy and air temperature differences are an efffective indicator of plant water status (Bartholic et al., 1972; Ehrler, 1973; Braunworth and Mack, 1989). The use of foliar temperatures has been suggested for irrigation timing. Due to the substantial latent heat of vaporization of water, the evaporation of leaf water causes cooling which is relative to the air temperature. When water stress limits evaporation from the leaf surface, the absorbed radiation is apportioned more to warming leaf temperature than to evaporating water (Braunworth and Mack, 1989).

As demonstrated by Alderfasi and Nielsen (2001), CWSI is a valuable tool for monitoring and quantifying water stress, as well as for timing irrigation. The main objective of their study was to develop a baseline equation for calculating CWSI to monitor water status and scheduling of irrigation of a wheat crop.

Since the development of the CWSI method, many researchers used it for irrigation management (Pinter and Reginato, 1982; Reginato, 1983; Howell et al., 1984b; O'Toole et al., 1984; Reginato and Garrot, 1987; Wanjura et al., 1990). The CWSI was

correlated to yield (Walker and Hatfield, 1983; Smith et al., 1985), leaf water potential (Pinter and Reginato, 1981; O'Toole et al., 1984; Jackson, 1991), and soil water availability (Hatfield, 1982; Reginato and Garrot, 1987).

Using the theoretical method for determining the baselines of CWSI for sweet corn, Braunworth and Mack (1989) found that CWSI measurements needed to be improved; however, it was possible to determine the upper and lower baselines from field data. Idso et al. (1981a) and Bonanno and Mack (1983) demonstrated such relationships for alfalfa and snap beans.

The field-measured lower limit has one possible advantage in that it averages the variable conditions for those terms set to a constant for theoretical lower limit. Another advantage is that all measurements of less-watered plots are compared to a field-measured, well-watered baseline rather than to a theoretical lower limit which may be much lower than the field-measured lower limit (Braunworth and Mack, 1989).

2.4 Water Deficit Index (WDI)

The CWSI is limited, however, to full vegetation cover. Moran et al. (1994) addressed this limitation by proposing the Water Deficit Index (WDI), a technique for determining irrigation management zones and reducing the soil samples needed to analyze plant-available water.

Colaizzi et al. (2003a) indicated that WDI was sensitive to differences in water treatments from partial to full canopy cover for cotton in Maricopa, Arizona. This information is crucial for irrigation management and has the potential of improving water use efficiency.

Moran et al. (1994) addressed the influence of soil background by accounting for soil temperature using the same energy balance principles employed in CWSI, and defined the water deficit index (WDI). Utilizing data from airborne multi-spectral and thermal sensors that were flown over a muskmelon farm west of Phoenix, Arizona, Clarke (1997) demonstrated that WDI could detect differences in water status (Colazzi et al., 2003a).

The CWSI is a commonly used index for detecting plant stress based on differences between foliage and air temperature. However, the difficulty of measuring the foliage temperature of partially vegetated fields has hampered the application of CWSI at local and regional levels. Most infrared sensors —hand-held, airborne and satellite-based— measure a composite of both soil and plant temperatures (Moran et al., 1994).

Jackson et al. (1981) warned that it is important that the soil background not appear in the field of view of the infrared thermometer. Soil temperatures can differ drastically from plant temperatures; hence, including them can cause serious errors in the CWSI. Attempts to combine spectral vegetation indices with composite surface temperature measurements to allow application of the CWSI theory to partially-vegetated fields without knowledge of foliage temperature has been carried out by use of the vegetation index / temperature (VIT) trapezoid. Based on this approach, Moran et al. (1994) introduced the water deficit index (WDI) for evaluating evapotranspiration rates for both full-cover and partially-vegetated sites. WDI is an extension of the CWSI, in which measured surface temperature is considered a composite of both vegetation cover and soil background.

Moran et al. (1994) concluded that the VIT trapezoid and WDI appear to have a potential for evaluating evapotranspiration rates and relative field water deficits for both full and partial vegetation cover. This represents an advantage over CWSI, which is limited in application to full-cover application period. In addition to remotely sensed data, WDI, like CWSI, requires few input parameters, and most input values are either known or can be adequately estimated. Furthermore, at local and regional scales with ground-, aircraft-, and satellite-based sensors, technology is available for providing simultaneous measurements of composite surface temperature and spectral reflectance.

The VIT trapezoid approach is based on the hypothesis that a trapezoidal shape would result from a plot of measured ground surface (soil and plant) minus air temperatures ($T_s - T_a$) versus vegetation cover (unitless, ranging from 0 = no vegetation cover to 1 = full vegetation cover). As shown in Figure 2.2, the trapezoid's vertices would correspond to 1) well-watered, full-cover vegetation, 2) water-stressed, full-cover vegetation, 3) saturated bare soil, and 4) dry bare soil (Moran et al., 1994).

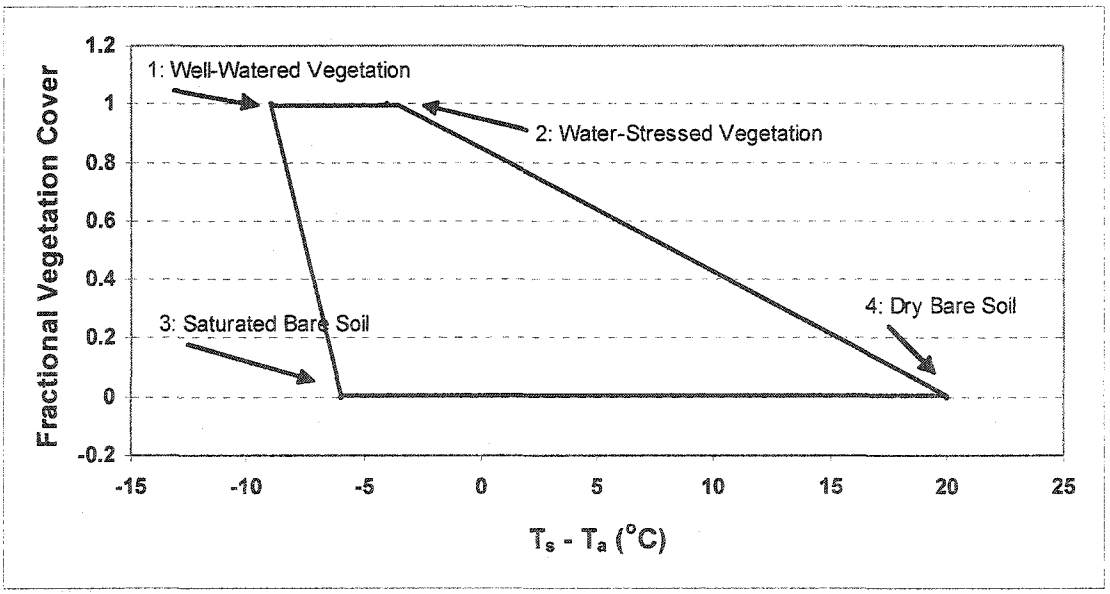

Figure 2.2. The VIT trapezoidal shape that would result from the relation between ($T_s - T_a$) and the fractional vegetation cover (Moran et al., 1994)

To determine WDI, the vegetation cover was plotted versus the difference in measured surface and air temperature ($T_s - T_a$) ($^{\circ}C$). There are three main methods for determining the vegetation cover: estimate, measure and theoretical methods. Hence, WDI can be calculated by using remote sensing measurements of reflectance data, and surface and air temperatures. The VIT trapezoid becomes noticeably more useful if the measurements of vegetation cover along the Y-axis are substituted with an estimate vegetation cover (vegetation index) that is linearly related to measured vegetation cover. There is confirmation that the relation of some vegetation indices (estimated vegetation cover) with measured vegetation cover is relatively linear in excess of a large range of measured vegetation cover values (Huete and Jackson, 1988; Huete 1988; Moran et al., 1994), though this relation is not unique but rather both crop- and site-specific. In addition, Price (1990) demonstrated that vegetation indices computed by band ratios do not satisfy the associative property for area measurements and are therefore affected by the spatial resolution of the sensor. Accordingly, two sites with the same vegetation cover but different vegetation distribution could yield different values of vegetation index. Though issues such as these must be addressed in each application of the VIT trapezoid, the confirmation that the relation is almost linear over a large range of values will be sufficient here for development and demonstration of the concept (Moran et al., 1994).

Since it is important for the vegetation index to be sensitive to increases in vegetation cover and insensitive to spectral changes in soil background (such as soil moisture-related differences), Moran et al., (1994) used the soil adjusted vegetation index (SAVI) to represent fractional vegetation cover in their study, as shown in Figure 2.3.

$$SAVI = [(\lambda_{NIR} - \lambda_R) / ((\lambda_{NIR} + \lambda_R) + L)] * (1 + L), \quad (2.4)$$

and λ_{NIR} and λ_R are the near-infrared (NIR) and red reflectances, respectively, and L is a unitless constant assumed to be 0.5 for a wide variety of leaf area index (LAI) values (Huete, 1988).

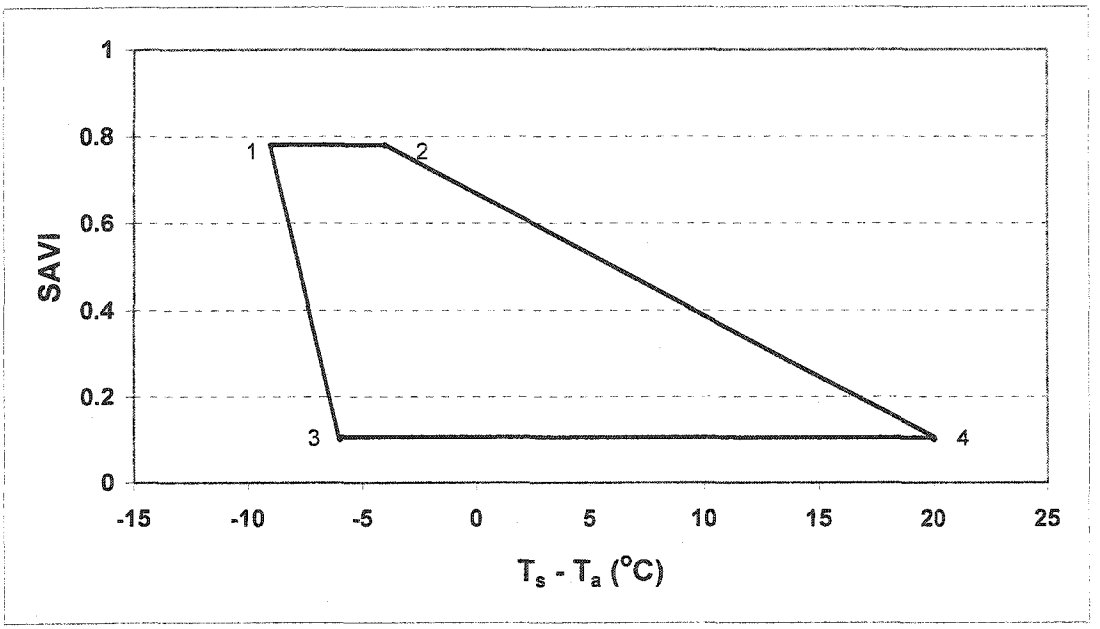

Figure 2.3. Substitution of SAVI for fractional vegetation cover to derive the VIT trapezoid (Moran et al., 1994).

Colaizzi et al. (2000) used a different estimated vegetation cover (vegetation index), i.e., the normalized difference vegetation index (NDVI), to establish the vegetation index / temperature (VIT) trapezoid. In their study, Colaizzi et al. (2000) found a strong linear relationship ($R^2 = 0.96$) using their experimental data for NDVI versus vegetation cover. Figure 2.4 shows the VIT trapezoid by estimating vegetation cover using NDVI.

$$NDVI = (\lambda_{NIR} - \lambda_R) / (\lambda_{NIR} + \lambda_R), \quad (2.5)$$

where λ_{NIR} and λ_R are reflectance in the near infrared (NIR) and red bands, respectively, of the measured plant canopy.

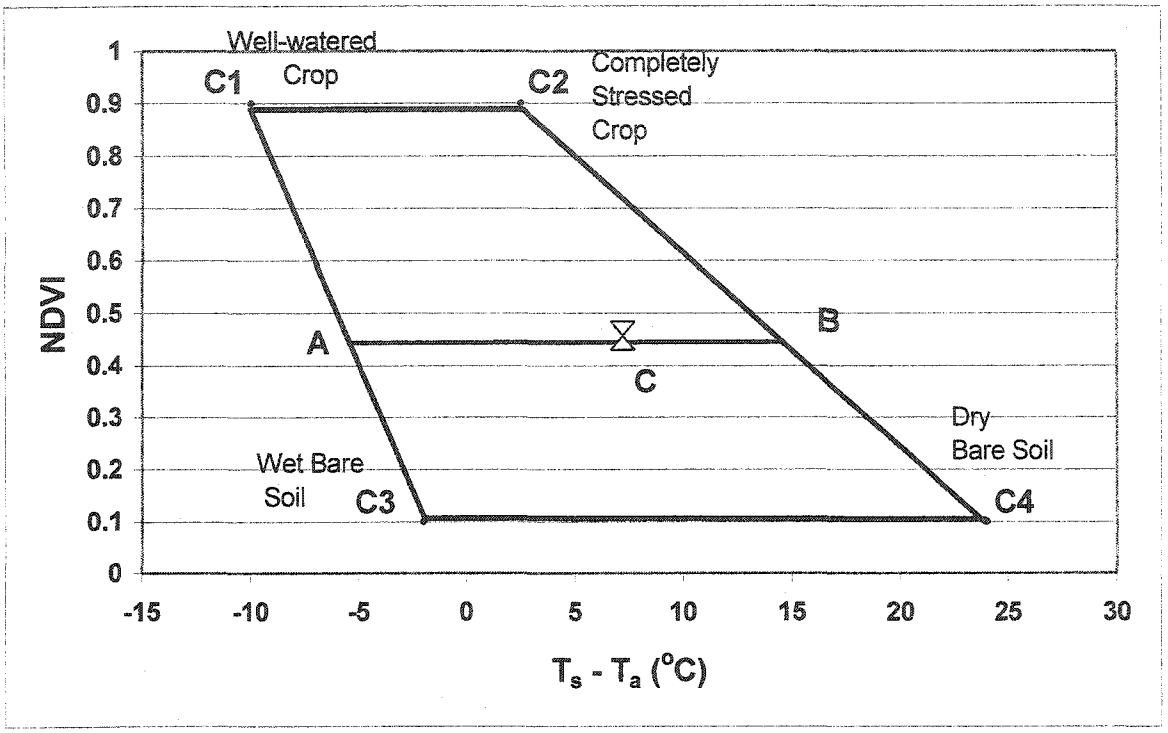

Figure 2.4. Vegetation index and temperature (VIT) trapezoid for cotton in Maricopa, Arizona (Colaizzi et al., 2000).

In Figure 2.4, the VIT trapezoid shows lines that connect the four corners, in which the left line contains point A and defines the range of (T_s - T_a) possible for full vegetation cover where water is not limited. In like manner, the right line contains point B and defines the possible range of (T_s - T_a) for conditions of no available water. The range of (T_s - T_a) possible for full vegetation cover is defined by the top line between corners C1 and C2, which is also the range of (T_s - T_a) possible for the CWSI. Consequently, if CWSI is used, point C will fall on the top line, while corners C1 and C2 will define the lower and upper limits, respectively.

Plotting NDVI versus the difference between measured or estimated surface and air temperature (T_s -T_a) (°C) results in a Vegetation Index / Temperature (VIT) trapezoid, as shown in Figure 2.4. For a surface with a crop present, the following four possible

extremes of NDVI versus (T_s -T_a) may be encountered, as represented by the four corners of the VIT trapezoid: (C1) = a crop that is well-watered with full vegetation cover transpiring at full potential; (C2) = a crop that is completely water-stressed, having full vegetation coverage where measurable transpiration is negligible; (C3) = soil that is bare and wet, where evaporation is at potential; and (C4) = soil that is dry and bare, where no water is available for evaporation (Colaizzi et al., 2000).

Energy balance between the surface and atmospheric boundary layer are in equilibrium for each of these four corners (point C), within which a point measurement of (T_s - T_a) and the corresponding vegetation cover (NDVI) will fall. The lower limit of (T_s - T_a), where water for evaporation and transpiration is not limiting, will occur at point A for a given amount of vegetation cover, while if no water is available, the upper limit will occur at point B. The WDI is defined as the ratio of the distances of AC to AB.

Moran et al. (1994) present the origin and underlying assumptions of the equations, as well as the assumptions underlying the VIT trapezoid. The required meteorological parameters include T_a, VPD, R_s and u (wind speed [m s^{-1}]) measured at height z, all of which are accessible from an on-site weather station.

With the measurement of actual (T_s - T_a) and vegetation cover (point C, Figure 2.4), (T_s - T_a) at the four corners of the VIT trapezoid must also be determined. At that stage, points A and B can be linearly interpolated between corners C1-C3 and C2-C4, respectively, while WDI can be computed. Computing (T_s - T_a) at each corner on a theoretical basis gives

$$(T_s - T_a)_1 = \frac{r_{a1}(R_{n1}-G_1)}{\rho_a C_p} * \frac{\gamma_1(1+(r_{cp}/r_{a1}))}{\Delta_1+\gamma_1(1+(r_{cp}/r_{a1}))} - \frac{VPD}{\Delta_1+\gamma_1(1+(r_{cp}/r_{a1}))}, \quad (2.6)$$

$$(T_s - T_a)_2 = \frac{r_{a2}(R_{n2}-G_2)}{\rho_a C_p} * \frac{\gamma_2(1+(r_{cp}/r_{a2}))}{\Delta_2+\gamma_2(1+(r_{cx}/r_{a2}))} - \frac{VPD}{\Delta_2+\gamma_2(1+(r_{cp}/r_{a2}))}, \quad (2.7)$$

$$(T_s - T_a)_3 = \frac{r_{a3}(R_{n3}-G_3)}{\rho_a C_p} * \frac{\gamma_3}{\Delta_3+\gamma_3} - \frac{VPD}{\Delta_3+\gamma_3}, \quad (2.8)$$

$$(T_s - T_a)_4 = \frac{r_{a4}(R_{n4}-G_4)}{\rho_a C_p}, \quad (2.9)$$

where subscripts 1-4 refer to corners C1-C4,

r_a: the aerodynamic resistance (s m^{-1}),

R_n: the net incoming radiant flux density (W m^{-2}),

G: the soil heat flux density (W m^{-2}),

ρ_a: the density of dry air (kg m^{-3}) and is assumed constant at 1.19,

C_p: the specific heat of dry air (J kg^{-1} $^{\circ}C^{-1}$) assumed to be constant at 1013 (Jensen et al., 1990),

γ: the psychrometric "constant" (kPa $^{\circ}C^{-1}$),

Δ: the slope of the saturated vapor pressure-temperature relation (kPa $^{\circ}C^{-1}$),

r_{cp}: the canopy resistance at potential transpiration (s m^{-1}),

r_{cx}: the canopy resistance under completely stressed conditions (s m^{-1}),

VPD: the vapor pressure deficit of air at T_a (kPa).

Utilizing the VIT trapezoid, WDI is calculated:

$$WDI = \overline{AC} / \overline{AB}, \quad (2.10)$$

As shown in Fig. 2.4, A, B, and C will occur on the plot of the WDI. Point A represents a non-limiting condition for evaporation and transpiration; point B is the upper limit at which no water is available, and point C represents the actual measurement.

The WDI may be useful to assess the irrigation needs of sandy soils. In this study, all four corners of the VIT trapezoid were found by using light bar (LB) and a ground-based remote sensing system. Determining the vegetation cover is the most important part of preparing the WDI. Both estimated and measured vegetation cover methods were used in this study.

Various techniques are used for estimating vegetation cover, such as Normalized Difference Vegetation Index (NDVI), Soil Adjusted Vegetation Index (SAVI), Modified Soil Adjusted Vegetation Index (MSAVI), Visible Atmospherically Resistant Indices ($VARI_{green}$), and Vegetation Index (VI_{green}). The measured vegetation cover was used as a guide for determining which of the estimated vegetation covers had a better relationship with the measured vegetation cover values.

Another use for the WDI deserves to be mentioned. As shown in Fig. 2.5 (Clarke, 1997), WDI is divided into three additional regions. Extending a line from C1 to $(T_s - T_a) = 0$ at zero vegetation cover; area (1) to the left of this line comprises a region where the soil background is completely wet. Drawing a second line from C1 to C4, area (3) to the right of this line comprises a region where the soil background is completely dry. Between areas (1) and (3) is an intermediate region, area (2), which has a drying or patchy wet soil background.

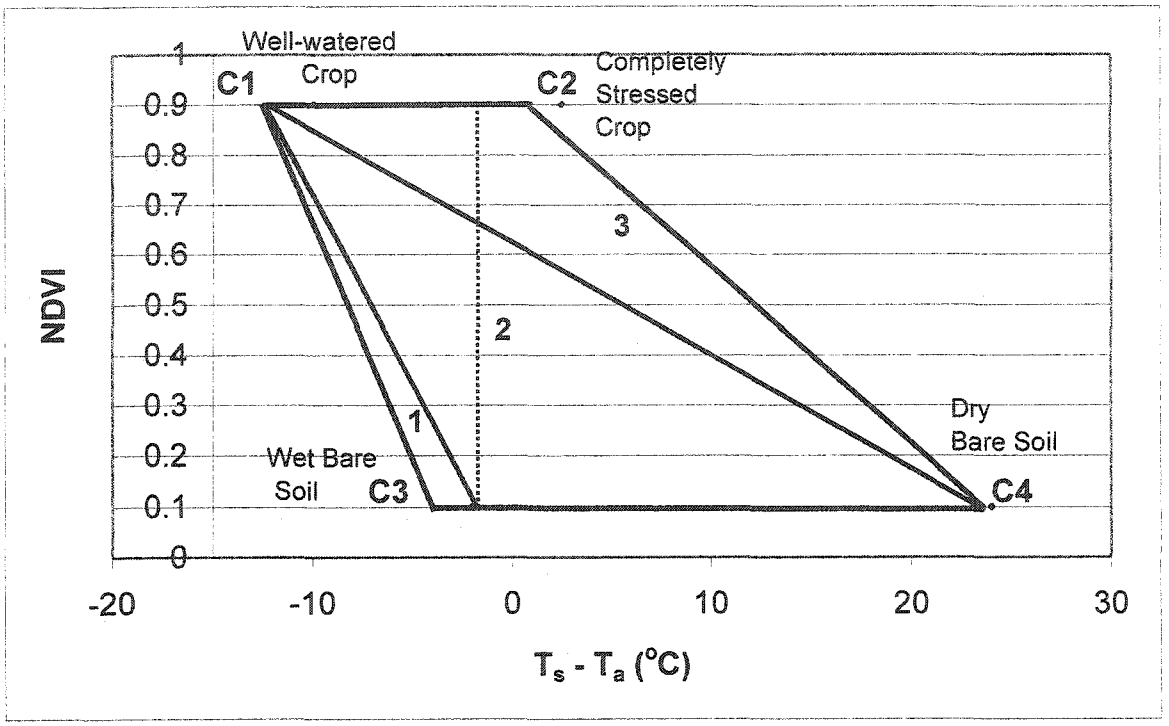

Figure 2.5. Vegetation index and temperature (VIT) trapezoid divided into three regions for cotton in Maricopa, Arizona (Colaizzi et al., 2000).

2.5 Vegetation Indices

As mentioned above, measured vegetation cover can be replaced with a vegetation index (estimated vegetation cover) by using reflectance data (Moran et al., 1994). Obviously, vegetation index has some advantages when compared with measured vegetation cover especially in large areas. These advantages are time, data availability, money and labor.

The growth response of plants in relation to measured or predicted climatic variables can be monitored by multispectral vegetation indices derived from canopy reflectance in relatively wide waveband (Hatfield and Pinter, 1993). Vegetation indices such as the perpendicular vegetation index (Richardson and Wiegand, 1977) and the normalized difference (Rouse et al., 1973; Deering et al., 1975; Deering, 1978; and Holben et al., 1980) have been developed to monitor vegetative growth. Vegetation

indices are usually ratios or linear combinations of signals from radiometer bands. These indices provide more highly correlated relationships than individual bands with canopy variables such as green leaf area index, wet and dry biomass, percent cover by vegetation, plant height, fraction of leaf chlorosis, and leaf water content (Bausch and Neale, 1987).

Tucker (1979) and Menenti (1986) proposed a normalized difference vegetation index (NDVI) to enhance the ability to classify crops into various condition groups. Some other indices—soil-adjusted vegetation index (SAVI) by Huete (1988) and modified soil adjusted vegetation index (MSAVI) by Qi et al. (1994)—were also proposed to minimize the back-scattering of canopy-transmitted-soil reflected radiation (Ambast et al., 2002). Recently, Gitelson et al. (2001) presented strong linear relationships between a visible atmospherically resistant index ($VARI_{green}$) and a vegetation index (VI_{green}) with measured vegetation cover for corn.

2.6 Time Domain Reflectometry (TDR)

Measurement of soil water content for the purpose of scheduling irrigation dates back to the origin of irrigated agriculture, and new methods continue to be developed. Existing techniques used for measuring soil water status in the field include tensiometers, electrical resistance sensors, neutron probes, the gravimetric method, soil hygrometers/psychrometers and time domain reflectometry.

While a tensiometer responds to reduced soil water potentials, as do plants, the tensiometer measures only a partial range of potentials and requires regular servicing to remove entrapped air. Electrical resistance sensor readings do not rely solely on the moisture content of the soil, since soluble salt concentration and soil texture also affect the readings.

By the gravimetric method, the sample is destroyed through the measuring process, and consequently continuous readings of soil water at a given point on the landscape cannot be taken. For repeated measurement, the gravimetric method is not an adequate technique. This method is also quite time-consuming. For neutron probes, the most significant restrictions are related to radiation licensing and inspection programs, the necessity of operator-controlled depth selection, and transportation difficulties. Soil hygrometers/psychrometers are not appropriate for sandy soils because they are indifferent to soil water potentials larger than –100 cbar (-1 bar). Time domain reflectometry (TDR) is a technique that also can be used to measure soil volumetric water content. It is a method that overcomes the majority of the previously-mentioned disadvantages (Irmak et al., 1999). As a technique that indirectly measures soil volumetric water content, time domain reflectrometry (TDR) is based on the effect of changing dielectric properties of the medium on applied electromagnetic waves. Many researchers have conducted studies between TDR and one of the above methods to ascertain the advantages of TDR. Each researcher concluded that TDR has become an accepted method of measuring soil water content, resulting in accurate and reliable operations (Hart et al., 1994; Van Clooster et al., 1995; Frueh and Hopmans, 1997; Hart and Lowery, 1998; Nissen et al., 1998; Irmak et al., 1999; Noborio et al., 1999; Huisman and Bouten, 1999; Ponizovsky et al., 1999; Robinson et al., 1999; Thomsen et al., 2000).

CHAPTER 3

MATERIALS AND METHODS

3.1 Materials

Experimental data were collected in a commercial cornfield (Figure 3.1) north of Wiggins, Colorado, in Morgan County, during the 2002 corn (Zea mays L.) growing season. The Morgan County soil survey indicated that Valentine and Valentine Dwyer sands (sandy, mixed, non-acid, mesic, typic ustipsamments), as well as Bijou loamy sand (coarse loamy, mixed, mesic, mollic haplargids), were the major soils.

The study had two sites. One of these, a small area of 1080 m^2, included six plots (trial area) immediately next to the field, as shown in Figure 3.2. Drip irrigation was used in this area in order to obtain greater control of water application. The trial area contained six plots; five of which were planted with corn and one left unplanted. This area was approximately 90 m long and 12 m wide with 16 rows oriented in the northwest/southeast direction. Row spacing was 0.76 m. Single plot size was 12 m x 15 m. The second site was the NW half of a commercial center pivot irrigated cornfield; the field was 47 ha in area. Both sites had the same row direction and same corn hybrid.

The WDI end points (the four corners of a vegetation index / temperature (VIT) trapezoid) and CWSI baselines (VPD upper and lower) were to be established from data collected in the drip irrigated plots. Plot #1 was well irrigated; i.e., no plant water stress was allowed to develop. The other four plots started in a well-watered condition and then

were water stressed at various growth stages in order to analyze crop reactions to water stress during the growing season. Crop water stress data were collected at these times to determine the stress (upper) baseline of VPD vs ($T_s - T_a$). The last plot, #6, was a bare soil area. To obtain wet bare soil data from the bare soil plot, a lawn sprinkler was used. Data were taken first from the dry soil (plot #6), which was irrigated while data were being taken from the other plots and finally GBRS returned to wet soil plot after data was taken on the last corn plot (plot #1).

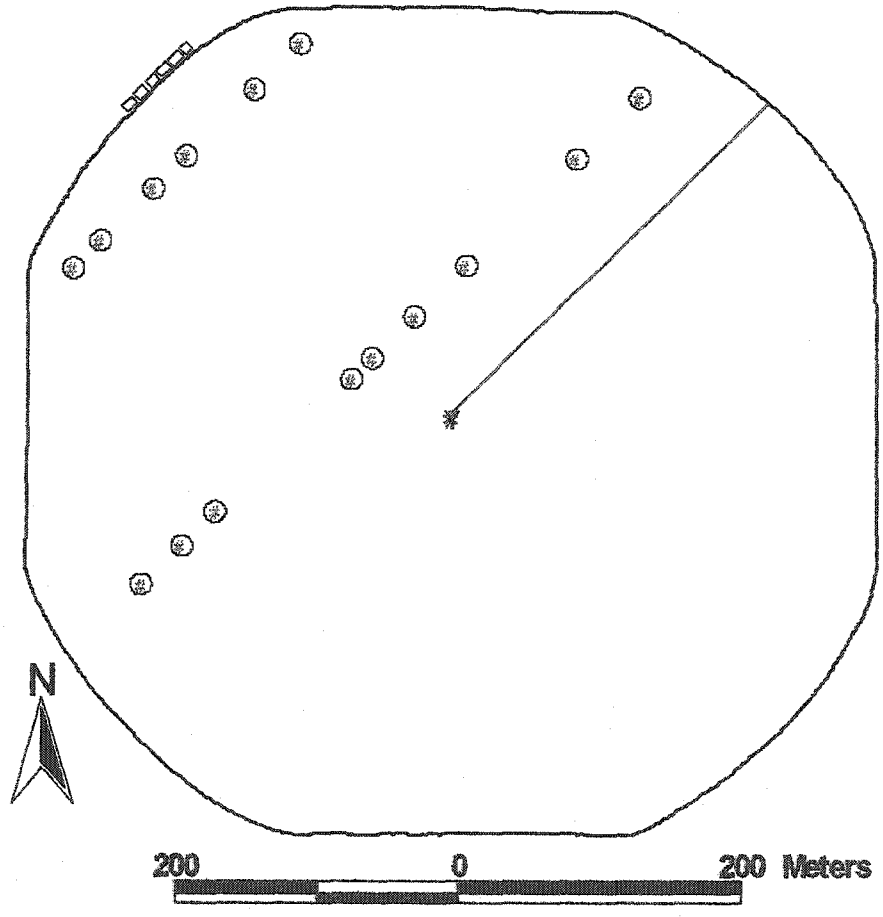

Figure 3.1. Locations of TDR probes.

Fifteen data collection sites which potentially represented yield variability were located on the NW half of the commercial field. These sites were geographically located by using DGPS based on field soil electrical conductivity (EC) maps (deep and shallow

maps) provided by Dr. Hamid Farahani (USDA-ARS Water Management Research Unit, Ft. Collins, CO).

As shown in Figure 3.1, TDR probes were installed in the commercial cornfield at these fifteen sites at two different depths (30 cm and 70 cm). TDR probes were also installed in each drip-irrigated plot in order to obtain data from the small plots as well.

The fifteen locations were selected along two transects through the field. These two transects had highly variable soil EC values as shown by shallow and deep EC maps (Figures 3.3 and 3.4, respectively). Nine of the 15 sites were located on the first row close to the center pivot road, and the remaining 6 sites were located in the second row (Figure 3.2). In this study, measurements were taken near solar noon; consequently there was limited time for collecting the necessary data from all locations.

Figure 3.2. Drip irrigated plots for imposing water deficits at various growth stages.

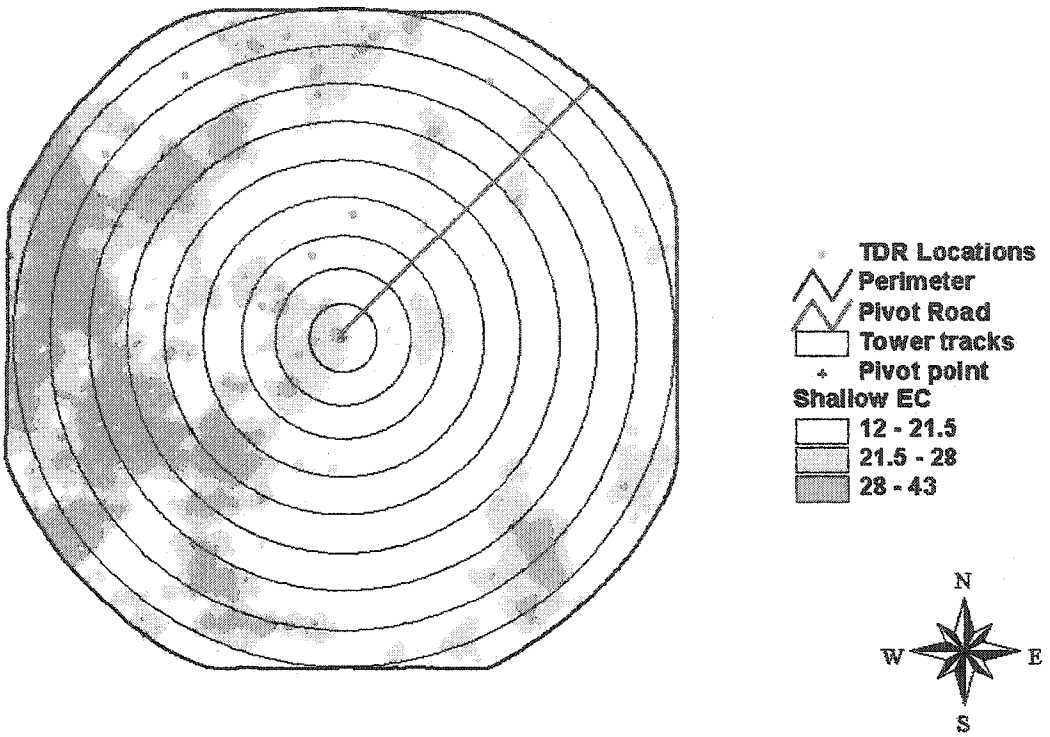

Figure 3.3. Shallow soil electrical conductivity (mS/l) map.

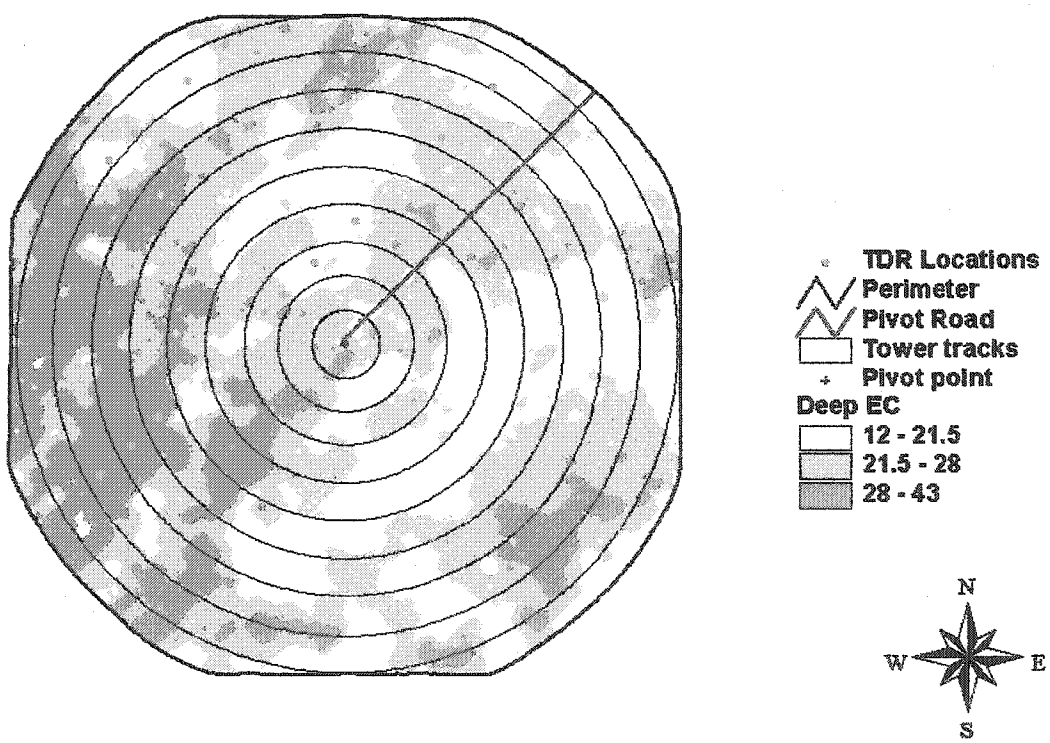

Figure 3.4. Deep soil electrical conductivity (mS/l) map.

3.2 Methods

3.2.1 Ground-Based Remote Sensing (GBRS) System

The Ground-Based Remote Sensing (GBRS) system used in this study was developed by Dr. Walter Bausch, USDA-ARS Water Management Research Unit, Ft. Collins, CO. This system is a modification of the one described by Bausch et al. (1990) and is partially described by Moran et al. (2003). As seen in Figure 3.5, the system consists of a high-clearance tractor for easy field access, a hydraulic-operated extendable boom, three instrument platforms with various instruments, and a data logger. One instrument platform is attached to the boom for a nadir view of the target, another is attached to the front of the tractor for oblique views of the target, and the third platform is mounted on the tractor's roll over protection system (ROPS) for up-looking sensors measuring irradiance. The nadir-view platform and the ROPS platform have two-way leveling to keep the instruments level. When the boom is fully raised and extended, instruments on the nadir-view platform are 10 m above ground. The oblique-view platform provides height adjustment, angle adjustment, and rotational capability for viewing on either side of the tractor. Typical orientation of this platform is to have the sensors look perpendicular to the crop row.

As shown in Figure 3.6, basic instrumentation on the nadir- and oblique-view sensor platforms consist of radiometers and infrared thermometers (IRT); one of each type of sensor is on each platform. However, film, digital, and/or video cameras are frequently mounted on one or both of these platforms. The up-looking sensor platform on the tractor ROPS carries a radiometer, a pyranometer, and a photosynthetic active radiation (PAR) sensor. A height adjustable, aspirated temperature-humidity probe is

attached on the right side of the tractor; its mounting is such that it can be switched to the other side of the tractor if so desired.

Figure 3.5. Set-up of reflectance data collection systems on the ground-based remote sensing system.

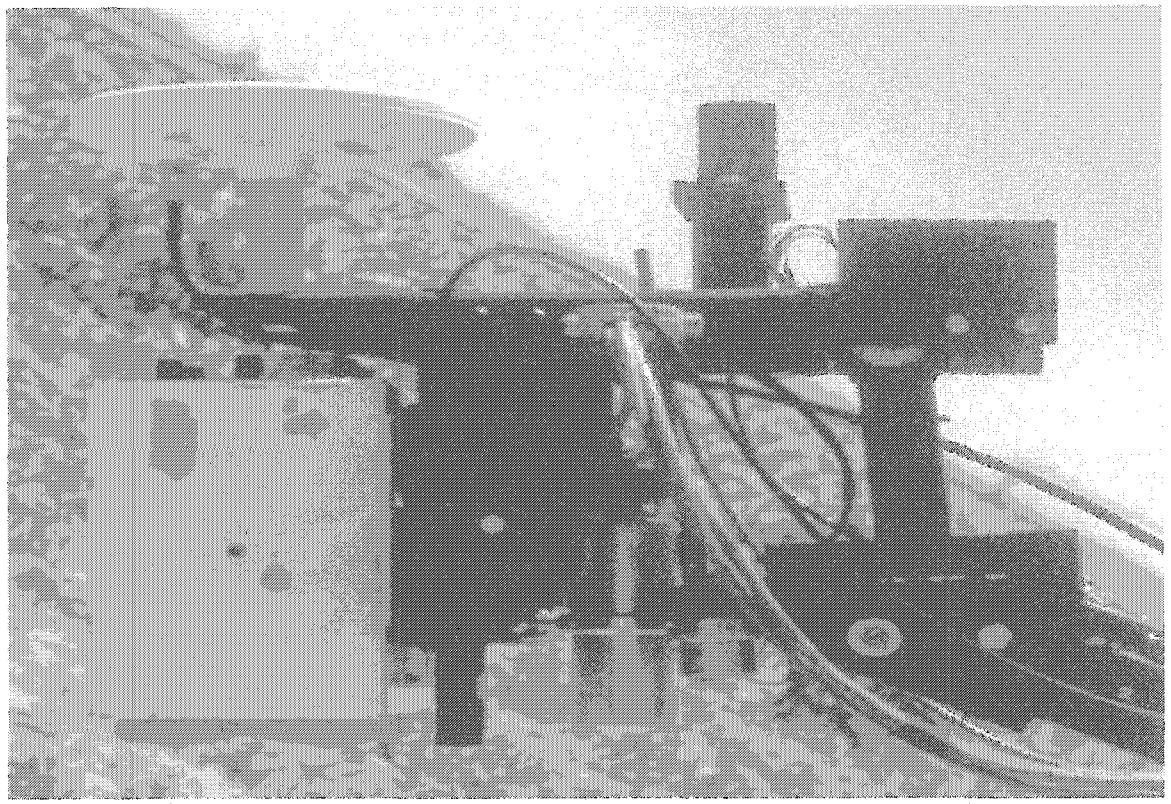

Figure 3.6. Radiometer, IR sensor, and GPS antenna on the nadir-view platform.

A data logger (Campbell Scientific CR23X) is used to sample and store sensor voltages as well as time of measurement. Data are acquired every two seconds as the tractor traverses a data transect through the field. Position (longitude and latitude) of each data point is determined with real-time differential GPS (Racal LandStar MkIV with Ashtech G12 Lite GPS card). The GPS antenna is mounted on the nadir-view platform directly above the radiometer; accuracy of the instantaneous horizontal position is sub-meter.

At the start of each measurement session, the data logger clock is synchronized to GPS time and all sensors go through a routine check to ensure proper operation. Also, measurements of crop height are made to determine height settings for the temperature humidity probe and the oblique-view sensors.

Figure 3.7 shows travel direction of high clearance tractor and the areas where the Exotech radiometer and IR sensor were looking. Data collected with these instruments were used to establish the CWSI and WDI. These two indices were used to determine the irrigation timing and soil water deficit (SWD).

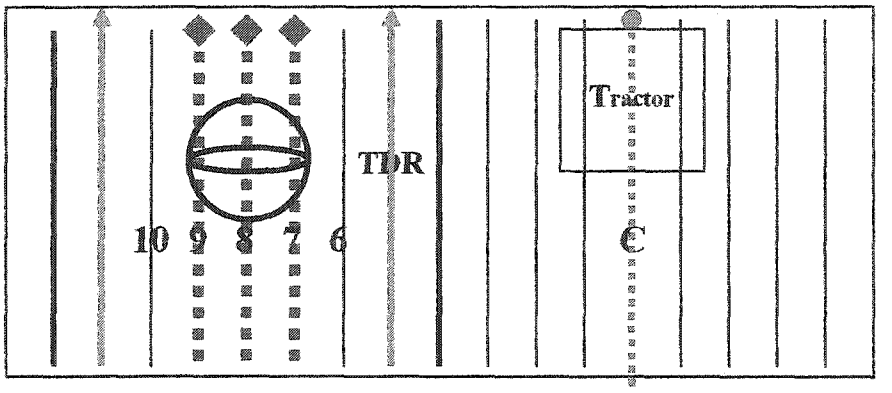

Tractor Center Line

Reflectance Rows

Measurements Rows

TDR TDR Locations Row

Reflectance (nadir view) Measurement Circle (Diameter = 2.6 m)

IR Sensor (80° view) Measurement Elipse (Axis Lengths = 2.4 m and 0.4 m)

Figure 3.7. Data collection areas with GBRS

3.2.1.1 Measurement of Surface Temperatures (T_s)

Surface temperature was measured using thermal infrared (IR) sensors. The nadir view IR sensor was an Apogee model IRTS-P infrared transducer with a 3:1 (≈19°) field of view (FOV) that viewed a circular spot 3.3 m in diameter. The IR sensor mounted in

front of the high clearance tractor was an Everest Interscience model 100.3ZL which had a 4° FOV. Its mounting provided an oblique view of the target which was perpendicular to the crop rows. The sensor was positioned 1 m above the target surface at an 80° view angle (10° below the horizontal). Thus, the sensor's view was an ellipse with major axis of 2.4 m and a minor axis of 0.4 m (Figure 3.7), centered very near the center (within 0.2 m) of the circular spot viewed by the nadir sensors. The 80° view angle was maintained via automatically positioned hardware and software. The height of the sensor above the target was adjusted for each measurement session based on mean height of the corn canopy. The sensor was rotated to always view the sunlit side of the canopy regardless of travel direction. As depicted by the photographs in Figure 3.8, the nadir view IR sensor was influenced by soil background temperature, while the oblique view IR sensor minimized the influence of soil temperature on canopy temperature measurements.

Bare soil temperature measurements for the small plot study were strictly from the nadir view IR sensor. For all other locations, canopy temperature measurements were made with the oblique view and nadir view IR sensors. Surface temperature measurements from both view angles were evaluated to determine their effect on CWSI and WDI.

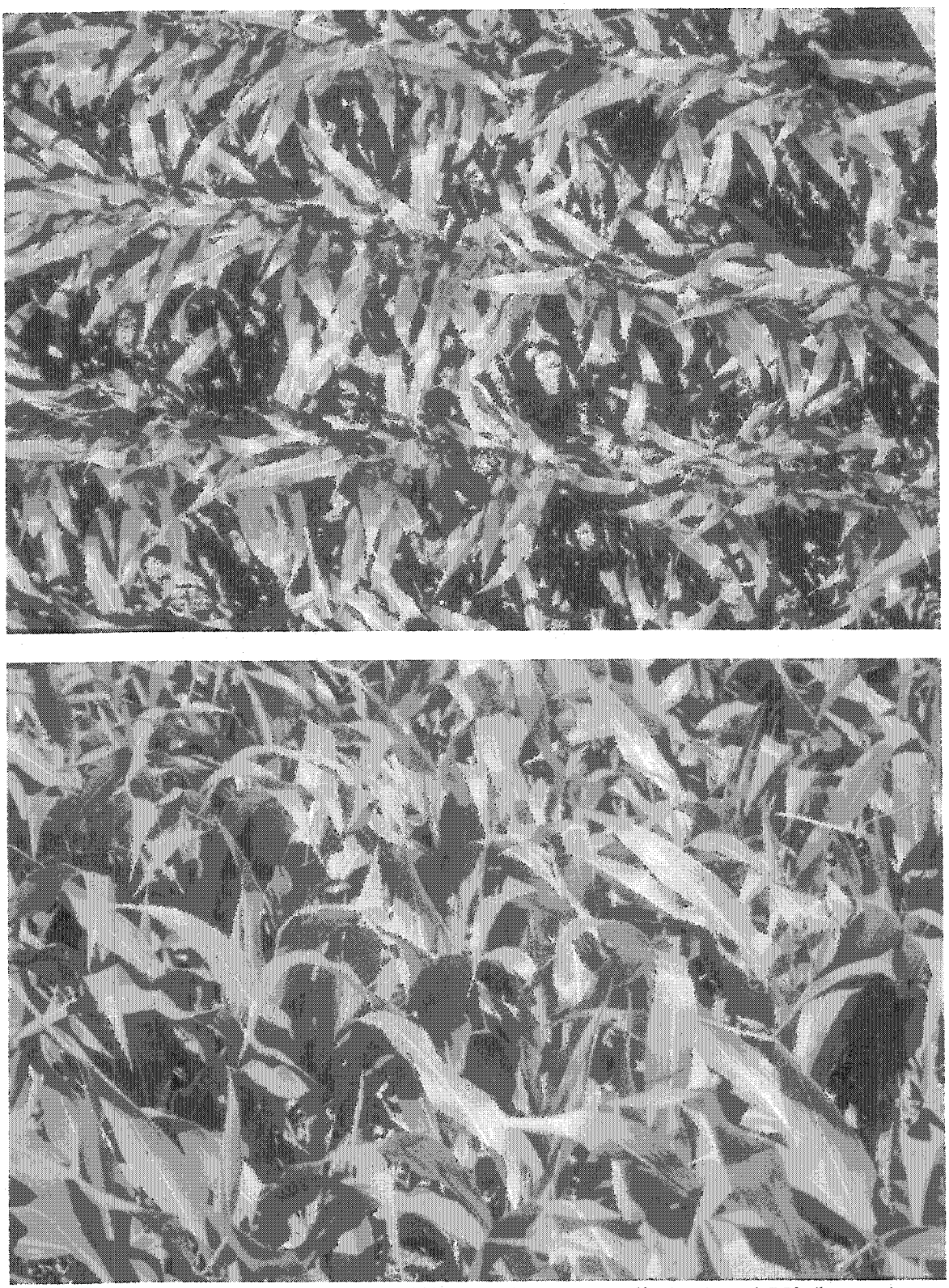

Figure 3.8. Photographs showing the difference between nadir (top) and 75° (bottom) views at the V9 growth stage.

3.2.1.2 Measurement of Air Temperature (T_a) and Relative Humidity (RH)

An aspirated Rotronic MP101A humidity temperature probe was mounted on the right side of the GBRS system near its front. The bracket holding this sensor was height adjustable to maintain the air intake to the sensor 1 m above the canopy surface. This sensor was checked against an Assman psychrometer before and after each set of measurements. As shown by Figure 3.9, air temperature measured by the humidity temperature probe compared very well with dry bulb air temperature measured by the Assman psychrometer. Relative humidity (RH) measured by the probe also compared well with RH calculated from Assman psychrometer dry bulb and wet bulb air temperature (Figure 3.10).

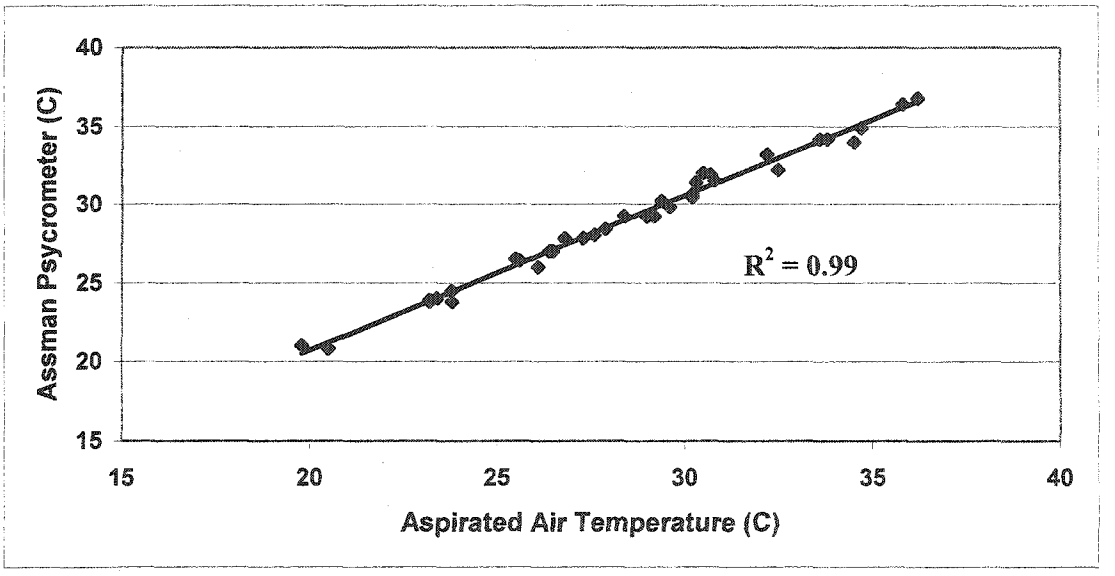

Figure 3.9. Aspirated air temperature checked against Assman psycrometer.

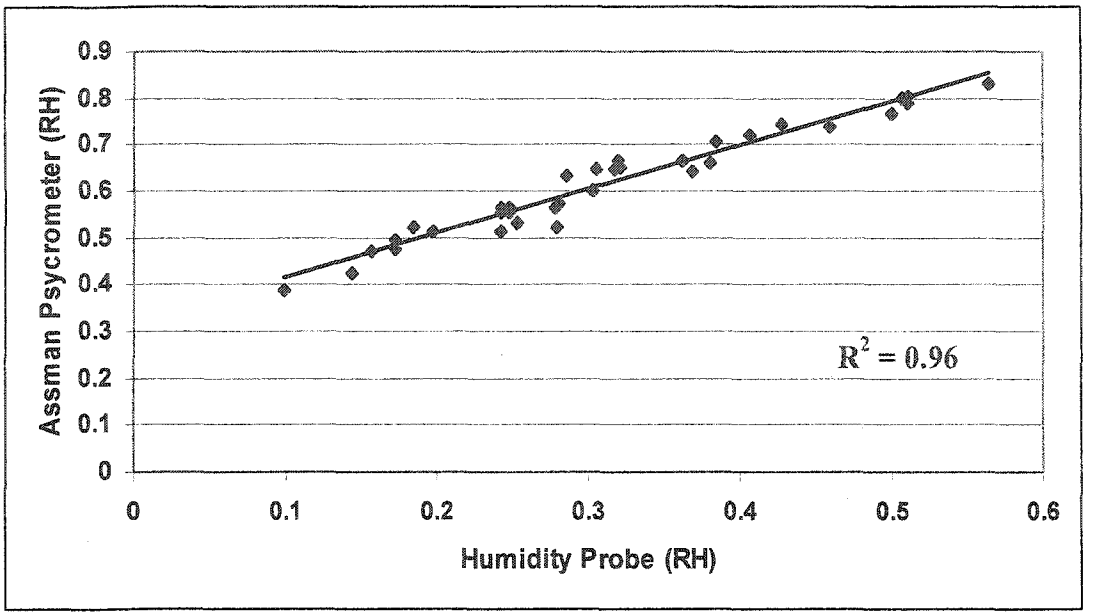

Figure 3.10. Humidity probe measurements checked against Assman psycrometer.

3.2.1.3 Canopy Reflectance Measurements

Corn canopy radiance and incoming irradiance were measured near solar noon with the GBRS system. Exotech 100 BX four band radiometers were used to measure radiant energy in the blue, green, red, and near-infrared areas of the electromagnetic spectrum (i.e., 450 to 520 nm, 520 to 600 nm, 630 to 690 nm, and 760 to 900 nm, respectively). These wavebands are similar to those in the Landsat Thematic Mapper, Ikonos, and QuickBird satellites. Canopy radiance measured from the nadir view (0°, which is perpendicular to the crop surface) was only important to this study. The nadir-view radiometer had a 15° FOV and viewed a circular spot 2.6 m in diameter whereas the up-looking radiometer had a 180° FOV to view the upper hemisphere. Each data point consisted of canopy radiance from 25 to 35 plants depending on crop height; the taller the plants grew, the smaller the viewed spot.

Bi-directional reflectance of the target was calculated for each of the four wavebands using a process described by Neale (1987) which was similar to that

presented by Duggin (1980) apart from the fact that the $BaSO_4$ reference panel was calibrated as described by Jackson et al. (1987). The computer program that calculated canopy reflectance from measured radiometer voltages also associated the GPS position with canopy reflectance data.

Canopy reflectance data were used to calculate several vegetation indices which were in turn used to estimate vegetation cover for the Water Deficit Index.

3.2.2 Crop Water Stress Index (CWSI) Determinations

Essential data were canopy temperature (T_s) from two different views (nadir "down-looking" view and 80° oblique view), air temperature (T_a) and relative humidity (RH). These data were used to calculate saturated vapor pressure (VP_{sat}), actual vapor pressure (VP), and vapor pressure deficit (VPD). VP_{sat} was calculated using the following expression presented by Bosen (1960):

$$VP_{sat} = 3.38639\,[(0.00738 * T_a + 0.8072)^8 - 0.000019\,|1.8 * T_a + 48| + 0.001316]$$

$$\text{for } -51^\circ C < T_a < 54^\circ C, \qquad (3.1)$$

where

VP_{sat} is the maximum vapor pressure for a given air temperature and pressure (the maximum water vapor the air can hold) (kPa)

T_a is air temperature (°C)

Calculated VP_{sat} and measured RH were used to calculate VP in kPa, i.e.,

$$VP = VP_{sat} * RH, \qquad (3.2)$$

Calculated VP and VP_{sat} were used to calculate the VPD in kPa, from the following equation:

$$VPD = VP_{sat} - VP\ , \qquad (3.3)$$

Calculated VPDs were used with two different views (nadir and oblique) of T_s measurements to establish the lower and upper VPD vs ($T_s - T_a$) baselines of CWSI by using measurements from the drip-irrigated plots. After CWSI was established for different percent of sandy soils, data from the low yield area were analyzed with special attention to the cornfield, as the study anticipated that plants might be water stressed in these locations because the center pivot irrigation system irrigated all locations with approximately the same amount of irrigation water. One of the objectives of the study was to develop the relationship between the calculated CWSI and measured volumetric water content (VWC) to determine the irrigation management effect on yield at the study site. Determined VPD vs ($T_s - T_a$) baselines were used to calculate CWSIs to estimate the irrigation timing at the study site. Consequently, the VPD vs ($T_s - T_a$) baselines were determined for different types of sandy soil in order to more accurately calculate the CWSI by using the following equation:

$$CWSI = \frac{(dT - dT_l)}{(dT_u - dT_l)}\ , \qquad (3.4)$$

where

dT = the current difference in canopy and air temperature °C.

dT_l = the baseline difference in canopy and air temperature of a well-watered, transpiring plant, °C.

dT_u = the baseline difference in canopy and air temperature of a fully stressed, non-transpiring plant, °C.

3.2.3 Water Deficit Index (WDI) Determination

One of the most important aspects of this study was to determine the four corners of the vegetation index/temperature (VIT) trapezoid to calculate the WDI to estimate the amount of irrigation water. $(T_s - T_a)$, and vegetation cover were the necessary parameters.

WDI was plotted using measured vegetation cover and the difference between surface and air temperatures $(T_s - T_a)$ (°C) from T_s measured by two view angles (nadir and 80° oblique view) to determine the four corners of the VIT trapezoid. After determining the VIT trapezoid, WDI was calculated for the drip irrigated plots. As mentioned before, four of the five drip-irrigated plots, which had various percentages of sand, were water stressed during different plant growth stages. Thus, four different WDIs were established for each surface temperature view angle. The other plot (plot #1) was well–irrigated. Consequently, the data from this plot was used to determine the well-irrigated line which set two of the four corners of the VIT trapezoid. The WDI was calculated using the following equation:

$$WDI = \overline{AC} / \overline{AB} \ , \qquad (3.5)$$

where

A is non-limiting condition for evaporation and transpiration (well-watered baseline on the plot)

B is the upper limit where no water was available (completely stressed crop baseline on the plot)

C is the actual measurement of plant status (see Figure 2.4).

The WDI range is similar to the CWSI, that is, from 0 (unlimited water) to 1 (no water available). Calculated WDIs were correlated with soil water deficit (SWD) determined from total available water (TAW) and volumetric water content (VWC).

3.2.3.1 Measured Vegetation Cover Determination

The fraction of soil surface obscured by the crop canopy (vegetation cover) was determined from measurements of light at the soil surface transmitted through the canopy. These measurements were made with a Decagon Sunfleck Ceptometer (model SF-80) which has a probe length of 80 cm. This light bar (LB) measures photosynthetically active radiation (PAR) in the 400 to 700 nm waveband with 80 light sensors placed at one-centimeter intervals along the probe. The Ceptometer displays an average of all the sensor readings each time the sample button is pressed. Readings below the canopy were made from the center of one plant row to the center of the neighboring plant row. At each location, ten below canopy readings were collected. Following the below canopy sampling at each location in the verification study, a measurement was obtained in full sunlight (above canopy) by holding the sensor level in the same orientation as it was for the under canopy measurement (Neale, 1987). The fraction (f) of soil surface covered by vegetation was then calculated as

$$f = \frac{Va - Vb}{Va}, \qquad (3.6)$$

where

Va = above canopy reading

Vb = below canopy reading.

The PAR (quantuum) sensor on the GBRS system was used for incoming photosynthetic active radiation. This required that the light bar (Sunfleck) and LiCor PAR sensor be intercalibrated which produced the following relationship:

$$\text{Sunfleck (umoles/m}^2\text{)} = 207.848 * \text{Quantum (mv)} - 329.3 \quad (3.7)$$

3.2.3.2 Estimated Vegetation Cover Determination

The fraction (f) method (measured vegetation cover) was found to be the best representative data for vegetation cover. However, it is difficult for irrigators to use the light bar (LB) during the entire growing season. LB also has some limitations, such as the time required to go from one location to other in order to complete the data set and damage to plants. There are techniques (vegetation indices) for estimating the vegetation cover by using reflectance measurements from remotely sensed measurements. Some major known vegetation indices were calculated by using the following equations:

$$NDVI = (\lambda_{NIR} - \lambda_R) / (\lambda_{NIR} + \lambda_R), \quad (3.8)$$

$$SAVI = [(\lambda_{NIR} - \lambda_R) / ((\lambda_{NIR} + \lambda_R) + L)] * (1 + L), \quad (3.9)$$

$$MSAVI = [2 * \lambda_{NIR} + 1 - SQRT ((2 * \lambda_{NIR} + 1)^2) - 8 * (\lambda_{NIR} - \lambda_R)] / 2, \quad (3.10)$$

$$VARI_{green} = (\lambda_G - \lambda_R) / (\lambda_G + \lambda_R - \lambda_B), \quad (3.11)$$

$$VI_{green} = (\lambda_G - \lambda_R) / (\lambda_G + \lambda_R), \quad (3.12)$$

where

I_{NDV}: Normalized difference vegetation index

I_{SAV}: Soil adjusted vegetation index

I_{MSAV}: Modified soil adjusted vegetation index

$VARI_{green}$: Visible atmospherically resistant index

VI_{green}: Vegetation index

λ_{NIR}: Near infrared spectral band

λ_R: Red spectral band

L: Correction for the plant factor; usually 0.5

λ_G: Green spectral band

λ_B: Blue spectral band.

Each of the above vegetation indices was evaluated to determine which had a better relationship with the fraction calculation (measured vegetation cover). Estimated vegetation cover has some advantages when compared to measured vegetation cover. One of the advantages could be obtaining vegetation cover faster for large fields that remotely sensed data were collected.

As mentioned above, measuring vegetation cover is labor intensive and irrigators may prefer to estimate vegetation cover. The high clearance tractor was used to measure canopy reflectance to calculate the vegetation indices. These indices were plotted against $(T_s - T_a)$ to determine the corners of the VIT trapezoid, which in turn established the WDI.

3.2.3.3 Determination of Soil Water Deficit (SWD)

There are many techniques to estimate the soil water deficit. Two frequently used techniques are estimating evapotranspiration (ET) and measuring VWC. All techniques require sampling and some plant damage occurs while taking soil and plant measurements. However, SWD must be known or estimated to determine appropriate irrigation depths. Remote sensing presents many advantages to data collection as mentioned previously. Thus, WDI may be a useful method to estimate the SWD to improve scientific irrigation management for agricultural areas.

Soil moisture determination is very important for estimating SWD. Field capacity (FC) and wilting point (WP) were measured to determine the total available water (TAW) by taking soil samples from the study site. Measured VWC and TAW were used to estimate the SWD for corn grown in sandy soil.

SWD was calculated for the 1.2 m soil profile by subtracting the measured VWC from the TAW. VWC was calculated by multiplying bulk density by gravimetric water content (GWC) measurements made at every 30 cm of soil depth. TAW was calculated as the difference between FC and WP for each 30 cm increment of the 1.2 m soil profile.

3.2.3.3.1 Soil Moisture Determination

Soil moisture is one of the most important factors affecting plant growth in irrigated agriculture. Soil moisture measurements are necessary data for assessing the effect of irrigation management techniques on agricultural output.

A center pivot irrigation system provided an assumed uniform amount of water across the commercial cornfield. Different sandy soil types at the 15 measurement locations should hold varying amounts of water according to their water-holding capacity. This might be one of the most important reasons for different yield values at different locations. Without proper irrigation management, various yield levels may occur in different soil textures.

The model 6050X1 Trase System uses TDR to instantaneously measure the dielectric constant (Ka) to determine the volumetric water content (VWC) of soils. Metal wave-guides for depth measurements ranging from 15 cm to 70 cm are available.

Soil moisture was measured in 30 cm and 70 cm soil profiles both before and after irrigations during the course of this experiment. Soil samples from the 0-30, 30-60, 60-90, 90-120, 120-150 cm depth were also taken gravimetrically.

During the middle of the growing season, farmers traditionally run the center pivot continuously; thus, it was very difficult to follow the farmer's schedule. Consequently, measurements were restricted to twice per week, sometimes once per week.

Measured Ka from TDR was used to determine the VWC. Techniques to convert Ka to VWC include the TDR manual's curve for soil texture (Figure 3.11), the Topp et al. (1980) equation, and TDR measurement calibration using the gravemetric soil sample method. As shown in Table 3.1, calibration was necessary to determine the VWC at the study site. The Topp et al. (1980) equation is the most used equation to determine the VWC from Ka:

$$VWC = -5.3 * 10^{-2} + 2.9 * 10^{-2} Ka - 5.5 * 10^{-4} Ka^2 + 4.3 * 10^{-6} Ka^3 , \qquad (3.13)$$

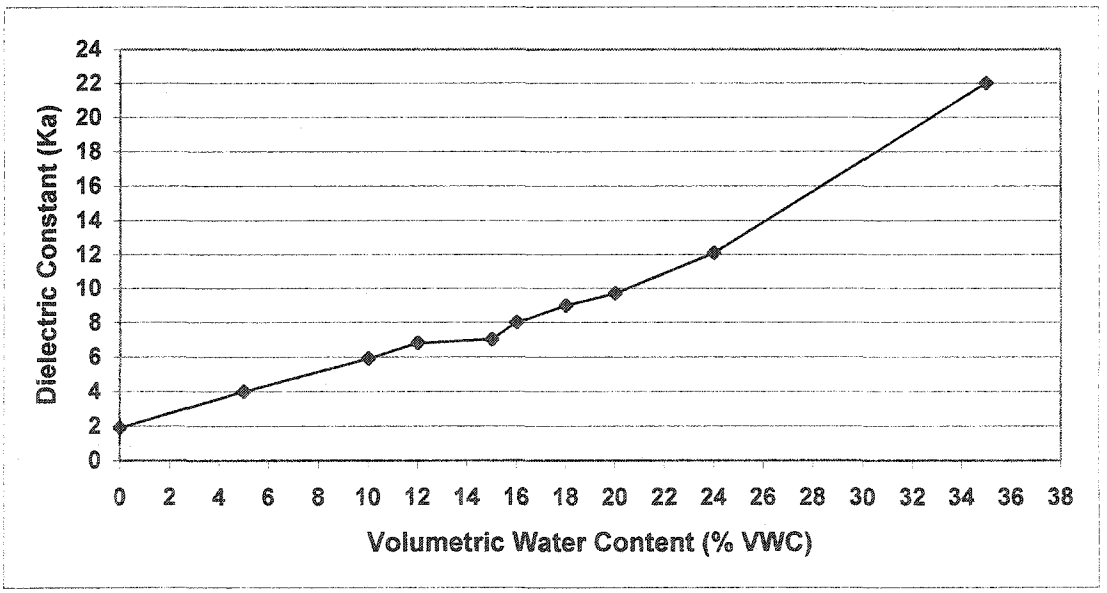

Figure 3.11. Relationship of dielectric constant, Ka, to VWC of sandy loam soil.

Table 3.1. Determination techniques for VWC by applying TDR measurements.

Measured Ka Using TDR	TDR Readings VWC (%)	TDR Manual VWC (%)	Topp et al (1980) equ. VWC (%)	Calibration Method VWC (%)	TDR Probes Length (cm)
5.9	10	11.25	9.78	6.7	70
6.8	12.5	13.33	11.81	7.91	70
9.1	18.7	18.64	16.66	12.43	70
13.5	26.7	28.81	24.68	17.62	70
5.4	8.6	10.1	8.62	3.52	30
7.1	13.3	14.02	12.47	10.01	30
8.9	18.3	18.18	16.26	10.9	30
11	22.6	23.03	20.32	14.22	30

TDR calibration data were completed for the 30 cm and 70 cm coated probes. As shown in Fig. 3.12, a 2 m x 2 m area was selected adjacent to the field, and TDR probes were installed in this area. Three different variations in sandy soils based on the texture analysis were selected very close to the field for TDR calibration.

Figure 3.12. One of three TDR calibration locations.

A pond was constructed on the soil surface. After heavy irrigation, the area was allowed to dry in order to obtain TDR readings during the natural drying cycle. TDR readings and three soil samples for gravimetric soil water content were collected. Soil samples were always taken at different locations; these locations were marked by yellow flags to keep from resampling in the same spot. TDR readings and soil samples were taken from a high to a low VWC value. By collecting TDR calibration data, a calibration curve and formula was produced to convert TDR Ka values to VWC during the growing season. The resulting equations were:

For 30 cm TDR probes: $VWC = 0.0263 * Ka - 0.048$ (3.14)

For 70 cm TDR probes: $VWC = 0.0219 * Ka - 0.0409$ (3.15)

Since TDR is limited to a measurement depth of 70 cm, the gravemetric soil sampling method was used to determine the soil VWC from 70 cm to 150 cm. After finding the soil VWC values at each location, these values were used to determine the calculated CWSI in order to compare the degree of stress with the soil VWC value at the same time and same location for irrigation timing. The same soil VWC values were also used to determine the calculated WDI in order to compare water deficit with soil VWC.

3.2.3.3.2 Soil Sampling

Soil sampling was conducted to determine field capacity (FC) and wilting point (WP), soil moisture, soil texture, and soil bulk density. Samples were collected at 20 sites and 3 TDR calibration sites.

Soil samples were collected near the TDR probes in the drip irrigated plots and from the 15 locations in the field. As shown in Figure 3.13, soil samples were collected by a hydraulic sampler mounted on the back of another high clearance tractor. When

TDR readings were collected, the soil samples were collected and placed in soil cans, which were taped shut to keep them avoid water loss, and then weighed. Subsequently, soil samples were dried in the oven at 105° C for one day. They were then taken to the laboratory and weighed again in order to calculate the water content in the soil profile. All soil samples were converted to percent VWC after the bulk density was measured.

To determine soil texture, some soil samples from each location were removed, mixed and analyzed in the laboratory to determine sand, silt and clay percentile.

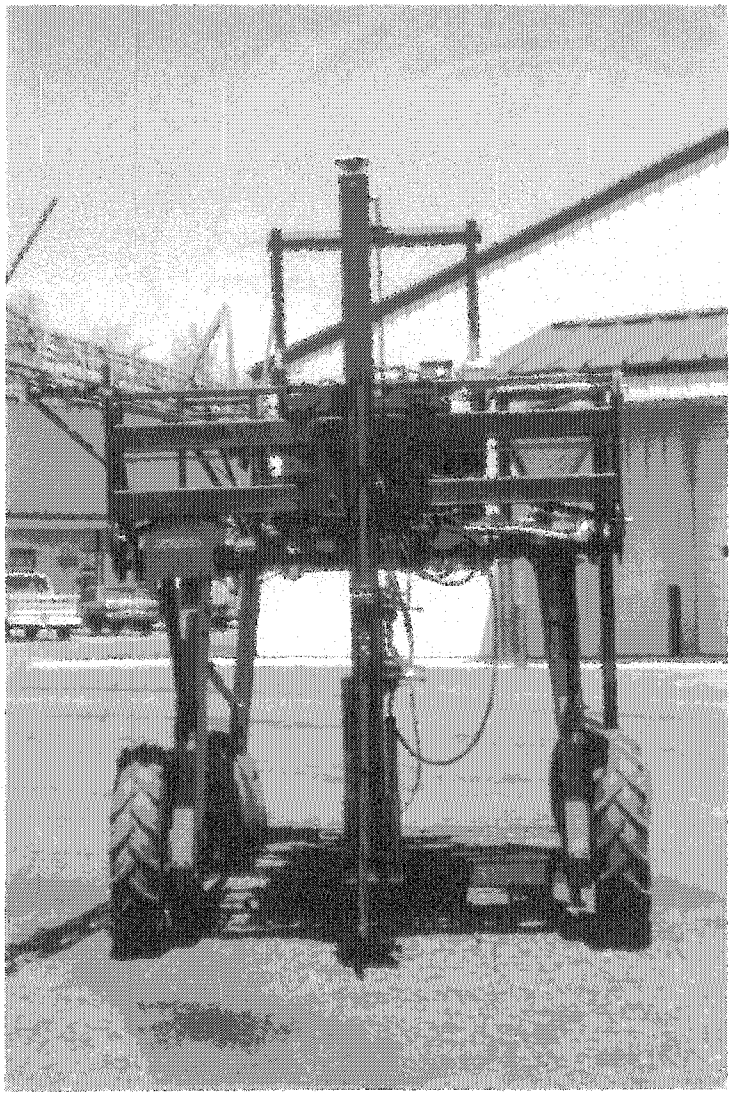

Figure 3.13. Soil sampler attached to the back of the high clearance tractor.

3.2.4 Location Data Collection

Location data were collected using a Racal Landstar MkIV with Ashtech G12 Lite GPS card. Because all data measurements were based on the TDR probe locations, these locations were determined immediately after they were installed. Soil samples were removed from within a 2 m distance from the TDR probes, and plot corners were located using GPS. Data were collected using static mode GPS with at least 5 minutes collection time. All the GPS positional data were based on the World Geodetic System of 1984 (WGS84).

3.2.5 Grain Yield

Corn yields were calculated by hand-harvesting one row on each side of the TDR probes from the 15 selected locations in the commercial cornfield and the drip irrigated plots. The harvested row was 3 m long and centered on the TDR probe location. The corn yields were adjusted to moisture content of 15.5%, wet basis. Hand-harvested yield data was used to determine the yield differences at the study sites (TDR locations).

3.2.6 Statistical Analysis on Experimental Data

Kendall's independence test based on signs was found to be appropriate for the data set, because this test is a nonparametric test, valid under the assumption of the n bivariate observations $(X_1, Y_1),\ldots,$ where (X_n, Y_n) are a random sample from a continuous bivariate population. The (X, Y) pairs are mutually independent and identically distributed consistent with some continuous bivariate population (Hollander and Wolfe, 1999).

As mentioned above, Kendall's independence test is a nonparametric test which has many advantages and was selected as the statistical test in this study. Some of these advantages are proposed by Hollander and Wolfe (1999) as following;

1. The nonparametric procedure requires few assumptions concerning the underlying populations from which the data are obtained. Principally, the nonparametric procedures skips the traditional assumption that the underlying populations are normal.
2. The nonparametric procedure is usually easy to understand.
3. The nonparametric procedure is mostly easier to apply than their normal theory counterparts.
4. The nonparametric procedure is applicable in numerous situations where normal theory procedure cannot be utilized.
5. The nonparametric method is comparatively insensitive to outlying observations.

In this study, the dependence among specific variables was tested using Kendall's independence test and regression analysis as well. The null hypothesis of interest was that the paired variables were independent and the alternative hypothesis was that there is a dependency among the variables that was of particular interest.

Using Kendall's independence test, the Kendall statistic (K) was calculated and these values were used in one-sided upper tail and one-sided lower tail tests. At the alpha level of significance, if the actual K value was greater than or equal to K_{alpha}, the null hypothesis was rejected (no correlation); otherwise it was not rejected. If the K value was positive and larger or equal, the K_{alpha}, X and Y were positively correlated, while if

the K value was negative and the actual K was larger or equal, the K_{alpha}, X and Y were negatively correlated.

CHAPTER 4

RESULTS AND DISCUSSION

4.1 CWSI Analysis

Each drip-irrigated plot was exposed to plant water stress at various growth stages, and each also had a different percentage of sand. Hence, the CWSI was established for each plot to determine the differences. CWSI was established by using drip-irrigated plot data to carry out all the calculations at twenty sites. CWSI was calculated using Equation 3.4, by using two angle views (nadir and oblique (80°)) of plant temperatures (T_s). Nadir (down-looking) and 80° views were used to represent T_s to determine the VPD baselines on CWSI. Figures 4.1 and 4.2 show the baselines of VPD for nadir view of T_s measurements.

As mentioned in Chapter 2, reported ($T_s - T_a$) of maximum stress commonly occurred in a range of 4 to 6° C. As shown in Figure 4.1, the upper VPD baseline occurred at approximately 8° C ($T_s - T_a$), which was quite high. Measured ($T_s - T_a$) data ranged from -0.5 to 19.5° C using nadir view-acquired T_s. However, measurements used to establish VPD baselines ranged from -0.5 to 13.0° C, as shown in Figure 4.1. Only four values of ($T_s - T_a$) measured under 0° C ($T_s < T_a$), even though the values ($T_s - T_a$) of the non-stress baseline showed that canopy temperatures were warmer than air temperature, which was impossible, because these results showed some degree of stress. If this approach was accepted, then the lower baseline of VPD determined the irrigation

timing for the entire growing season since T_s was higher than T_a. Basically, the CWSI established by using nadir view of T_s in Figures 4.1 and 4.2 showed some degree of stress even at non-stress baselines.

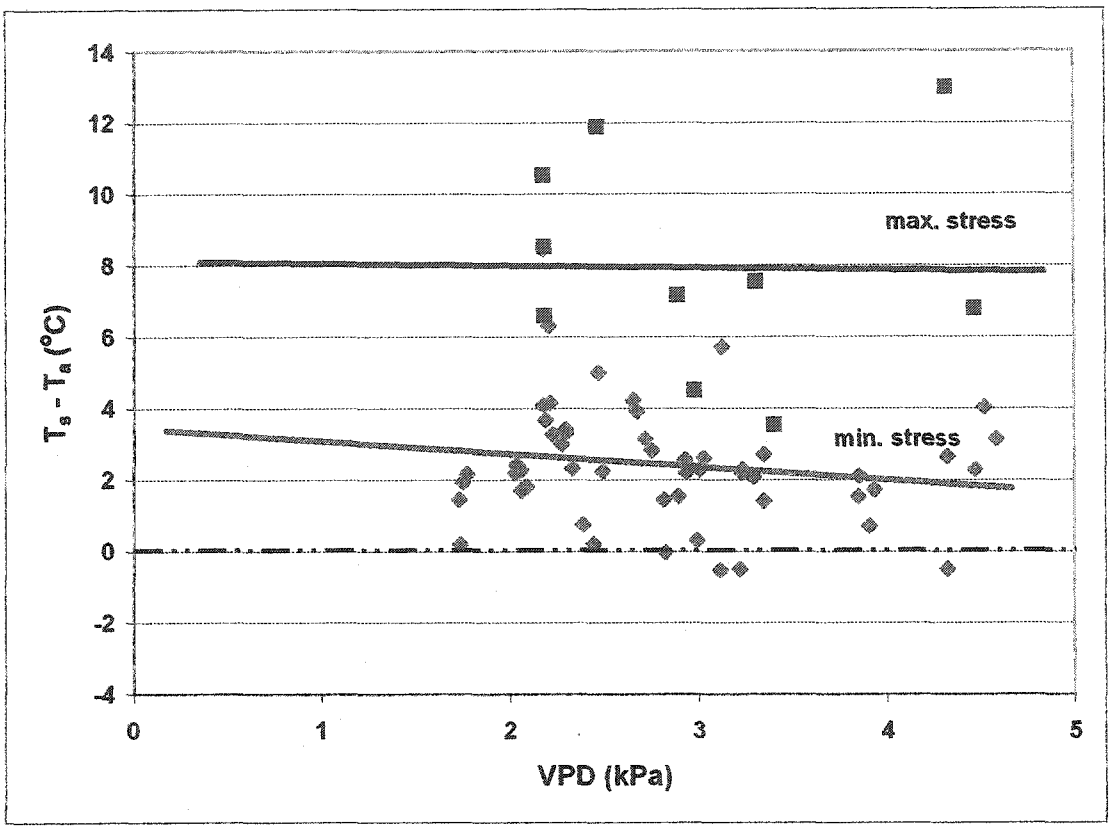

Fi

Figure 4.1. Established CWSI after determined VPD baselines by using nadir view of T_s measurements from drip-irrigated plots.

The lower baseline of the VPD increased due to the stresses introduced at different growth stages. At the non-stress condition (plot #1), it started from the $T_s - T_a$ value of 2, and the stress introduced increased it above 2. As seen in Figure 4.2, it went even higher with the stress introduced in the other plots between the V12 and V14 growth stages. The stress between V15 and VT (Figure 4.2d) resulted in a situation similar to that seen in the non-stress condition, except that the line was shifted up by about 2° C. These results indicate that irrigation timings would be different if the crop were introduced to a stress at any growth stage.

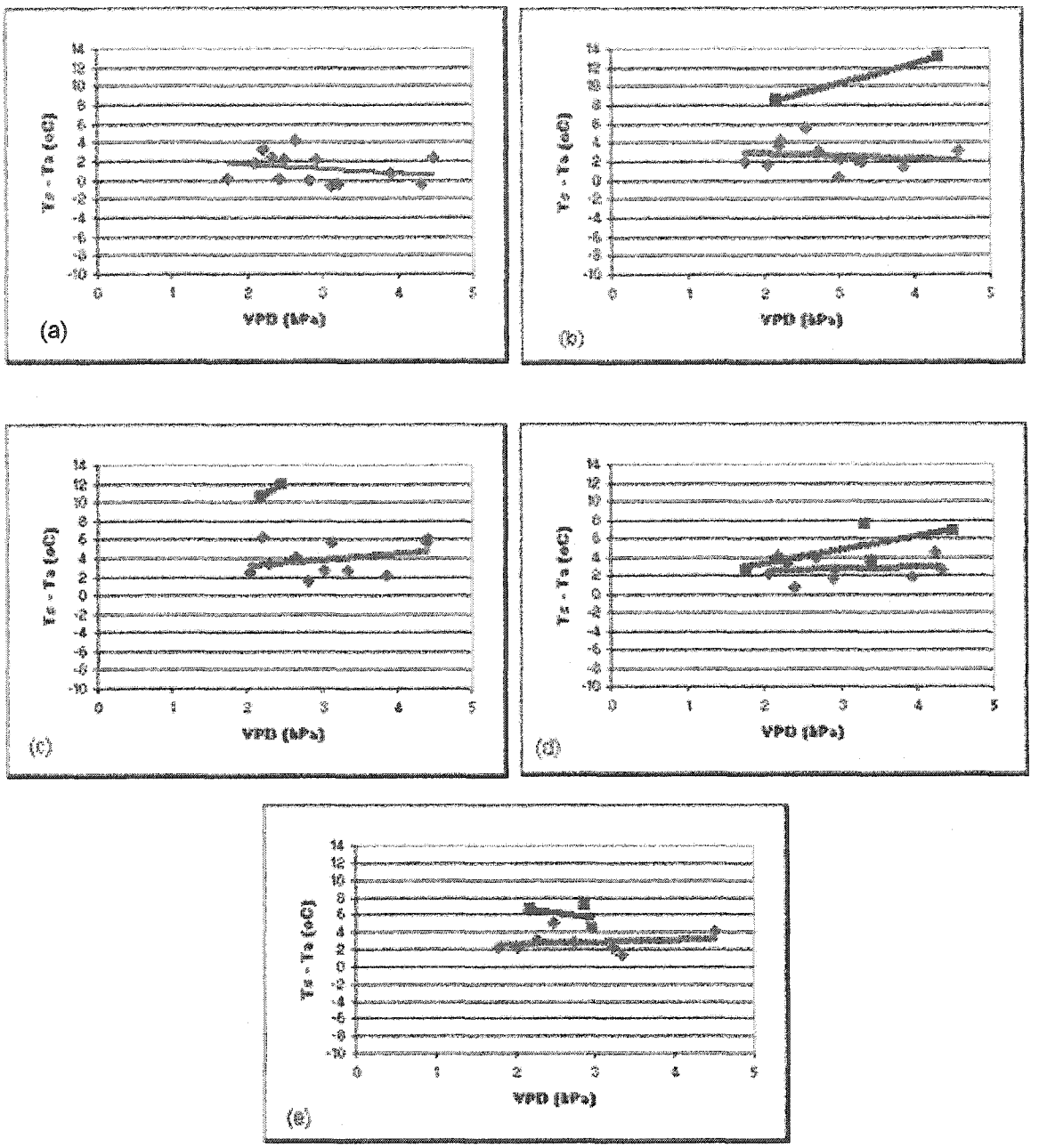

Figure 4.2. Established CWSI based on the irrigation treatments by using nadir (down-looking) view of T_s measurements (a) non stress (b) water stress between V8-V10 (c) water stress between V12-V14 (d) water stress between V15-VT (e) water stress between R2-R3. Pink lines represent the VPD upper baselines (max. stress), blue lines represent the VPD lower baselines (min. stress).

Canopy temperature and even leaf temperature were closely linked to the soil thermal environment when the plants were small. However, $(T_s - T_a)$ differed from the unstressed baseline measured in partial canopy cover. In the early growing season when plants are small, or for low plant populations, a part of the soil surface may be viewed by the IR sensor when surface temperature measurements are made.

Despite these findings, it is often reported that early season CWSI values are particularly difficult to obtain because of partial canopy cover (Howell et al., 1984b; Wanjura et al., 1984; Hatfield et al., 1985; Reginato and Howe, 1985; Irmak et al., 2000). The unstressed baselines of CWSI for cotton under full and partial ground cover were determined by Hatfield et al. (1985), who reported that unstressed baselines for full cover had slopes of about twice those under partial canopy cover due to the effect of nadir view measurements, which "see" soil background and result in higher T_s measurements. This study had the same limitation—namely, that T_s measurements were not able to represent canopy temperature in periods of partial vegetation cover. Hence, some of the data were not used to establish CWSI, since they were obtained before the V7 vegetative growth stage. Consequently, it was suggested to use oblique view readings in place of the nadir view IR sensor's readings to determine plant surface temperature from the GBRS system to represent more accurate measurements of T_s. This approach could be supported by Figures 4.3 and 4.4, where both view angles "see" almost the same amount of soil background prior to the V7 growth stage.

Figure 4.5 shows the V8 vegetation stage; one can observe that the soil background is less than that visible at the V6 growth stage. Also, almost no soil background is visible in the oblique view. A considerable amount of soil background

was visible before the V7 stage, which created high ($T_s - T_a$) because T_s did not represent the corn leaves very well, even with the 80° oblique view of the IR sensor measurements. Therefore, at V8 growth stage and there after an 80° oblique view of T_s measurements was used.

As mentioned in Chapter 3, the T_s of CWSI must represent canopy temperature only; therefore, the oblique view (80°) can be safely recommended over the nadir view in this study. Otherwise, T_s measurements were not reliable for creating the VPD baselines of CWSI. As seen in Figures 4.1 and 4.2, when T_s measurements were taken by using nadir (down-looking) view, ($T_s - T_a$) values were quite high because of the soil background effect on T_s. Even in well-watered conditions, it was found that positive values ($T_s > T_a$) mostly represented ($T_s - T_a$) instead of the more negative values ($T_s < T_a$) found at the study site. Our findings are in agreement with those of Jackson et al. (1981) regarding the fact that the soil background must not appear in the field of view of the infrared thermometer.

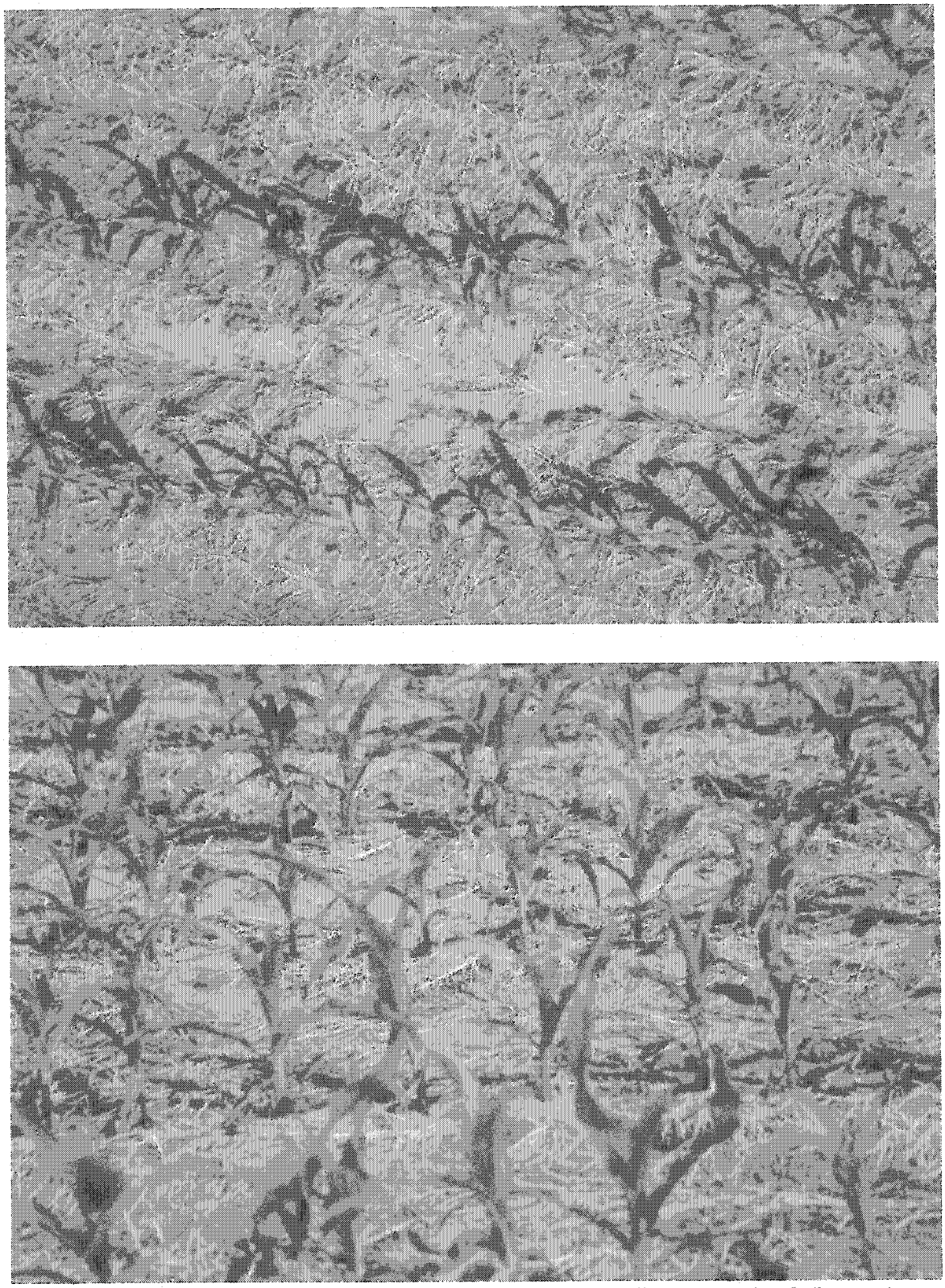

Figure 4.3. Photographs showing the difference between nadir (top) and 75° (bottom) views at the V5 growth stage.

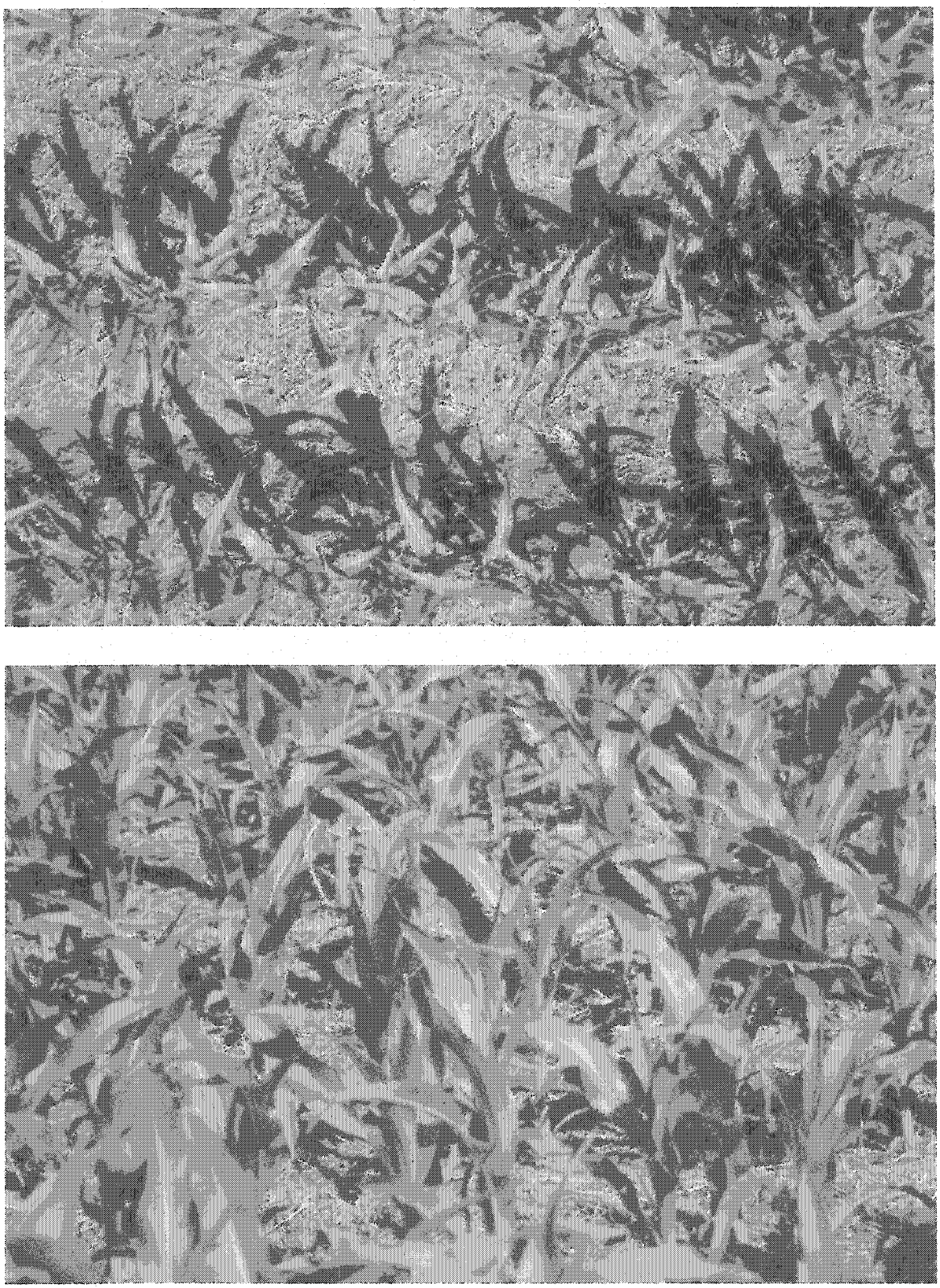

Figure 4.4. Photographs showing the difference between nadir (top) and 75° (bottom) views at the V6 growth stage.

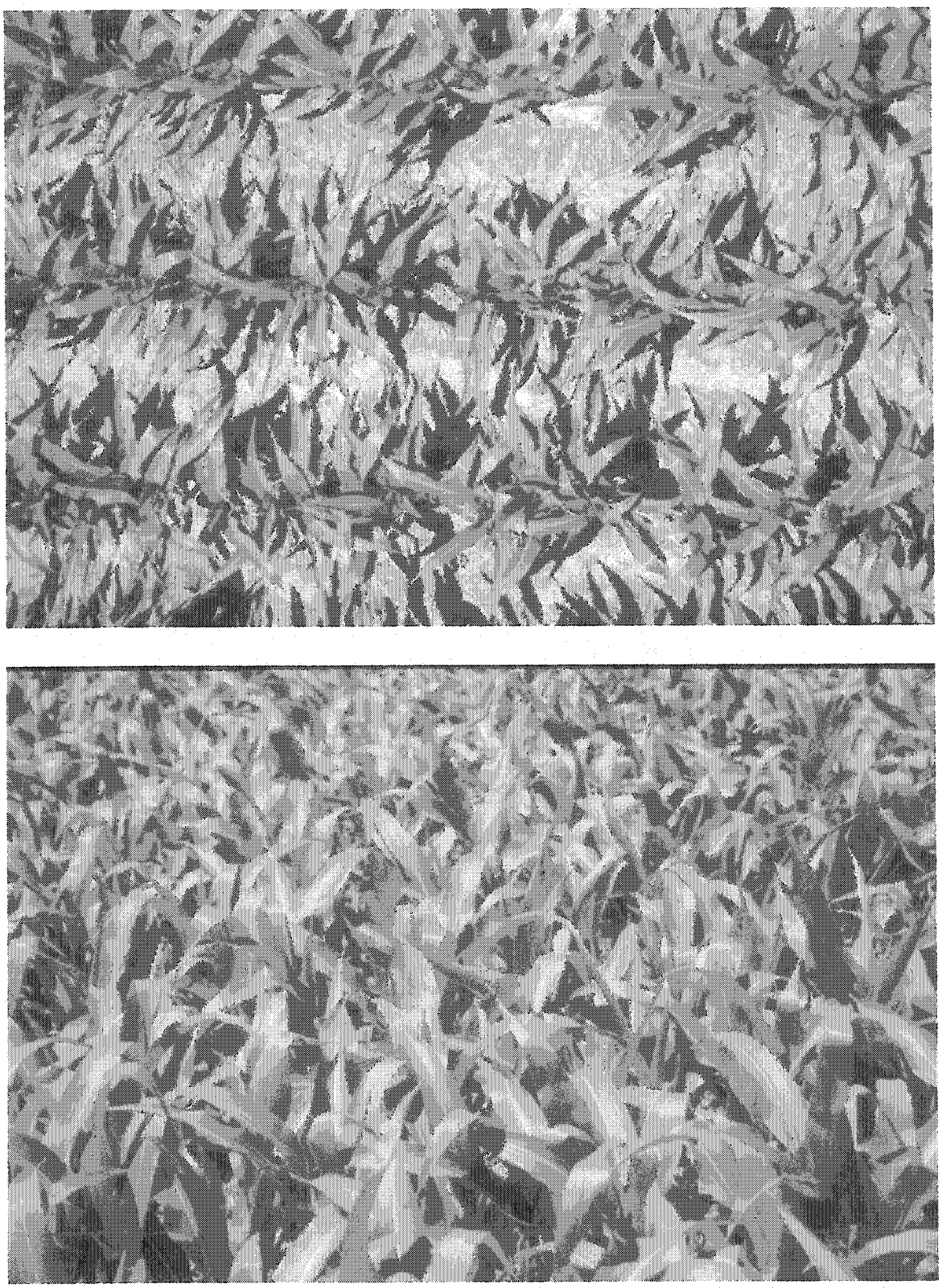

Figure 4.5. Photographs showing the difference between nadir (top) and 75° (bottom) views at the V8 growth stage.

Most CWSIs calculated using the 80° view of plant temperatures (T_s) were 0 (no degree of stress) at the field sites, but variable results were found by calculating CWSIs on drip-irrigated plots due to imposed water stress (Tables A.1 and A.2). CWSI results were between 0 to 1 for the study site, indicating that there was some degree of stress in the early growing season (V8) (Table A.1), which might have affected the yield. At the same time, the rest of the growing season was mostly stress-free at the cornfield sites (Tables A.1 and A.2). Therefore, since CWSI values did not reveal any degree of crop water stress, corn was not under-irrigated during most of the growth stages in the cornfield site. The bold numbers in Tables A.1 and A.2 represent plant stress periods for drip-irrigated plots. The upper and lower baselines of CWSI in Figure 4.6 were established by using all the data of drip-irrigated plots from Tables A.1 and A.2.

As shown in Tables A.1 and A.2, CWSIs were calculated from 0 to 0.44 in the cornfield site. These results were found to be the effect of the oblique views of T_s, which were measured and revealed clearly different measurements than those of the nadir view of T_s measurements. Figure 4.7 shows the results of individual measurements at the drip-irrigated plots. As shown in Figure 4.6, the maximum stress (upper VPD) baseline was approximately 2° C, with actual data ranging from -1.6 to 8.9° C. The no-stress (lower VPD) baseline in Figure 4.6 was established using all ($T_s - T_a$) values from drip-irrigated plots; measured ($T_s - T_a$) values ranged from 3.7 to -7.3° C. Only four of these ($T_s - T_a$) values were found to exceed 0° C ($T_s > T_a$), while the remainder of the ($T_s - T_a$) values measured below 0° C ($T_s < T_a$).

Comparing the graphs in Figures 4.1 and 4.6, it can be seen that the oblique view maximum stress baseline went down by about 6° C. Similarly, the no-stress baseline

went down by about 4° C. It can be concluded from these results that if a nadir view T_s is used in CWSI calculations for determining irrigation timing, irrigation applications would be more frequent than if an oblique view T_s is used. This might result in over-irrigation and water wastage and, in turn, result in groundwater pollution.

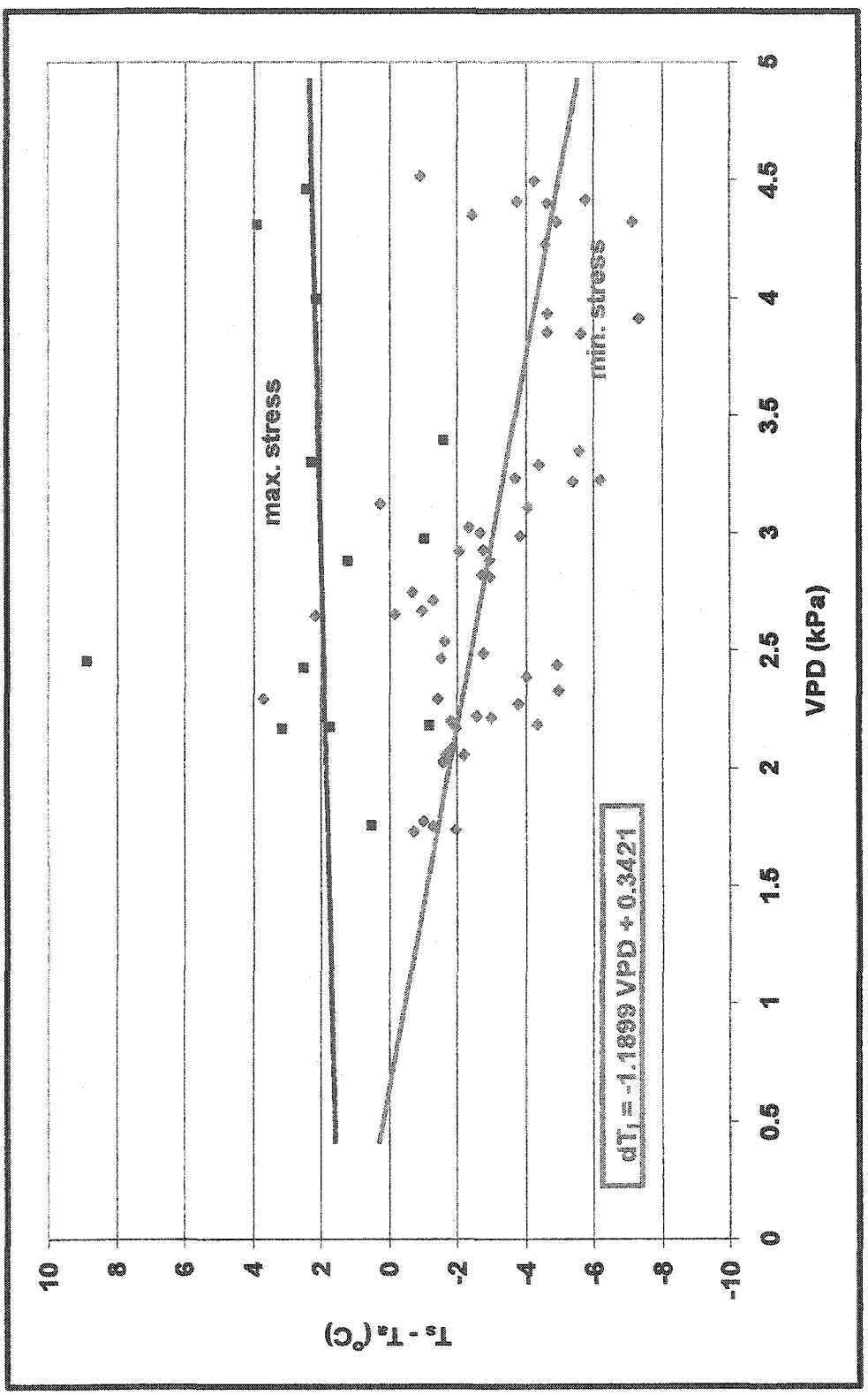

Figure 4.6. Established CWSI after determined VPD baselines by using oblique view of Ts measurements from drip-irrigated plots.

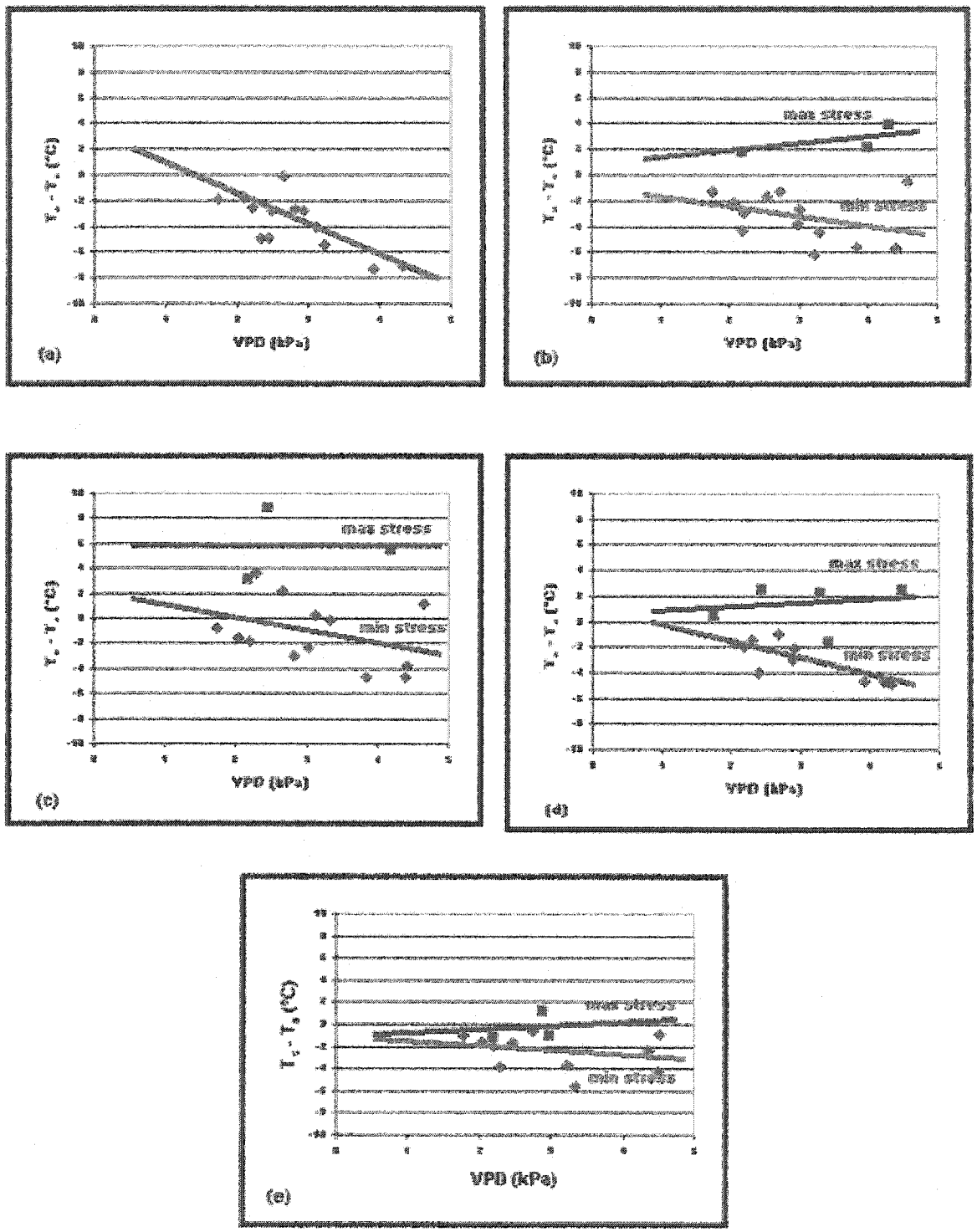

Figure 4.7. Established CWSI based on the irrigation treatments by using oblique (80°) view of T_s measurements (a) no stress (b) water stress between V8-V10 (c) water stress between V12-V14 (d) water stress between V15-VT (e) water stress between R2-R3.

CWSI determines the timing of irrigations. Methods of estimating irrigation timing were mentioned in earlier research using different techniques. Braunworth and Mack (1989) analyzed five irrigation levels ranging from 0% to 100%, in which the 100% level was intended to refill the root zone to field capacity at each irrigation after depletion of 50% of the available water. Wanjura et al. (1992) noted that irrigation was applied only when average canopy temperatures exceeded pre-determined threshold values. Alves and Pereira (2000) proposed the non-water-stressed baseline as a useful concept that could effectively guide the irrigator in obtaining maximum yields when ($T_s - T_a$) measurements were located between the lower and upper VPD baselines of CWSI, which is the recommended irrigation time in this study.

By timing irrigations based on a given threshold value determined by VPD baselines, CWSI can reduce water use without significantly compromising the final yield (Wanjura et al., 1990; Shae et al., 1999). While water is one of the most important issues for agriculture, the use of CWSI offers a significant opportunity to conserve water. More importantly, CWSI is a highly useful tool for large agricultural areas because CWSI can be calculated by using remotely-sensed data. However, CWSI and other canopy temperature-based indices indicate the timing but not the amount of irrigation (Colaizzi et al., 2003b), which in this study was determined in addition to the timing of irrigation by using WDI results.

4.2 WDI Analysis

The WDI was developed from the drip-irrigated plots and field sampling locations. These six different plots were used to determine WDI for different purposes. Irrigation was applied to plot #1 over evapotiranspiration (ET) to determine the best-

watered corner of the VIT trapezoid. Plots #2, #3, #4 and #5 were left to experience stress at different times, V15 to VT/R1, V12 to V14, V8 to V10, and R2 to R3, respectively. Plot #6 was used to represent bare soil, and data were taken from it during wet and dry conditions. As shown in Figure 4.8, the four corners of VIT were determined individually by nadir (down-looking) views of T_s measurements for each plot, while all measurements were used to calculate WDI for all the study sites.

The two corners of VIT trapezoid which determined the beginning (wet bare soil) and ending (well-watered full vegetation cover) of the well-watered baseline were represented with positive (T_s - T_a) measurements by using the nadir (down-looking) view of T_s. WDI studies by Moran et al. (1994) and Colaizzi et al. (2000) showed the well-watered baseline to be represented with $(T_s - T_a) < 0$. However, Figure 4.8 shows that in this study the well-watered baseline is determined by positive temperature differences. Due to soil temperature influences, the nadir view measurements of T_s created high values of $(T_s - T_a)$. Subsequently oblique view measurements of T_s were investigated to establish the four corners of VIT trapezoid.

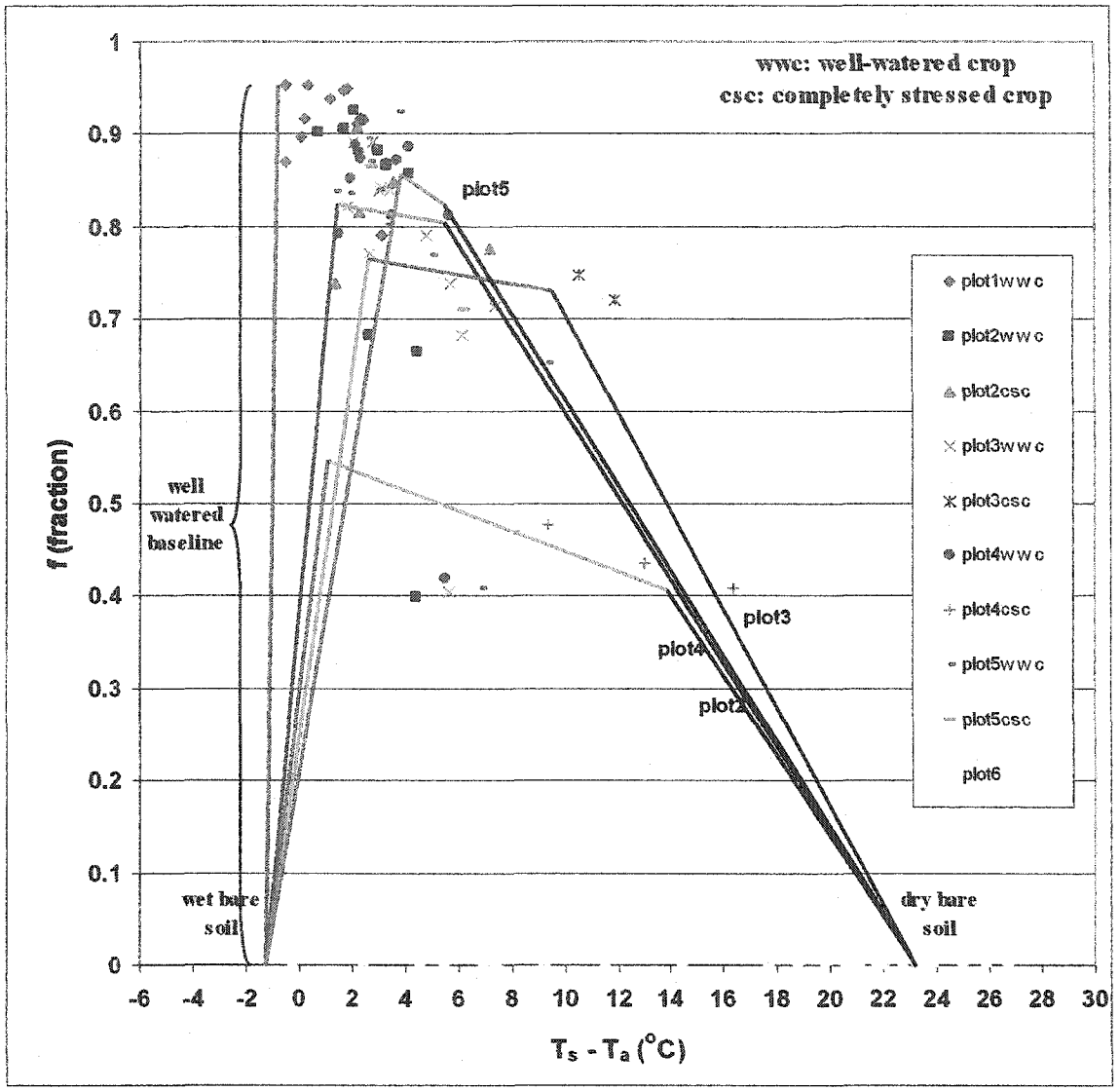

Figure 4.8. Graphic representation of WDI after establishing the four corners of the VIT trapezoid by using nadir view of T_s from drip irrigated plots.

($T_s - T_a$) versus fraction cover was plotted for each drip-irrigated plot, as shown in Figure 4.9, and for all data (Figure 4.10), based on the oblique (80°) view of T_s measurements. Tables A.3 and A.4 show calculated values of WDI using Equation 3.5 from Chapter 3. As shown in Figure 4.9, there was no stress on plot #1; consequently, WDI was represented by only two corners of the well-watered baselines of the VIT trapezoid. However, in the other drip-irrigated plots, four corners of VIT trapezoid were established.

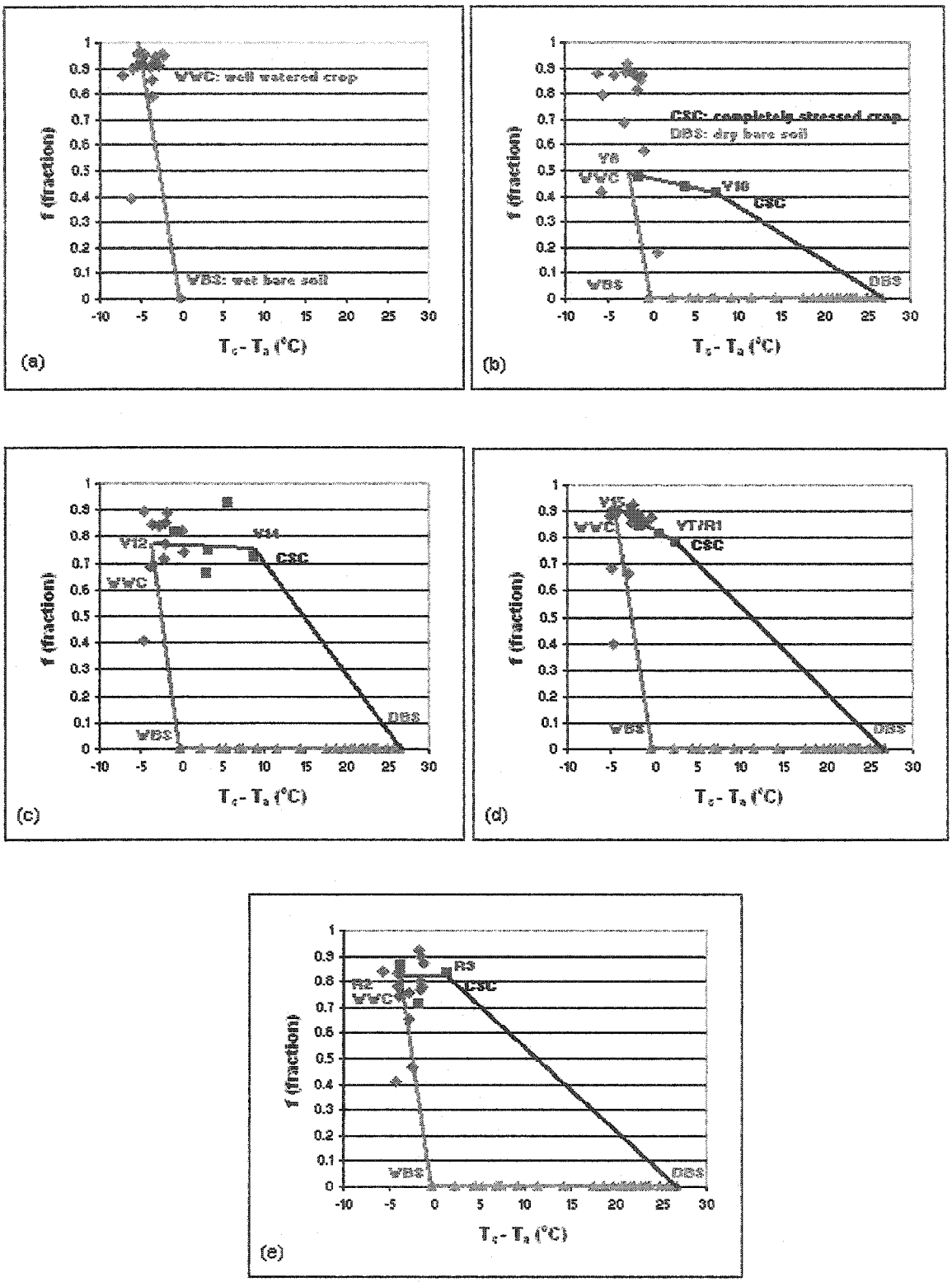

Figure 4.9. Established WDI based on the irrigation treatments by using oblique (80°) view of Ts measurements (a) none stress (b) water stress between V15-VT (c) water stress between V12-V14 (d) water stress between V8-V10 (e) water stress between R2-R3.

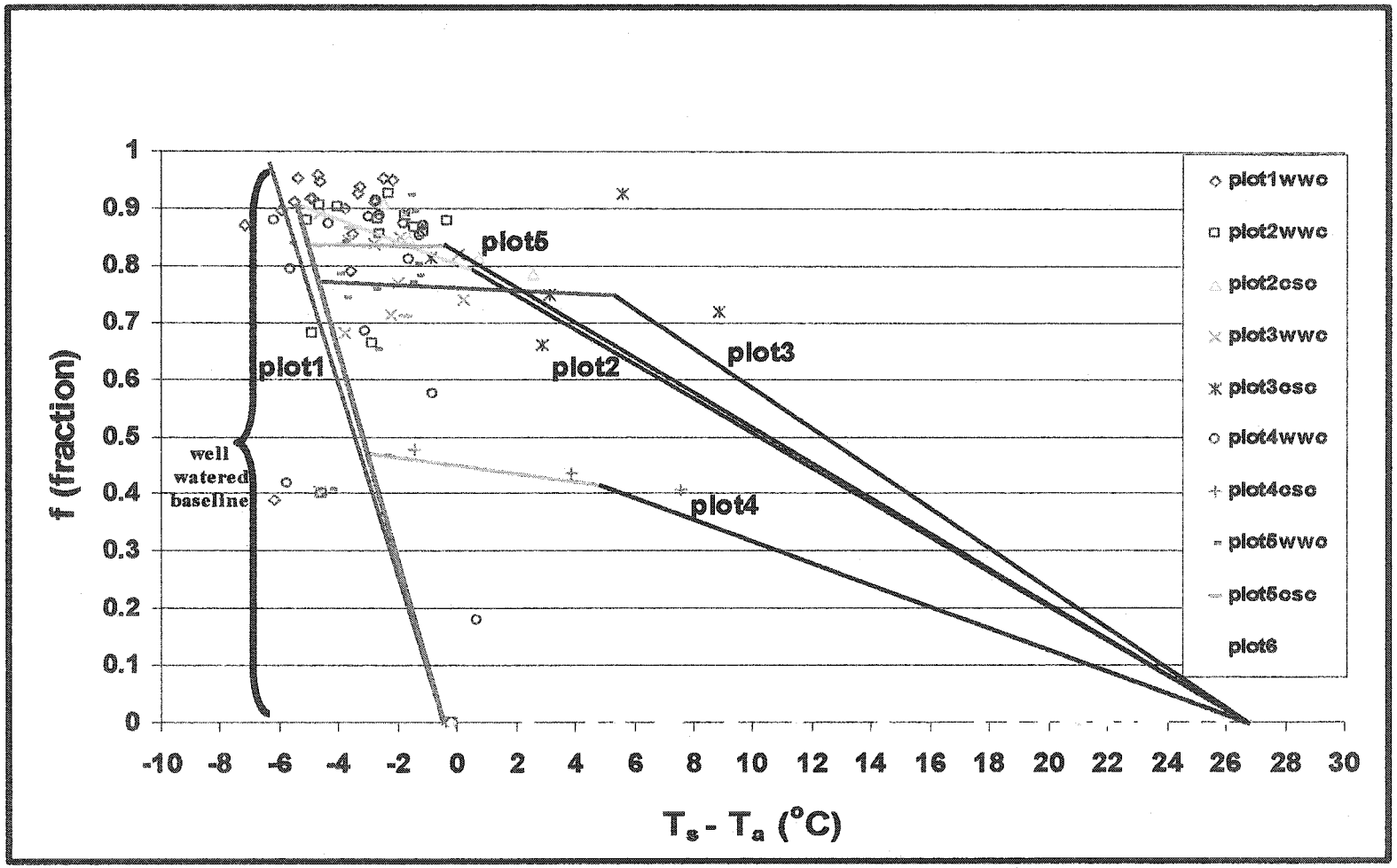

Figure 4.10. WDI after establishing the four corners of VIT trapezoid using the oblique (80°) view of T_s measurements from drip-irrigated plots.

Comparing nadir view results in Figure 4.8 with oblique view results given in Figure 4.10, it can be seen that the completely stressed points of graphs from the nadir view T_s had shifted on the X-axis by about 8° C ($T_s - T_a$). This may be very significant when the nadir view is used for determining the VIT trapezoid because it may lead to stress conditions. For example, the oblique view results indicate that stress starts at 8° C ($T_s - T_a$), while the nadir view, on the other hand, indicates that it starts at about 14° C ($T_s - T_a$). Thus, the oblique view is more conservative in determining the stress timing.

4.2.1 Relationship Between Measured and Estimated Vegetation Cover

In most previous studies (Moran et al., 1994 and Colaizzi et al., 2000), estimated vegetation cover (vegetation indices) was used to calculate WDI. Measured vegetation cover (fraction) requires more fieldwork to determine vegetation cover compared to estimated vegetation cover. For large agricultural areas, determining the vegetation cover using the measurement technique is almost impossible. However, it is easy to determine vegetation indices by using remotely-sensed data. Both techniques were used in this study.

Figure 4.11 shows the differences between the two techniques. Five different vegetation indices were investigated, namely: normalized difference vegetation index (NDVI), soil adjusted vegetation index (SAVI), modified soil adjusted vegetation index (MSAVI), visible atmospherically resistant indices ($VARI_{green}$), and vegetation index (VI_{green}). These vegetation indices were plotted against the fraction technique to determine their relationship in representing vegetation cover. Statistically, NDVI had the highest R^2, which was 0.922, in representing the vegetation cover. SAVI and MSAVI had the next highest R^2s of 0.916 and 0.907, respectively. In particular, NDVI and SAVI

having the best relationship with the measured vegetation cover had almost the same R^2, 0.92.

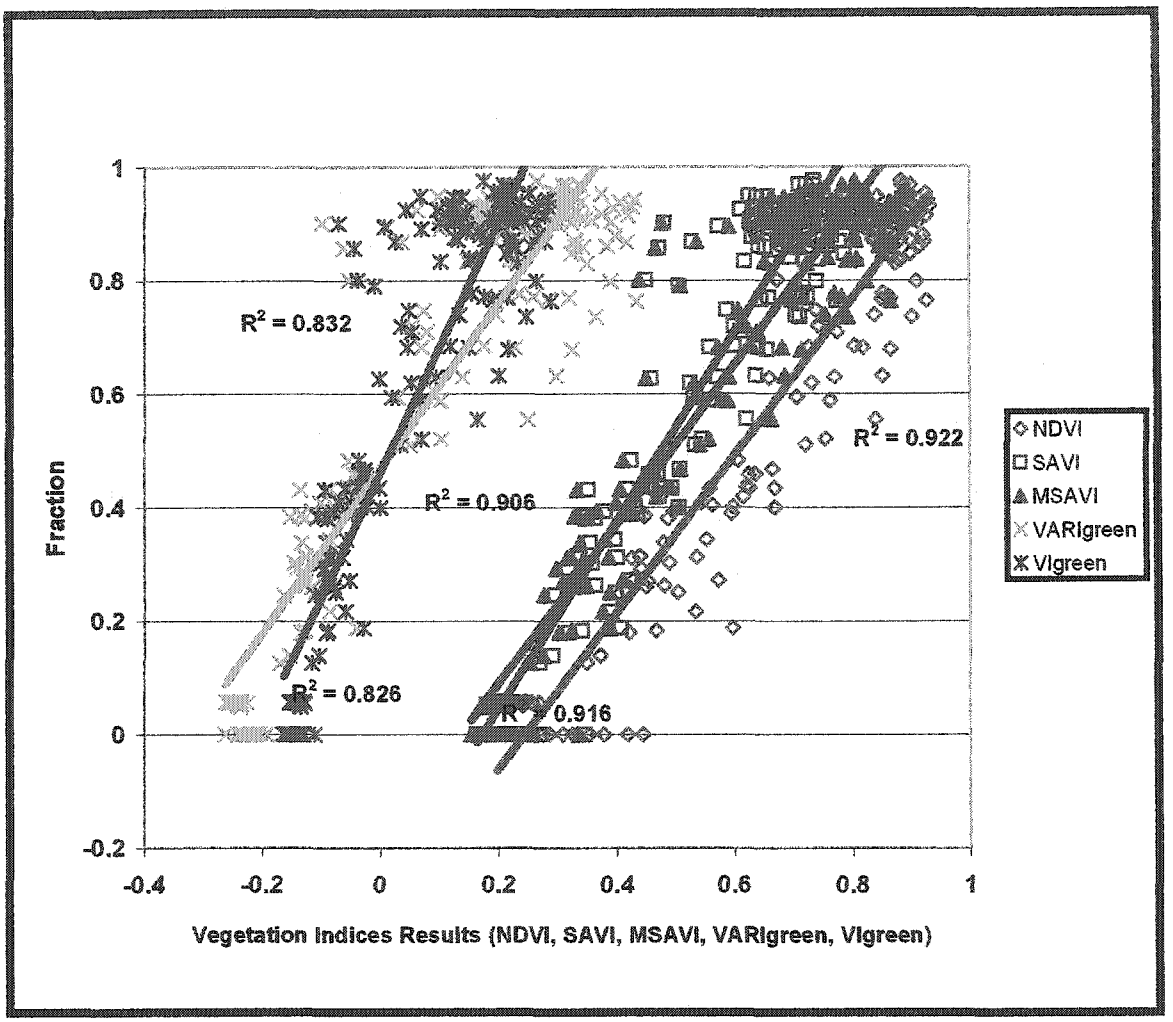

Figure 4.11. Comparison between measured and estimated vegetation cover.

4.2.2 WDI Results Using Estimated Vegetation Cover

As mentioned before, vegetation indices have advantages in representing the vegetation cover, especially in large agricultural areas. Consequently, determining the best relationship between vegetation indices and vegetation cover was very important in this study. NDVI provided the best vegetation index among all the vegetation indices. However, SAVI and MSAVI could not be ignored when compared to measured vegetation cover.

NDVI has a limitation when compared to SAVI, as soil background has an effect on the measurements of NDVI. After an irrigation, the soil surface is wet (darker color), red (λ_R) and near-infrared (λ_{NIR}) reflectance values were lower; therefore, NDVIs were calculated as higher values (Table 4.1). Hence, NDVI is not representative of the vegetation cover.

Table 4.1. Comparison between wet and dry measurements of NDVI.

DOY	Status	λ_P	λ_{PIN}	NDVI
210	wet	0.20	0.38	0.31
210	dry	0.11	0.23	0.35
212	wet	0.13	0.26	0.33
212	dry	0.10	0.20	0.35
233	wet	0.18	0.44	0.42
233	dry	0.09	0.25	0.44
238	wet	0.16	0.29	0.30
238	dry	0.10	0.27	0.45
241	wet	0.14	0.28	0.32
241	dry	0.09	0.20	0.38
263	wet	0.16	0.28	0.29
263	dry	0.09	0.18	0.35

SAVI was calculated by using equation 3.9, in which L = 0.5. "With L = 0, SAVI is identical to NDVI" (Bausch, 1993). This L was used to minimize the effect of soil surface color or moisture in representing vegetation cover. Vegetation indices were compared with measured vegetation cover in the drip-irrigated plots, as the drip irrigation system did not wet the soil surface between the crop rows. However, the center pivot system used in the commercial cornfield, created in a darker soil background color after irrigation, which influenced canopy reflectance measurements.

Since it is important for the spectral vegetation index to be sensitive to increases in vegetation cover and insensitive to spectral changes in soil background, the soil-adjusted vegetation index (SAVI) was used in this study to estimate vegetation cover

(Figure 4.12). Moran et al. (1994) also used SAVI to represent vegetation cover.

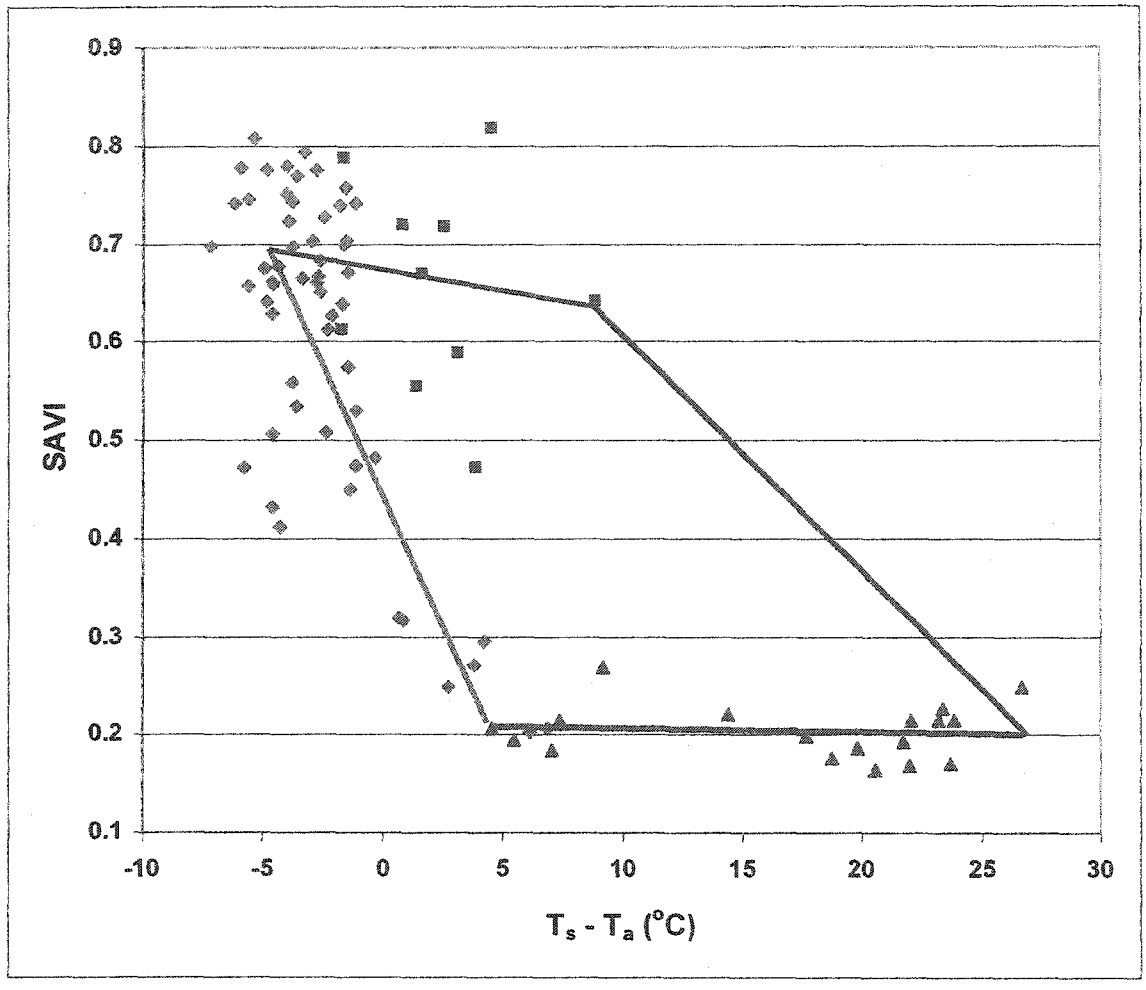

Figure 4.12. WDI results by using SAVI to represent vegetation cover.

4.2.3 Determination of Soil Water Deficit (SWD)

Calculated SWD and WDI values for the same time and location were correlated to develop the relationship. Figure 4.13 shows the relationship between calculated SWD and WDI results for sandy soil in this study.

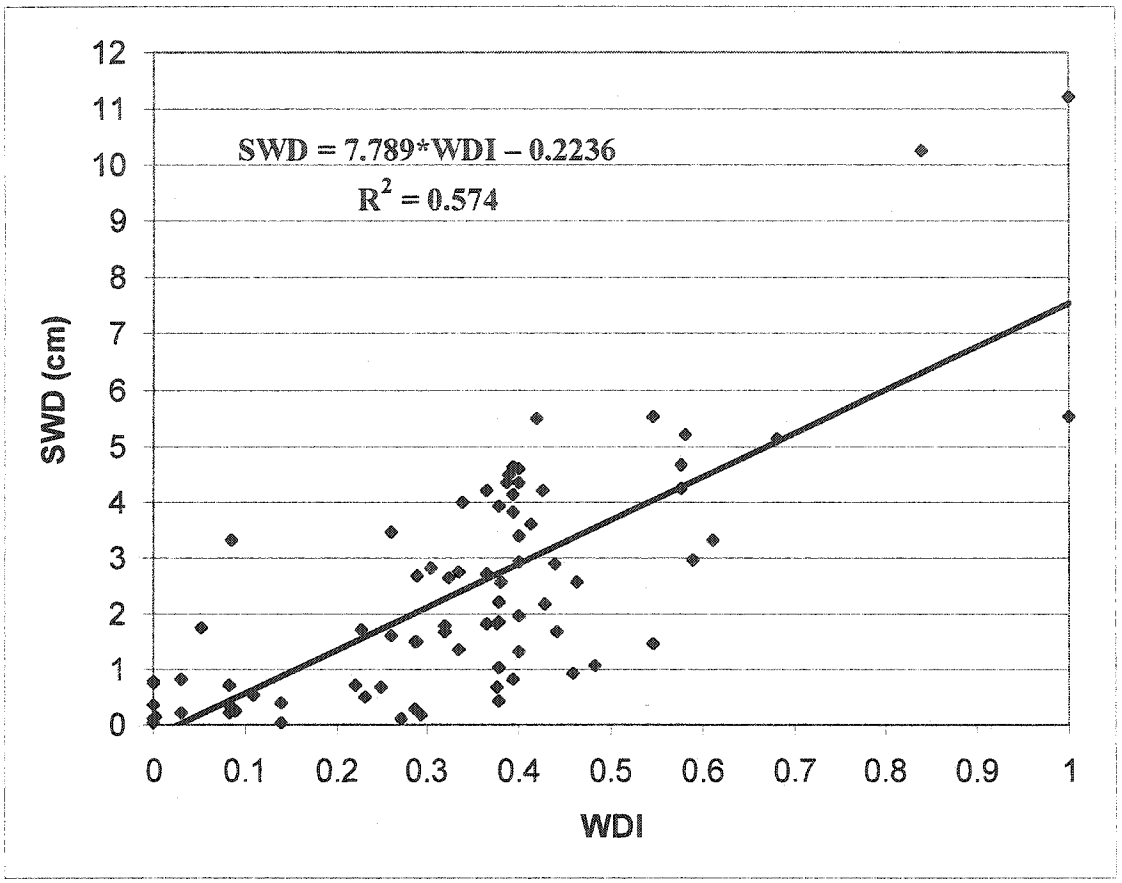

Figure 4.13. A comparison of SWD to WDI in estimating SWD for sandy soil and corn at the study site.

The relationship developed between the SWD and WDI is given below:

$$SWD = 7.79 * WDI - 0.22. \quad (4.1)$$

This relationship had a R^2 value of 0.57, which means that SWD correlates relatively well with WDI in the 1.2 m soil profile, which is the effective rooting depth of corn covering large areas in northeastern Colorado. This is very important when irrigation management for large agricultural fields is under investigation. Since remotely-sensed data can be used to estimate SWD spatially in the field, this could have considerable applications in precision water applications based on SWD estimates from WDI. This equation could therefore be used to estimate SWD in the sandy soils of northeastern Colorado, where it was developed. It might also be used for other areas with similar soil and weather

conditions, however, it may need testing to develop new relationships using the methodology utilized in this study.

4.3 Experimental Data Analysis

After establishing the baselines for CWSI and WDI, their values were calculated at the study sites for the entire growing season to determine their relationship to other parameters (soil texture, soil moisture and yield). Soil texture, yield and volumetric water content (VWC) in 30 cm and 70 cm soil profiles were also calculated for all sites. Table 4.2 represents the results for the drip-irrigated plots and Table 4.3 represents the results for the commercial cornfield. The bold lines in Table 4.2 represent plant water stress periods for drip-irrigated plots.

Table 4.2. Calculated parameters for drip-irrigated plots.

SITES	IRRIGATION (cm)	YIELD (Kg/ha)	% SAND 0-150 cm	DOY	GROWTH STAGES	CWSI	WDI	VWC 30 cm	VWC 70 cm
PLOT 1	71.1	12369	80.25	186	V8/9	0.000	0.000	0.220	0.176
PLOT 1	71.1	12369	80.25	190	V9/10	0.000	0.000	0.183	0.215
PLOT 1	71.1	12369	80.25	203	V16	0.000	0.000	0.244	0.224
PLOT 1	71.1	12369	80.25	205	V17/18	0.000	0.000	0.152	0.321
PLOT 1	71.1	12369	80.25	210	VT/R1	0.061	0.000	0.244	0.261
PLOT 1	71.1	12369	80.25	263	R5	0.593	0.000	0.241	0.248
PLOT 2	65.5	7890	84.00	186	V8	0.072	0.042	0.078	0.096
PLOT 2	65.5	7890	84.00	190	V9/10	0.062	0.000	0.186	0.128
PLOT 2	65.5	7890	84.00	203	V15	0.000	0.143	0.081	0.077
PLOT 2	**65.5**	**7890**	**84.00**	**205**	**V15**	**0.349**	**0.521**	**0.160**	**0.119**
PLOT 2	**65.5**	**7890**	**84.00**	**210**	**VT**	**1.000**	**1.000**	**0.081**	**0.073**
PLOT 2	65.5	7890	84.00	263	R5	0.421	0.682	0.157	0.156
PLOT 3	66.0	10745	84.75	186	V8	0.114	0.076	0.236	0.204
PLOT 3	66.0	10745	84.75	190	V9	0.155	0.000	0.207	0.117
PLOT 3	**66.0**	**10745**	**84.75**	**203**	**V14**	**1.000**	**0.524**	**0.091**	**0.112**
PLOT 3	66.0	10745	84.75	205	V15	0.644	0.289	0.015	0.071
PLOT 3	66.0	10745	84.75	210	VT	0.601	0.155	0.199	0.158
PLOT 3	66.0	10745	84.75	263	R5	0.810	0.227	0.173	0.156
PLOT 4	**66.6**	**10513**	**90.00**	**186**	**V8**	**0.369**	**0.145**	**0.236**	**0.121**
PLOT 4	**66.6**	**10513**	**90.00**	**190**	**V9/10**	**1.000**	**0.337**	**0.070**	**0.064**
PLOT 4	66.6	10513	90.00	203	V14	0.000	0.222	0.239	0.108
PLOT 4	66.6	10513	90.00	205	V16	0.000	0.000	0.115	0.086
PLOT 4	66.6	10513	90.00	210	VT	0.000	0.489	0.212	0.117
PLOT 4	66.6	10513	90.00	263	R5	0.346	0.577	0.160	0.121
PLOT 5	59.9	8775	86.25	186	V8	0.068	0.025	0.228	0.115
PLOT 5	59.9	8775	86.25	190	V9	0.333	0.000	0.118	0.119
PLOT 5	59.9	8775	86.25	203	V15	0.000	0.000	0.081	0.088
PLOT 5	59.9	8775	86.25	205	V16	0.000	0.000	0.139	0.091
PLOT 5	59.9	8775	86.25	210	VT	0.000	0.000	0.205	0.156
PLOT 5	**59.9**	**8775**	**86.25**	**233**	**R3**	**0.313**	**1.000**	**0.078**	**0.100**
PLOT 5	59.9	8775	86.25	263	R5	0.492	0.393	0.097	0.183

Table 4.3. Calculated parameters for the commercial cornfield.

SITES	YIELD (kg/ha)	% SAND 0-150 cm	DOY	GROWTH STAGES	CWSI	WDI	VWC 30 cm	VWC 70 cm
1	13033	83.00	186	V8	0.289	0.366	0.118	0.117
1	13033	83.00	190	V9	0.000	0.000	0.076	0.104
1	13033	83.00	263	R5	0.000	0.400	0.136	0.229
2	13881	78.25	186	V8/9	0.198	0.218	0.183	0.165
2	13881	78.25	190	V9/10	0.000	0.000	0.118	0.152
2	13881	78.25	263	R5	0.000	0.286	0.220	0.242
3	11979	87.25	186	V8	0.438	0.393	0.086	0.088
3	11979	87.25	190	V9	0.000	0.000	0.070	0.082
3	11979	87.25	263	R5	0.000	0.364	0.089	0.187
4	12123	88.25	186	V9	0.397	0.399	0.068	0.082
4	12123	88.25	190	V10	0.000	0.000	0.070	0.073
4	12123	88.25	263	R5	0.000	0.261	0.084	0.123
5	13367	79.75	186	V8/9	0.279	0.238	0.134	0.134
5	13367	79.75	190	V9/10	0.000	0.000	0.120	0.147
5	13367	79.75	263	R5	0.068	0.304	0.173	0.226
6	13315	83.13	186	V8/9	0.300	0.229	0.126	0.128
6	13315	83.13	190	V9/10	0.000	0.000	0.112	0.169
6	13315	83.13	263	R5	0.000	0.400	0.181	0.183
7	13705	77.50	186	V8/9	0.227	0.258	0.118	0.163
7	13705	77.50	190	V9/10	0.000	0.000	0.205	0.261
7	13705	77.50	263	R5	0.000	0.140	0.170	0.200
8	12215	84.75	186	V8	0.420	0.390	0.068	0.082
8	12215	84.75	190	V9	0.000	0.000	0.247	0.073
8	12215	84.75	263	R5	0.000	0.546	0.105	0.073
9	14011	78.25	186	V9	0.135	0.219	0.139	0.163
9	14011	78.25	190	V10	0.000	0.000	0.223	0.152
9	14011	78.25	263	R5	0.000	0.393	0.218	0.233
10	13824	76.25	186	V8	0.168	0.344	0.139	0.163
10	13824	76.25	190	V9	0.000	0.000	0.278	0.279
10	13824	76.25	263	R5	0.000	0.083	0.283	0.246

Table 4.3. continued

11	13216	77.00	186	V8	0.352	0.378	0.139	0.163
11	13216	77.00	190	V9	0.000	0.000	0.320	0.152
11	13216	77.00	263	R5	0.000	0.378	0.194	0.202
12	13317	81.75	186	V8	0.334	0.195	0.157	0.130
12	13317	81.75	190	V9	0.000	0.000	0.170	0.150
12	13317	81.75	263	R5	0.000	0.289	0.186	0.119
13	13612	81.75	186	V8	0.140	0.238	0.110	0.121
13	13612	81.75	190	V9	0.000	0.000	0.268	0.285
13	13612	81.75	263	R5	0.000	0.612	0.128	0.176
14	11885	87.50	186	V8	0.352	0.275	0.086	0.088
14	11885	87.50	190	V9	0.000	0.000	0.173	0.108
14	11885	87.50	263	R5	0.000	0.318	0.089	0.086
15	13882	81.00	186	V8	0.300	0.321	0.139	0.143
15	13882	81.00	190	V9	0.000	0.000	0.223	0.152
15	13882	81.00	263	R5	0.000	0.378	0.178	0.152

The study determined the relationships between yield, CWSI, WDI, VWC and soil texture at the study site. The study also determined the statistical relationship between two specific variables included in the bivariate structure. In particular, the type of dependence among such variables was analyzed by using Kendall's independence test.

As shown in Tables 4.4 and 4.5, these relationships were determined to understand varied levels of importance of CWSI and WDI, the relationships were determined at the study site. Drip-irrigated plots were prepared to establish CWSI and WDI with all independent parameters, which were studied based on the cornfield. Established CWSI and WDI were used to calculate the results in the cornfield. The cornfield was given approximately the same amount of irrigation water (≅74 cm), and CWSI, WDI and VWC were dependent on this irrigation water.

Table 4.4. The results of Kendall's independence test (a) V8 growth stage, (b) VT (tasselling) growth stage for drip-irrigated plots.

(a) V8 growth stage

Relationship between	Calculated K by Kendall test	Correlation exists at
CWSI & Sand	6	$\alpha \geq 0.117$
CWSI & Yield	-2	$\alpha \geq 0.408$
CWSI & Irrigation	2	$\alpha \geq 0.408$
CWSI & VWC_{70}	-2	$\alpha \geq 0.408$
CWSI & VWC_{30}	1	$\alpha \geq 0.592$
WDI & Sand	6	$\alpha \geq 0.117$
WDI & VWC_{30}	5	$\alpha \geq 0.242$
WDI & Yield	-2	$\alpha \geq 0.408$
WDI & Irrigation	2	$\alpha \geq 0.408$
WDI & VWC_{70}	0	$\alpha \geq 0.592$

(b) VT growth stage

Relationship between	Calculated K by Kendall test	Correlation exists at
CWSI & VWC_{30}	-8	$\alpha \geq 0.042$
CWSI & VWC_{70}	-6	$\alpha \geq 0.117$
CWSI & Yield	-4	$\alpha \geq 0.242$
CWSI & Irrigation	-4	$\alpha \geq 0.242$
CWSI & Sand	0	$\alpha \geq 0.592$
WDI & VWC_{70}	-8	$\alpha \geq 0.042$
WDI & VWC_{30}	-6	$\alpha \geq 0.117$
WDI & Yield	-6	$\alpha \geq 0.117$
WDI & Irrigation	-2	$\alpha \geq 0.408$
WDI & Sand	2	$\alpha \geq 0.408$

Table 4.5. The results of Kendall's Independence test for the commercial cornfield (a) V8/V9 vegetation period, (b) R5 growth stage.

(a) V8/9 growth stage.

Relationship between	Calculated K by Kendall test	Correlation exists at
CWSI & Yield	-66	$\alpha \geq 0.000$
CWSI & Sand	52	$\alpha \geq 0.006$
CWSI & VWC_{70}	-50	$\alpha \geq 0.008$
CWSI & VWC_{30}	-33	$\alpha \geq 0.057$
WDI & VWC_{30}	-57	$\alpha \geq 0.002$
WDI & VWC_{70}	-46	$\alpha \geq 0.014$
WDI & Yield	-46	$\alpha \geq 0.014$
WDI & Sand	40	$\alpha \geq 0.029$

(b) R5 growth stage.

Relationship between	Calculated K by Kendall test	Correlation exists at
CWSI & Yield	0 (no stress)	n/a
CWSI & Sand	0 (no stress)	n/a
CWSI & VWC_{70}	0 (no stress)	n/a
CWSI & VWC_{30}	0 (no stress)	n/a
WDI & Sand	24	$\alpha \geq 0.141$
WDI & VWC_{70}	-22	$\alpha \geq 0.164$
WDI & VWC_{30}	-15	$\alpha \geq 0.248$
WDI & Yield	-10	$\alpha \geq 0.349$

As shown in Table 4.5(b), calculated CWSI values were found to be 0, which means there was no stress at the R5 growth stage at the cornfield. Consequently, Kendall's independence test was not able to determine the correlation between the parameters.

4.4 Soil Texture Analysis

Due to its water-holding capacity, soil texture may affect yield. Consequently, soil texture analysis was carried out in this study. One time in 7 to 10 days during the growing season, soil samples were taken from the cornfield, from the drip-irrigated plots and from the TDR calibration centers. These soil samples were used to spatially analyze soil texture and to determine the TDR calibration equations.

The soil texture analysis shown in Table 4.6 demonstrates that the locations at the study site had mostly sandy soils. Figure 4.14 shows the relationship between yield and percentage of sand in all study sites. As seen in Figures 4.14b and 4.14c, the relationship developed between yield and the percent sand for drip-irrigated plots was poorer as compared to that for commercial cornfield sites. This was expected because in the case of cornfield sites irrigations were approximately similar, therefore, the effect of the sand on the yield was determined. In case of drip-irrigated plots, however, various levels of irrigation water were applied due to the water stress treatments. This was confounding with the sand effect, therefore R^2 was low.

Table 4.6. The results of determined percentage of sand at the study site.

SITES	% SAND 0-150 cm	SITES	% SAND 0-150 cm
PLOT 1	80.25	6	83.13
PLOT 2	84	7	77.5
PLOT 3	84.75	8	84.75
PLOT 4	90	9	78.25
PLOT 5	86.25	10	76.25
1	83	11	77
2	78.25	12	81.75
3	87.25	13	81.75
4	88.25	14	87.5
5	79.75	15	81

(a) For all study sites

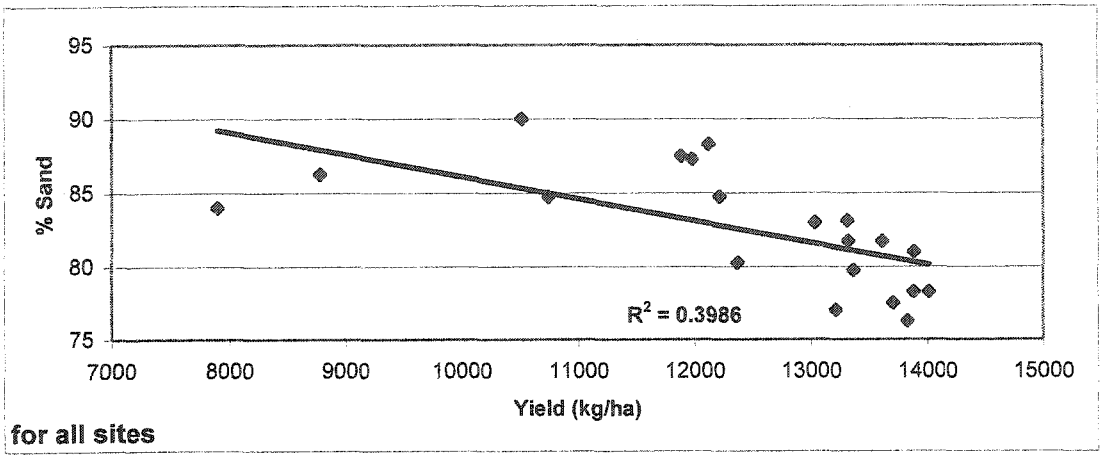

(b) For drip-irrigated plots only

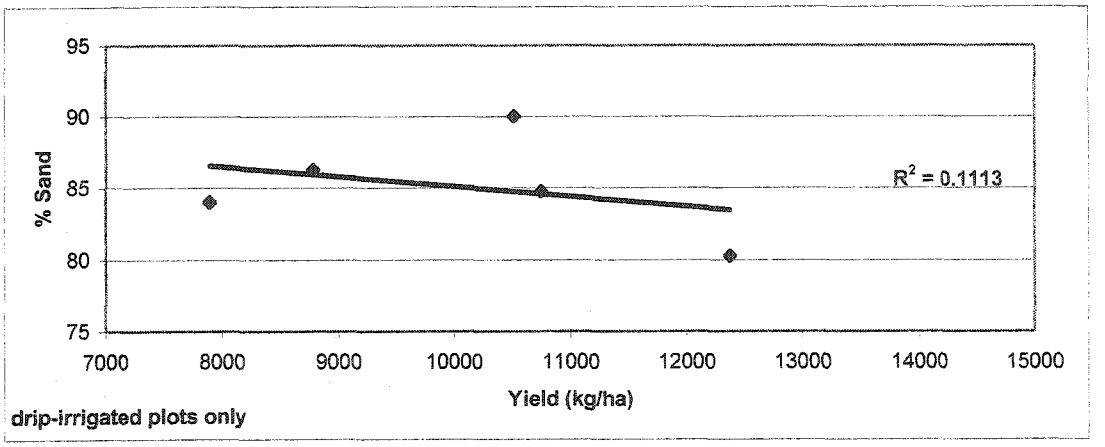

(c) For commercial cornfield sites only

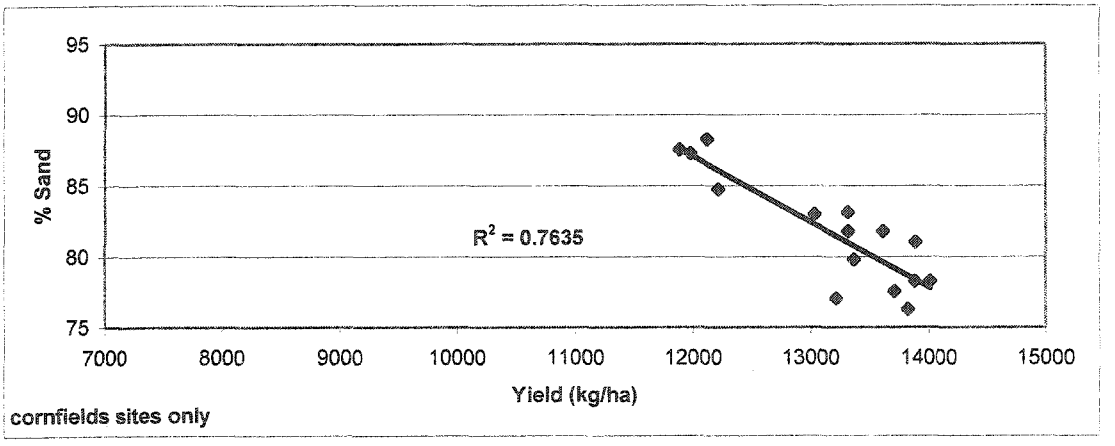

Figure 4.14. Relationship between yield and percentage of sand (a) for all sites, (b) for drip-irrigated plots only, (c) for commercial cornfield sites only.

4.4.1 Relationship Between Soil Texture and CWSI

CWSIs were calculated to analyze the degree of stress on twenty sites in the cornfield and drip-irrigated plots. Figure 4.15 shows the relationship between the results of CWSI and the percentage of sand in the cornfield. The Kendall statistic (K) was calculated to be 52, and according to K at alpha (α) $\geq$ 0.006, there was a correlation between CWSI and percentage of sand. Thus, the study determined a positive relationship between CWSI and soil texture. The study also anticipated that soil texture differences might result in a variable yield from approximately the same amount of irrigation water.

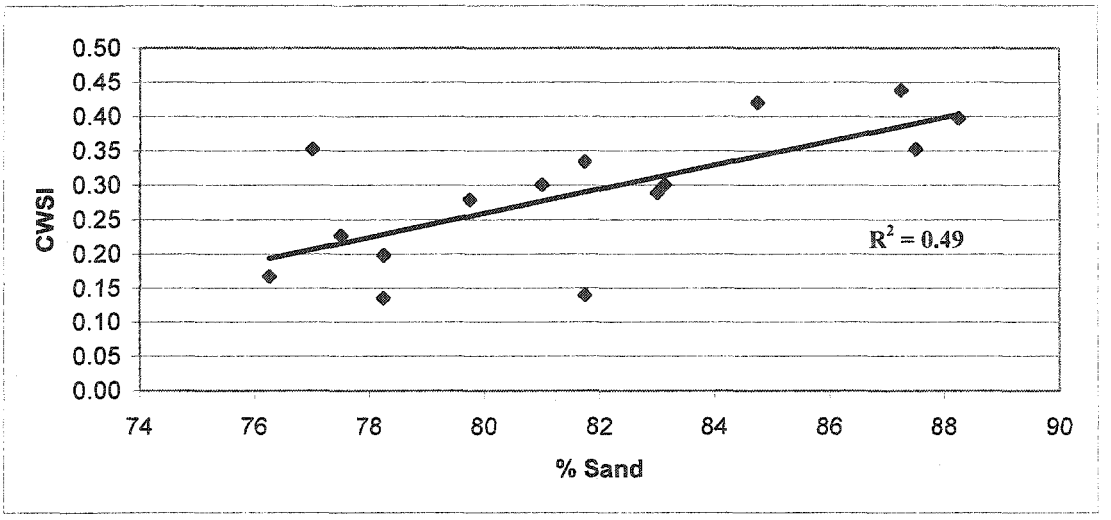

Figure 4.15. The relationship between the CWSI and percentage of sand in the cornfield.

4.4.2 Relationship Between Soil Texture and WDI

The results for WDI and percentage of sand for the V8/V9 growth stage are provided in Tables 4.2 and 4.3, while their relationship is shown in Figure 4.16. Statistically, there was a low correlation between WDI and percentage of sand at the cornfield. The calculated K of 40 determined a positive relationship between them at 0.029 and higher α levels.

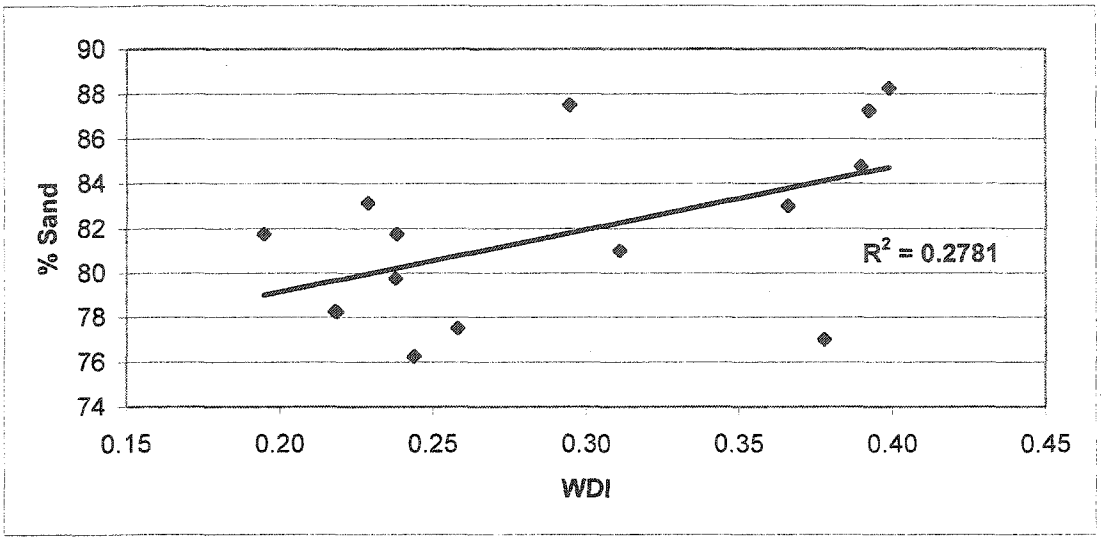

Figure 4.16. The relationship between WDI and percentage of sand at the cornfield.

4.5 Soil Moisture Analysis

Soil moisture data were taken at all the study sites using TDR probes at 30 cm and 70 cm. Soil samples were also taken to determine soil moisture. All TDR readings were calibrated based on the dielectric constant (Ka). Figures 4.17 and 4.18 show the calibration equations for the 30 cm and 70 cm TDR probes, respectively.

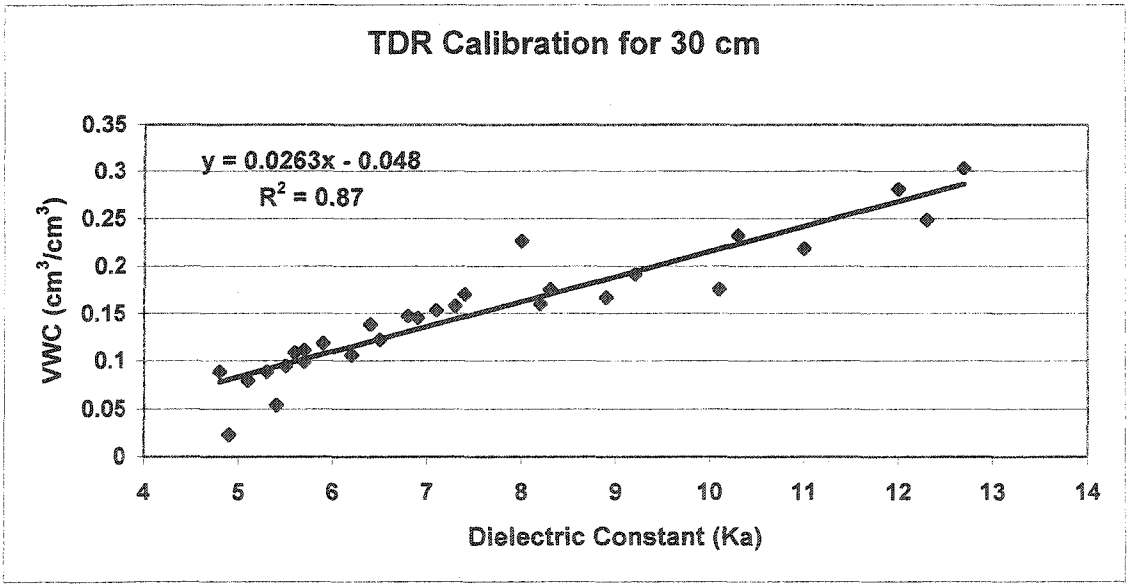

Figure 4.17. The calibration equation for 30 cm depth TDR readings based on Ka.

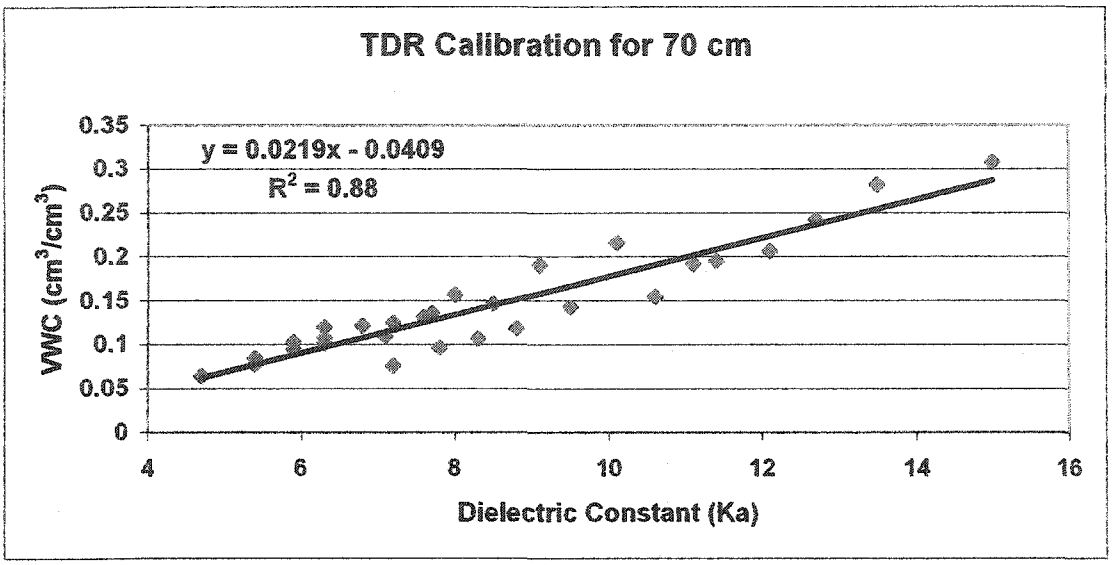

Figure 4.18. The calibration equation for 70 cm depth TDR readings based on Ka.

Kendall's statistical test demonstrated that VWC_{30} and VWC_{70} were the parameters most highly correlated with CWSI and WDI for the drip-irrigated plots at VT growth stage (Table 4.4b). Since corn is most sensitive to water stress during the VT growth stage, such statistical results were anticipated in this study.

Figures 4.19 shows VWCs for the lowest and highest yield locations at the commercial cornfield.

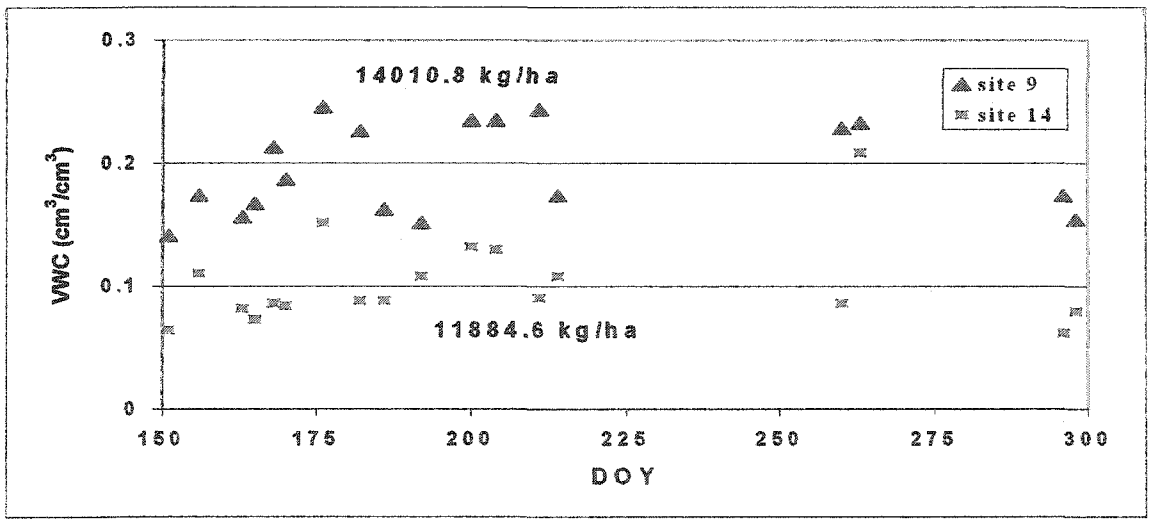

Figure 4.19. Some selected VWCs for 70 cm depth at the lowest and highest yield locations.

4.5.1 Relationship Between Soil Moisture and CWSI

VWC_{30} and VWC_{70} did not have good relationships with CWSI when compared with other parameters such as yield and sand percentage except at the VT growth stage in the cornfield and drip-irrigated plots (Tables 4.4a-b and 4.5a-b). As shown in Figure 4.20, the relationships were determined between CWSI and VWC in 30 and 70 cm at the cornfield. Negative relationships occurred at $\alpha \geq 0.008$ and $\alpha \geq 0.057$ between CWSI and VWC_{70}, VWC_{30}, respectively (Table 4.5a).

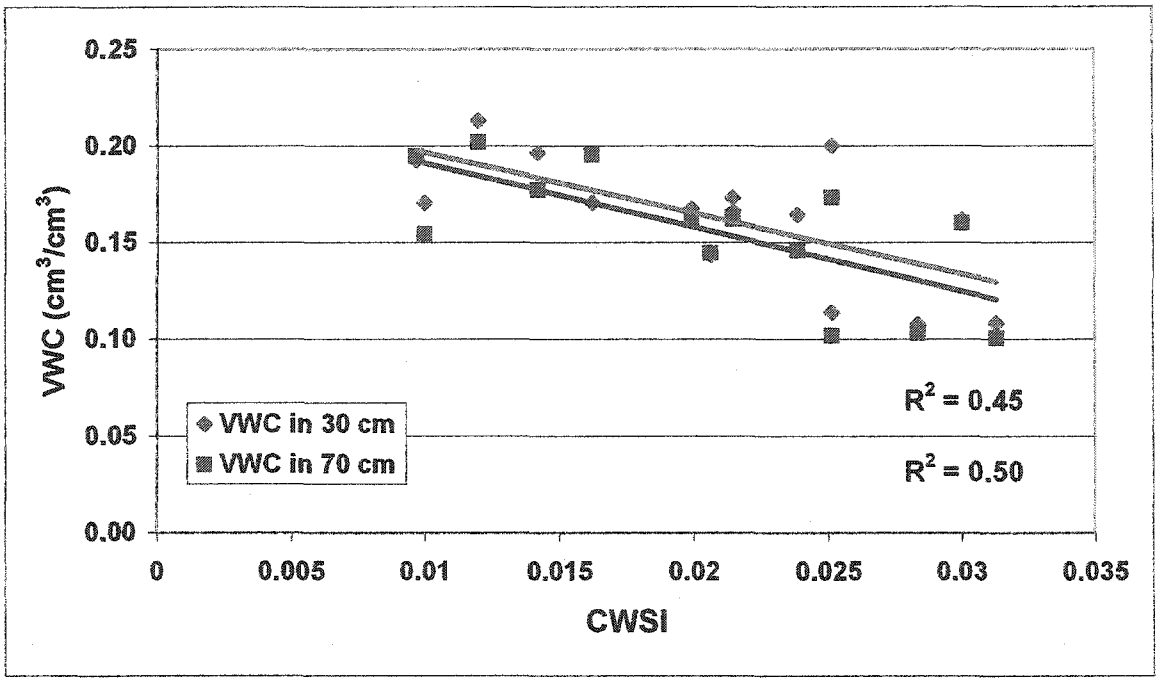

Figure 4.20. The relationship between CWSI and VWC at the cornfield.

4.5.2 Relationship Between Soil Moisture and WDI

The Kendall statistics (K = -57 and -46) were calculated at $\alpha \geq 0.002$ and $\alpha \geq 0.014$, and negative relationships were determined between WDI, VWC_{30} and VWC_{70}, respectively (Table 4.5a), which was the highest K value for all correlations between WDI and other parameters. This result was anticipated in this study because WDIs represent soil moisture combined with VWC. This relationship is shown in Figure

4.21 below. As mentioned before, SWD can be calculated using WDIs, thus affording a good opportunity to carry out scientific irrigation management to improve yield values in agricultural fields. Therefore, ascertaining the relationship between WDI and VWC was very important in making a better determination of SWD at the study site.

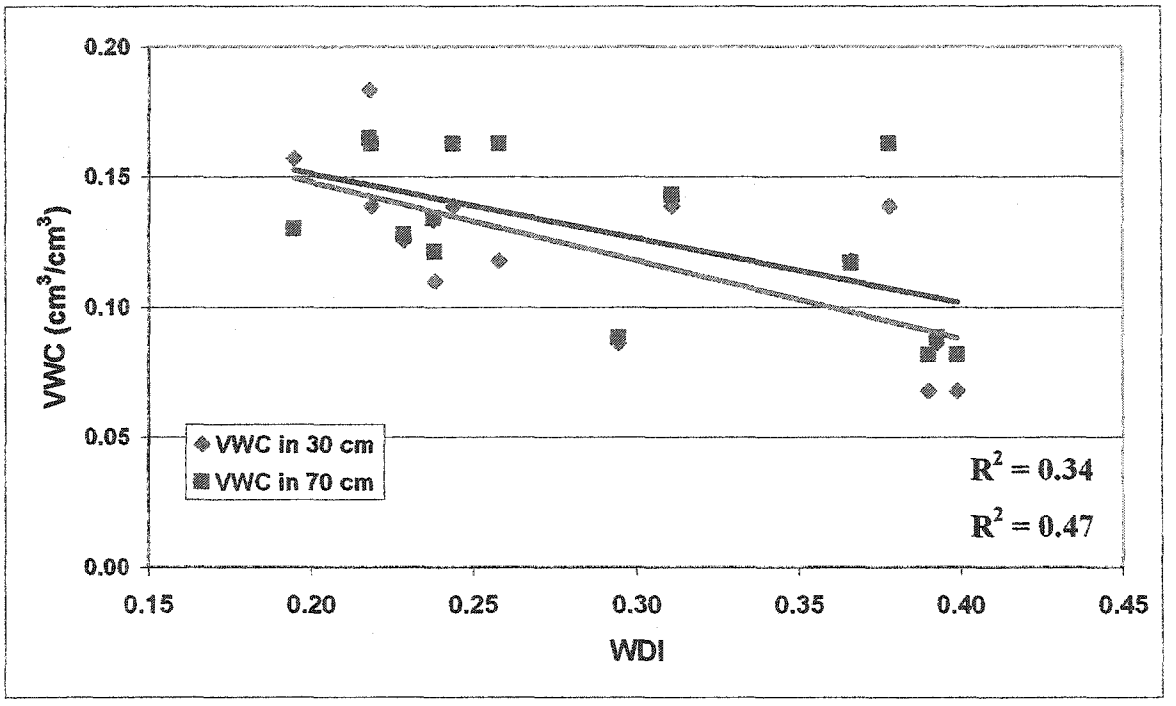

Figure 4.21. The relationship between WDI and VWC at the cornfield.

4.6 Yield Analysis

As mentioned previously, yield data were obtained from the study site by hand-harvesting. Yield varied for drip-irrigated plots, which were under stress during various stages of the corn-growing season. Table 4.7 shows the yield results for drip-irrigated plots, which indicate that stress during the middle and late growing season had a greater effect on yield. Hence it is clear that stress was a very important factor during various phases of the growing season (especially during the tasselling period) when compared with the entire corn-growing season.

Table 4.7. Yield results in different stress periods for drip-irrigated plots.

SITES	STRESS PERIOD	IRRIGATION (cm)	YIELD (Kg/ha)
PLOT 1	None	71.1	12368.7
PLOT 2	V15 - VT/R1	65.5	7889.6
PLOT 3	V12 - V14	66.0	10745.2
PLOT 4	V8 - V10	66.6	10512.8
PLOT 5	R2 - R3	59.9	8774.5

As shown in Table 4.7, irrigation amount has a positive relationship to yield. If the data in this table are analyzed, it becomes clear that duration of the stress period and irrigation amounts affect the yield considerably. For example, although plot 5 had the lowest irrigation amount during the growing season, it had a higher yield than plot 2 because plot 2 underwent stress during the tasselling period of the growing season. Thus, it is seen that timing of stress and irrigation amount are both important and have an effect on yield.

Table 4.8 shows yield results for the commercial cornfield. Although all sites were irrigated with approximately the same amount of water (≅74 cm) by the center pivot system, the yield results were not similar for these locations.

Table 4.8. Hand-harvesting yield results from the commercial cornfield.

SITES	YIELD (Kg/ha)		SITES	YIELD (Kg/ha)
1	13033		9	14011
2	13881		10	13824
3	11979		11	13216
4	12123		12	13317
5	13367		13	13612
6	13315		14	11885
7	13705		15	13882
8	12215		**AVERAGE**	**13158**

The yield values were determined for all locations in the study site, and these yields were analyzed with CWSI and WDI to determine the relationships among them. As shown in Table 4.5a, yield had a negative relationship to CWSI and WDI. CWSI was correlated with yield at any level of α, while WDI had a significant relationship with yield statistically ($\alpha \geq 0.014$). Table 4.8 demonstrates that yield varied from 11885 kg/ha to 14011 kg/ha, and that sites 3, 4, 8 and 14 had lowest yield values because they had the highest percentage of sand.

4.6.1 Relationship Between Yield and CWSI

As mentioned previously, the relationship between yield and other parameters was determined by using Kendall's statistical test. As shown in Table 4.5a, the best relationship for any α levels at the cornfield sites was found between yield and CWSI. Thus, the study demonstrated the importance of CWSI values to describe the corn yield. Using Kendall's independence test, the K value was calculated and found to be –66 at any level of α for the relationship between yield and CWSI. The calculated K was higher than all K_α values; consequently, it is evident that the correlation between yield and CWSI exists at any alpha level. Tables 4.2 and 4.3 show the results of yield and CWSI at the cornfield and drip-irrigated plots, while Figure 4.22 depicts their relationship. Since the study found that CWSI had a strong relationship to yield, irrigators have control over yield by using CWSI as an irrigation timing technique. When ($T_s - T_a$) measurements were located above the lower VPD baseline of CWSI, which is the recommended irrigation time in this study.

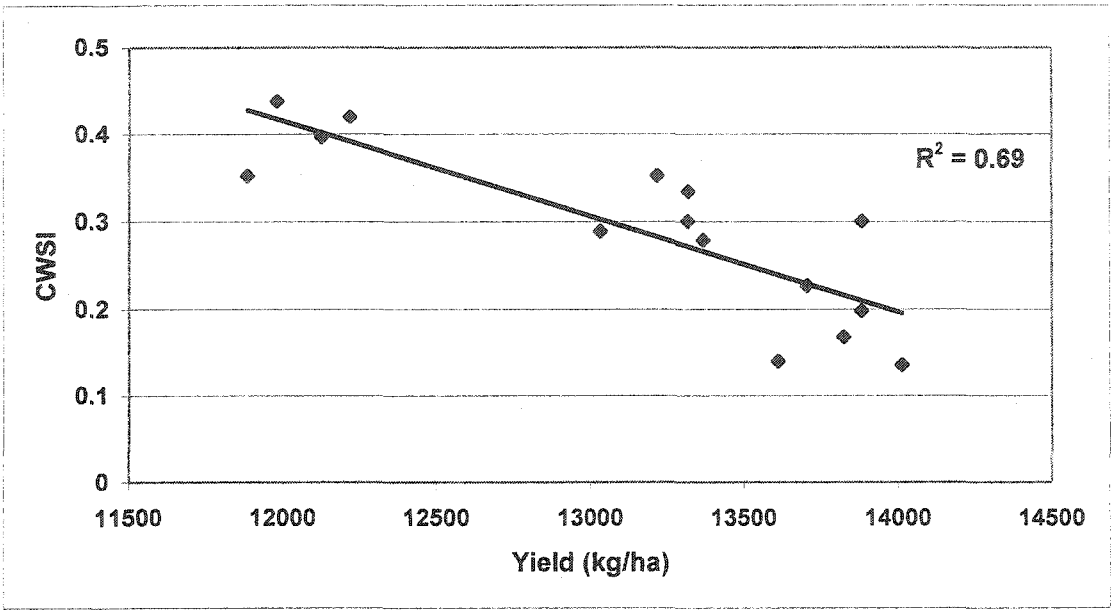

Figure 4.22. The relationship between yield and CWSI at the cornfield.

4.6.2 Relationship Between Yield and WDI

A low value of K (-46) was found with an α of 0.408 and higher (Table 4.4a) in the early growing season at V8 growth stage; however, during the tasselling period, the relationship was found with an α of 0.117 and higher levels in the drip irrigated plots (Table 4.4b). It is therefore clear that WDI has an important role to describe the corn yield, especially during tasselling time water deficit was significant effect on corn yield. Also, for the drip-irrigated plots, the lowest yield (7889.6 kg/ha) was found at plot 2, which was under water stress during V15-VT. Thus, it is clear that irrigation water was more important during these growth stages than others, and WDI demonstrated the ability to describe the situation.

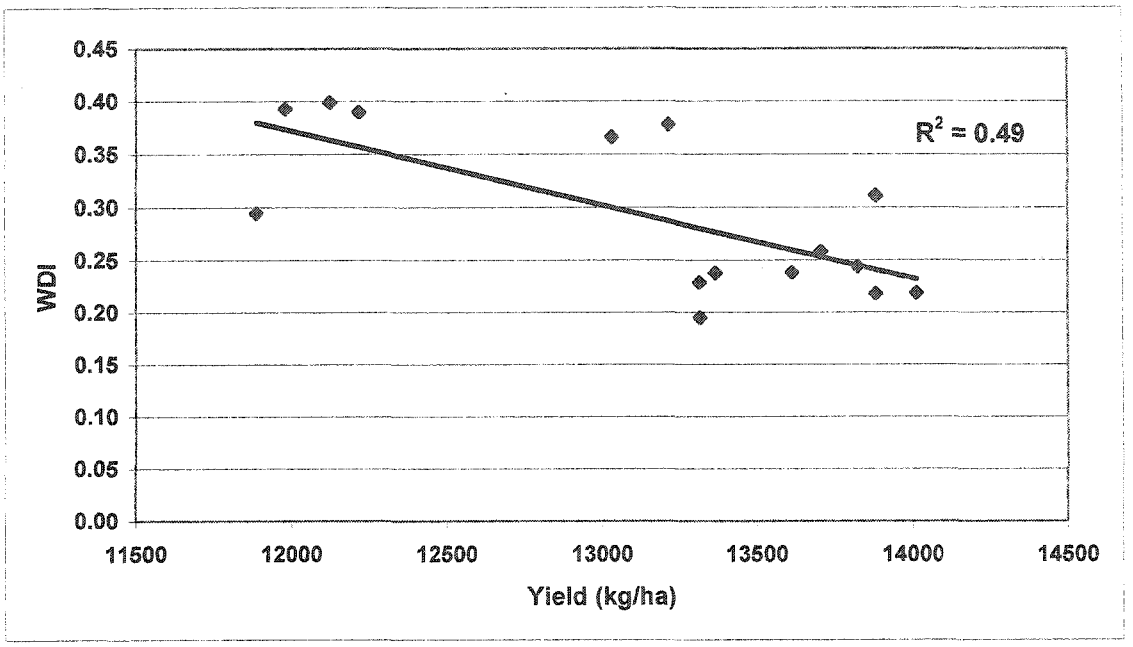

Figure 4.23. The relationship between yield and WDI at the cornfield.

CHAPTER 5

SUMMARY, CONCLUSIONS AND RECOMMENDATIONS

5.1 Summary

The overall objective of this study was to assess the potential of the crop water stress index (CWSI) and water deficit index (WDI) to improve irrigation management by determining irrigation timing and amount of irrigation water to apply on a sandy soil using ground-based remote sensing.

The study had two experimental corn sites. The first site consisted of six non-replicated drip-irrigated plots where the CWSI and the WDI were developed. The second site consisted of half of a commercial center pivot where corn was grown this year and it was used to test the CWSI and WDI values.

All remote sensing (RS) data were collected by a ground-based remote sensing system. The RS data from the nadir (down-looking) and oblique (80^{o}) views were used in this study to represent more accurate plant surface temperature data, apart from the bare soil plot. The effect of soil background was the major problem encountered during the early plant growth stage measurements of T_s.

Both the CWSI and WDI baselines for corn grown in the sandy soils of northeastern Colorado were developed. These parameters were then evaluated for their performance in improving irrigation management. They were also correlated with other plant and soil parameters.

Although CWSI could be used to estimate irrigation timing, it is not reliable, especially during the early growing season for corn. Canopy temperature is the main measurement for developing CWSI which was found to be inaccurate before the V8 growth stage.

In the present study, WDI was found to be a better index when compared with CWSI. Although the both indices used T_s as well, T_s represents soil and canopy temperature for WDI. Consequently, T_s measurements were more reliable in determining the four corners of VIT. Another advantage of WDI was estimated soil water deficit (SWD), which was one of the most important objectives of this study. Estimating SWD determined the necessary irrigation amount; hence, CWSI was not necessary for estimating irrigation timing.

The relationships of CWSI and WDI with soil and plant parameters were analyzed using Kendall's Independence test and regression analysis. Measured VWC using TDR and gravimetric soil sample technique correlated well with WDI. This high correlation helped to estimate SWD.

In this study, a comparison was made between measured vegetation cover and vegetation indices (estimated vegetation cover) such as NDVI, SAVI, MSAVI, $VARI_{green}$ and VI_{green}. The measured vegetation cover (f) was correlated with all vegetation indices. The vegetation index found to be best correlated with f was NDVI (R^2= 0.922), followed by SAVI (R^2= 0.916).

5.2 Conclusions

Results indicated that the WDI was superior to the CWSI since it enables users to determine the amount of irrigation water to be applied to the soil by estimating SWD at

each irrigation besides the irrigation timing that the CWSI is able to determine. Estimating SWD using remote sensing data is an innovative technique. SWD conveys the necessary information to the irrigator with less fieldwork, and is useful in saving money, time and labor. It can be used with remotely-sensed data measurements, which is a very important feature, especially for large agricultural areas.

In addition, the study revealed the difficulties of obtaining measurements of T_s, which must represent canopy temperatures for CWSI, especially during the partial vegetation cover period because of the influence of soil background. Surface temperatures (T_s) were measured with two angles which were nadir (down-looking) and oblique (80°) view. The remote sensing data from the 80° view angle were a better estimator of plant surface temperature compared to the nadir view angle of T_s. However, even before the V8 growth stage, the 80° view did not constitute reliable data because of soil background influences.

Vegetation indices have a reliable relationship with measured vegetation cover (f); hence, the study suggests the importance of using vegetation indices, which are quick and easy to calculate. For measured vegetation cover, it is especially difficult to complete the data set with the limited time (during noon) available in large agricultural areas. The study found that NDVI and SAVI had the highest positive relationship (R^2 = 0.92) with the vegetation cover. However, SAVI was found to be a better indicator vegetation index for determining the measured vegetation cover because the color of the soil background altered the results of NDVI by reducing red and near IR measurements when the soil was wet. Consequently, NDVI did not represent the vegetation color as accurately as SAVI.

The study demonstrated the relationships between CWSI, WDI and the other parameters such as percentage of sand, VWC at 30 and 70 cm depths of soil profile, and yield. At the drip-irrigated plots, the Kendall statistic (K) indicated that WDI and CWSI correlated well with parameters in the following order: VWC, yield, and percentage of sand at the VT growth stage. Based on K, the correlation between WDI and parameters at the cornfield were ranked VWC, yield, and percentage of sand at the V8/V9 growth stages as well as the VT growth stage of drip-irrigated plots. However, based on the Kendall statistic, the correlation between CWSI and parameters were ranked as follows: yield, percentage of sand, and VWC at V8/V9 growth stages of corn in the commercial cornfield. The change in the rank of correlation between WDI and CWSI could be the influence of the soil background on T_s measurements which were used in both indices to establish the baselines. T_s measurements were represented by soil and canopy temperatures in WDI, however, they should be only canopy temperature in CWSI.

5.3 Recommendations

Since the WDI enables the estimation of the SWD to be applied in addition to the irrigation timing, it is recommended that the WDI should be used instead of CWSI for better irrigation management.

SWD is a common tool for irrigators; however, its estimation by remotely-sensed data is an innovative approach. While this study produced an equation for SWD using GBRS for sandy soil and corn for northern Colorado, this equation may not produce similar results for different atmospheric, soil or vegetation conditions.

Use of the 80° view in this study seemed to produce more reliable surface temperature (T_s) when compared to T_s measurements of nadir view. Thus, oblique (80°) view measurements were used in computing both WDI and CWSI.

Data set were collected two or three times a week during the growing season by using GBRS. If remotely-sensed data had been collected on a daily basis for CWSI and WDI, a more accurate data set would have been available for analyzing CWSI and WDI and their effects. Daily data would also have provided a better understanding of VWC in the soil profile and would therefore be a better tool for improving irrigation management at the study site.

During partial vegetation cover, T_s measurements represented very high values of temperature because of soil influences. It is therefore recommended to use hand-held IR sensors to obtain the measurements of T_s at partial vegetation periods. Using a hand-held IR sensor would have measured T_s more accurately by decreasing the distance between the IR sensor and plant.

REFERENCES

Abernethy, C.L. 1986. Performance measurement in canal water management: a discussion. Irrigation Management Network Paper, 86/2d, ODI/IIMI.

Alderfasi, A.A., and D.C. Nielsen. 2001. Use of crop water stress index for monitoring water status and scheduling irrigation in wheat. Agricultural Water Management, Vol. 47(1): 69-75.

Andrews P.K., D.J. Chalmers, M. Moremong. Canopy air-temperature differences and soil-water as predictors of water-stress of apple-trees grown in a humid, temperate climate. Journal of the American Society for Horticultural Science, Vol. 117(3): 453-458.

Alves I. and L.S. Pereira. 2000. Non-water-stressed baselines for irrigation scheduling with infrared thermometers: a new approach. Irrigation Science, Vol. 19: 101-106.

Ambast, S.K., A.K. Keshari, A.K. Gosain. 2002. Satellite remote sensing to support management of irrigation systems: concepts and approaches. Irrigation and Drainage, Vol. 51: 25-39.

Bartholic, J.F., L.N. Namken, C.L. Wiegand. 1972. Aerial thermal scanner to determine temperatures of soils and of crop canopies differing in water stress. Agron. Journal, Vol. 64: 603-608.

Bastiaanssen V.G.M., T. Van Der Wal, T.N.M. Visser. Diagnosis of regional evaporation by remote sensing to support irrigation performance assessment. Irrigation and Drainage Systems, Vol. 10: 1-23.

Bausch, W.C., and C.M.U. Neale. 1987. Crop coefficients derived from reflected canopy radiation: a concept. Trans. ASAE, Vol. 30: 703-709.

Bausch, W.C., D.M. Lund, M.C. Blue. 1990. Robotic data acquisition of directional reflectance factors. Remote Sens. Environ. Vol. 46: 213-222.

Bausch, W.C. 1993. Soil background effects on reflectance-based crop coefficients for corn. Remote Sens. Environ. Vol. 46: 213-222.

Biswas, A.K. 1990. Monitoring and evaluation of irrigation projects. Journal of Irrigation and Drainage Engineering (ASCE), Vol. 116(2): 227-242.

Bonanno, A.R., and H.J. Mack. 1983. Use of canopy-air differentials as a method for scheduling irrigations in snap beans. J. Amer. Soc. Hort. Sci., Vol. 108:826-831.

Bosen, J.F. 1960. A formula for approximation of saturation vapor pressure over water. Monthly WeatherRev., Vol. 88(8): 275-276.

Bouman, B.A.M., and T.P. Tuong. 2001. Field water management to save water and increase its productivity in irrigated lowland rice. Agricultural Water Management, Vol. 49: 11-30.

Boyer, J.S. 1982. Plant productivity and environment. Science, Vol. 218: 443-448.

Braunworth, W.S., and H.J. Mack. 1989. The possible use of crop water stress index as an indicator of evapotranspiration deficits and yield reductions in sweet corn. J. Amer. Soc. Hort. Sci., Vol. 114(4): 542-546.

Clarke, T.R. 1997. An empirical approach for detecting crop water stress using multispectral airborne sensors. HortTech., Vol. 7(1): 9-16

Clawson, K.L., and B.L. Blad. 1982. Infrared thermometry for scheduling irrigation of corn. Agron. Journal, Vol. 74:311-316.

Clemmens, A.J., and M.G. Bos. 1990. Statistical methods for irrigation system water delivery performance evaluation. Irrigation and Drainage Systems, Vol. 4: 345-365.

Colaizzi, P.D., C.Y. Choi, P.M. Waller, E.M. Barnes, T.R.Clarke. 2000. Determining irrigation management zones in precision agriculture using the water deficit index at high spatial resolutions. 2000 ASAE Annual International Meeting. Pp. 1-19.

Colaizzi, P.D., E.M. Barnes, T.R. Clarke, C.Y. Choi, P.M. Waller, J. Haberland, M. Kostrzewski. 2003a. Water stress detection under high frequency sprinkler irrigation with water deficit index. Journal of Irrigation and Drainage Engineering, Vol. 129(1): 36-43.

Colaizzi, P.D., E.M. Barnes, T.R. Clarke, C.Y. Choi, P.M. Waller. 2003b. Estimating soil moisture under low frequency surface irrigation using crop water stress index. Journal of Irrigation and Drainage Engineering, Vol. 129(1): 27-35.

Deering, D.W., J.W. Rouse, R.H. Haas, J.A. Schell. 1975. Measuring forage production of grazing units from Landsat MSS data. Proceedings, Tenth Intern. Symposium of Remote Sensing of Environment, ERIM, Ann Arbor, MI. pp. 1169-1178.

Deering, D.W. 1978. Rangeland reflectance characteristics measured by aircraft and spacecraft sensors. Ph.D. dissertation. Texas A&M University, College Station, 338 pp.

Duggin, M.J. 1980. The field measurement of reflectance factors. Photogramm. Eng. Remote Sens., Vol. 46(5): 643-647.

Ehrler, W.L. 1973. Cotton leaf temperatures as related to soil water depletion and meteorological factors. Agron. J., Vol. 65: 404-409.

Ehrler, W.L., S.B. Idso, R.D. Jackson, R.J. Reginato. 1978. Wheat canopy temperature: Relation to plant water potential. Agronomy Journal, Vol. 70(2): 251-256.

Engman, E.T., and R.J. Gurney. 1991. Remote Sensing in Hydrology. Chapman & Hall: London.

Frueh, W.T. and J.W. Hopmans. 1997. Soil moisture calibration of a TDR multilevel probe in gravely soils. Soil Science, Vol. 162: 554-565.

Fuchs, M., and C.B. Tanner. 1966. Infrared thermometry of vegetation. Agronomy Journal, Vol. 58: 597-601.

Fuchs, M., E.T. Kanemasu, J.P. Kerr, C.B. Tanner. 1967. Effect of viewing angle on canopy temperature measurements with infrared thermometers. Agronomy Journal, Vol. 59: 494-496.

Gardner, B.R., and C.C. Shock. 1989. Interpreting the crop water stress index. ASAE Paper 89-2642. Trans. ASAE, St. Joseph, MI.

Gardner, B.R., D.C. Nielsen, C.C. Shock. 1992a. Infrared thermometry and the crop water stress index. I. History, theory, and baselines. J. Prod. Agric. Vol. 5: 462-466.

Garrot, D.J., Jr. M.W. Kilby, S.W. Stedman, D.D. Fangmeier, M.J. Ottman, J.M. Harper, S.H. Husman, D.T. Ray. 1990. Irrigation scheduling using the crop water stress index. In Visions of the Future, Proceedings of the Third National Irrigation Symposium, St. Joseph, MI: ASAE, 281-286.

Gitelson, A., D. Rundquist, D. Derry, J. Ramirez, G. Keydan, R. Stark, R. Perg. 2001. Using remote sensing to quantify vegetation fraction in corn canopies. Third International Conference on Geospatial Information in Agriculture and Forestry, Denver, CO, 5-7 November 2001.

Gonzalez, C.E.A. 1998. Water management in the Americas. Water Resources Development, Vol. 14: 289-291.

Gregory, P.J., L.P. Simmonds, C.J. Pilbeam. 2000. Soil type, climatic regime, and the response of water use efficiency to crop management. Agronomy Journal, Vol. 92-5: 814-820.

Hart, G.L., B. Lowery, K. McSweeney, K. Fermanich. 1994. In-situ characterization of hydrologic properties of Sparta sand: Relation to solute movement. Geoderma, Vol. 64: 41-55.

Hart, G.L. and B. Lowery. 1998. Measuring instantaneous solute flux and loading with Time Domain Reflectometry. Soil Sci. Soc. Am. J., Vol. 62: 23-35.

Hatfield, J.L. 1982. The utilization of thermal infrared radiation measurement inputs from grain sorghum crops as a method of assessing their irrigation requirements. Irrigation Science, Vol. 3: 259-268.

Hatfield, J.L., D.F. Wanjura, G.L. Barker. 1985. Canopy temperature response to water stress under partial canopy. Trans. ASAE, Vol. 28: 1607-1611.

Hatfield, J.L. 1990. Measuring plant stress with an infrared thermometer. Hortscience, Vol. 25(12): 1535-1538.

Hatfield, J.L. and P.J. Pinter. 1993. Remote sensing for crop protection. Crop Protection, Vol. 12(6): 403-413.

Hatfield, J.L., T.J. Sauer, J.H. Prueger. 2001. Managing soils to achieve greater water use efficiency. Agronomy Journal, Vol. 93-2: 271-280.

Hiler E.A. and R.N. Clark. 1971. Stress day index to characterize effects of water stress on crop yields. Trans. ASAE, Vol. 17: 757-761.

Hiler E.A., T.A. Howell, R.B. Lewis, R.P. Boos. 1974. Irrigation timing by the stress day index method. Trans. ASAE, Vol. 17: 393-398.

Hiler E.A., T.A. Howell. 1983. Irrigation options to avoid critical stress. Chapter 11. In: Limitations to Efficient Water Use in Crop Production, ASA, pp 479-497.

Holben, B.N., C.J. Tucker, C. Fan. 1980. Spectral assessment of soybean leaf area and leaf biomass. Photogram. Eng. and Remote Sens., Vol. 46(5): 651-656.

Hollander, M. and D.A. Wolfe. 1999. Nonparametric statistical methods (second edition). John Wiley & sons, 605 3rd Ave, New York, NY 10158-0012.

Howell, T.A. and J.T. Musick. 1984a. Responses of cotton water stress indicators to soil salinity. Irrigation Science. Vol. 5: 25-36.

Howell, T.A., J.L. Harfield, H. Yamada, and K.R. Davis. 1984b. Evaluation of cotton temperature to detect water stress. Trans. ASAE, Vol. 27: 84-88

Huete, A.R. 1988. A soil-adjusted vegetation index (SAVI). Remote Sens. Environ., Vol. 27: 47-57.

Huete, A.R. and R.D. Jackson. 1988. Soil and atmosphere influences on the spectra of partial canopies. Remote Sens. Environ., Vol 25: 89-105.

Huggins, D.R. and R.D. Alderfer. 1995. Yield variability within a long-term corn management study: Implications for precision farming. *In* Proc. Site-Specific Management for Agricultural Systems. P.C. Robert, R.H. Rust, and W.E. Larson (eds.). Am. Soc. of Agronomy, ASA, Publisher. Pp. 417-426.

Huisman J.A. and W. Bouten. 1999. Comparison of calibration and direct measurement of cable and probe properties in time domain reflectometry. Soil Sci. Soc. Am. J., Vol. 63: 1615-1617.

Idso, S.B., R.D. Jackson, R.J. Reginato. 1977. Remote sensing of crop yields. Science, Vol. 196: 19-25

Idso, S.B., R.D. Jackson, P.J. Pinter, R.J. Reginato, J.L. Hatfield. 1981a. Normalizing the stress-degree-day parameter for environmental variability. Agricultural Meteorology, Vol. 24: 45-55.

Idso, S.B., R.J. Reginato, D.C. Reicosky, and J.L. Hatfield. 1981b. Determining soil-induced plant water potential depressions in alfalfa by means of infrared thermometry. Agron. J., Vol. 73: 826-830.

Idso, S.B., R.J. Reginato, R.D. Jackson, P.J. Pinter. 1981c. Measuring yield-reducing plant water potential depressions in wheat by infrared thermometry. Irrigation Sci., Vol. 2: 205-212.

Idso, S.B., R.J. Reginato, S.M. Farah. 1982. Soil and atmosphere-induced plant water stress in cotton as inferred from foliage temperatures. Water Resour. Res., Vol. 18: 1143-1148.

Idso, S.B., P.J. Pinter, R.J. Reginato, K.L. Clawson. 1984. Stomatal conductance and photosynthesis in water hyacinth: effects of removing water from roots as quantified by a foliage-temperature-based plant water stress index. Agricultural and Forest Meteorology, Vol. 32: 249-256.

Irmak, S., D.Z. Haman, A.G. Smajstrla. 1999. Continuous water content measurements with Time-Domain Reflectometry for sandy soils. Soil Crop Sci. Soc. Florida Proc., Vol 58: 77-81.

Irmak, S., D.Z. Haman, R. Bastug. 2000. Determination of crop water stress index for irrigation timing and yield estimation of corn. Agronomy Journal, Vol. 92: 1221-1227.

Jackson, R.D. and S.B. Idso. 1969. Ambient temperature effect in infrared thermometry. Agronomy Journal, Vol. 61:324-325.

Jackson, R.D., S.B. Idso, R.J. Reginato, P.J. Pinter, Jr. 1981. Canopy temperatures as a crop water stress indicator. Water Resources Research, Vol. 17: 1133-1138.

Jackson, R.D. 1982. Canopy temperatures and crop water stress. In Advances in Irrigation, D.I. Hillel, Editor, Academic Press. Vol. 1: 43-85.

Jackson, R.D., M.S. Moran, P.N. Slater, and S.F. Biggar. 1987. Field calibration of reference reflectance panels. Remote Sens. Environ. Vol. 22: 145-158.

Jackson, S.H. 1991. Relationship between normalized leaf water potential and crop water stress index values for acala cotton. Agric. Water Manage., Vol. 20: 109-118.

Jensen, M.E., R.D. Burman, and R.G. Allen. 1990. Evapotranspiration and irrigation water requirememnts. ASCE Manuals and Reports on Engineering Practice No. 7, ASCE, 345 E. 47th St., New York, NY, USA.

Jones H.G., 1999. Use of infrared thermometry for estimation of stomatal conductance as a possible aid to irrigation scheduling. Agricultural and Forest Meteorology, Vol. 95: 139-149.

Kanemasu, E.T., G. Asrar, M. Yoshida. 1985. Remote sensing techniques for assessing water deficits and modeling crop response. HortScience, Vol. 20(6): 1043-1046.

Malhotra, S.P., S.K. Raheja, D. Seckler. 1984. A methodology for monitoring the performance of large scale irrigation systems: a case study of the warabandi system of northwest India. Agricultural Administration, Vol. 17: 231-259.

Mateos L., R.C.G. Smith, R. Slides. 1991. The effect of soil surface temperature on the crop water stress index. Irrigation Science, Vol. 12: 37-43.

Menenti, M. 1986. Physical aspects of determination of evaporation in deserts applying remote sensing techniques. Report No. 10, Institute of Land and Water Management Research: Wageningen, the Netherlands.

Moran, M.S., T.R. Clarke, Y. Inoue, A. Vidal. 1994. Estimating crop water deficit using the relation between surface-air temperature and spectral vegetation index. Remote Sensing Environment, Vol. 32: 125-141.

Moran, S., G. Fitzgerald, A. Rango, C. Walthall, E. Barnes, W. Bausch, T. Clarke, C. Daughtry, J. Everitt, D. Escobar, J. Hatfield, K. Havstad, T. Jackson, N. Kitchen, W. Kustas, M. NcGuire, P. Pinter, Jr., K. Sudduth, J. Schepers, T. Schmugge, P. Starks, and D. Upchurch. 2003. Sensor development and radiometric correction for agricultural applications. Photogram. Eng. and Remote Sens., Vol. 69(6): 705-718.

Mulla, D.J. and J.S. Schepers. 1997. Key processes and properties for site-specific soil and crop management. Pp.1-18. In F.J. Pierce and E. J. Sadler (eds.) *The State of Site-Specific Management for Agriculture*. American Society of Agronomy, Madison, WI.

Neale, C.M.U. 1987. Development of reflectance based crop coefficients for corn. Ph.D. Dissertation, Department of Agricultural and Chemical Engineering, Colorado State University, Ft. Collins, CO. 170 pp.

Nissen, H.H., P. Moldrup, K. Henriksen. 1998. High-resolution time domain reflectrometry coil probe for measuring soil water content. Soil Sci. Soc. Am. J. Vol. 62: 1203-1211.

Noborio, K., R. Horton, C.S. Tan. 1999. Time domain reflectometry probe for simultaneous measurement of soil matric potential and water content. Soil Sci. Soc. Am. J. Vol. 63: 1500-1505.

O'Toole, J.C., N.C. Turner, O.P. Namuco, M. Dingkukn, K.A. Gomez. 1984. Comparison of some crop water stress measurement methods. Crop Science, Vol. 24: 1121-1128.

Penuelas, J., R. Save, O. Marfa, L. Serrano. 1992. Remotely measured canopy temperature of greenhouse strawberries as indicator of water status and yield under mild water stress conditions. Agricultural and Forest Meteorology, Vol. 58: 63-77.

Pinter, P.J. and R.J. Reginato. 1981. Thermal infrared techniques for assessing plant water stress. Proc ASAE Irrigation Scheduling Conference, pp 43-85.

Pinter, P.J. and R.J. Reginato. 1982. A thermal infrared technique for monitoring cotton water stress and scheduling irrigations. Trans. ASAE, Vol. 25: 1651-1655.

Ponizovsky, A.A., S.M. Chudinova, and Y.A. Pachepsky. 1999. Performance of TDR calibration models as affected by soil texture. Journal of Hydrology, Vol.218: 35-43.

Price, J.P. 1990. Using spatial context in satellite data to infer regional scale evapotranspiration. IEEE Trans. Geosci. Remote Sens., Vol.28: 940-948.

Qi, J., A.L. Chehbouni, A.R. Huete, Y.H. Kerr, S. Sorooshian. 1994. A modified soil adjusted vegetation index (MSAVI). Remote Sensing of Environment, Vol. 48: 119-126.

Reginato, R.J. 1983. Field quantification of crop water stress. Trans. ASAE, Vol. 26(3): 772-775.

Reginato, R.J., and J. Howe. 1985. Irrigation scheduling using crop indicators. Journal of Irrigation and Drainage Engineering, Vol. 111(2): 125-133.

Reginato, R.J., and Jr. D.J. Garrot. 1987. Irrigation scheduling with the crop water stress index. pp. 7-10. In Western Cotton Production Conf. Summary Proc., Phoenix, AZ. 18-20 August, 1987. Cotton Growers Assoc., Memphis, TN.

Richardson, A.J. and C.L. Wiegand. 1977. Distinguishing vegetation from soil background information. Photogrammetry Engineering and Remote Sensing, Vol. 43: 1541-1552.

Ritchie, S.W., J.J. Hanway, G.O. Benson. 1989. How a corn plant develops. Special Report No. 48, pp 21, Iowa State University of Science and Technology Cooperative Extension Service Ames, Iowa.

Robinson, D.A., C.M.K. Gardner, J.D. Cooper. 1999. Measurement of relative permittivity in sandy soils using TDR, capacitance and theta probes: comparison, including the effects of bulk soil electrical conductivity. Journal of Hydrology, Vol. 223: 198-211.

Rouse, J.W., R.H. Haas, J.A. Schell, D.W. Deering. 1973. Monitoring vegetation systems in the great plains with ERTS. Third ERTS Symposium, NASA SP-351 I: 309-317.

Seckler, D., R.K. Sampath, S.K. Raheja. 1988. An index for measuring the performance of irrigation management systems with an application. Water Resources Bulletin, Vol. 24(4): 855-860.

Shae, J.B., D.D. Steele, B.L. Gregor. 1999. Irrigation scheduling methods for potatoes in the Northern Great Plains. Trans. ASAE, Vol. 42(2): 351-360.

Skeen, T. S., 1996. Crop water stress index. http://weather.nmsu.edu/Teaching_material/soil698/CWSI.html Pp. 1-2.

Smith, R.G.C., H.D. Barrs, J.L. Stainer, M. Stapper. 1985. Relationship between wheat yield and foliage temperature: Theory and its application to infrared measurements. Agric. For. Meteorol., Vol. 36: 129-143.

Steele, D.D., E.C. Stegman, R.E. Knighton. 2000. Irrigation management for corn in the northern Great Plains, USA. Irrigation Science, Vol. 19: 107-114.

Stegman, E.C. and M. Soderlund. 1992. Irrigation scheduling of spring wheat using infrared thermometry. American Society of Agricultural Engineers, Vol. 35(1): 143-152.

Stegman, E.C., L.H. Schiele, A. Bauer. 1976. Plant water stress criteria for irrigation scheduling. Trans. ASAE, Vol. 19: 850-855.

Stockle, C.O. and W.A. Dugas. 1992. Evaluating canopy temperature-based indices for irrigation scheduling. Irrigation Sci., Vol. 13: 31-37.

Thiruvengdachari, S. 1993. Remote Sensing in Water Resources. Training Course in Water Resources. NRSA: Hyderabad, India.

Thomsen, A., B. Hansen, K. Schelde. 2000. Application of TDR to water level measurement. Journal of Hydrology, Vol. 236: 252-258.

Topp, G.C., J.L. Davis, and A.P. Annan. 1980. Electromagnetic determination of soil water content: Measurement in coaxial transmission lines. Water Resour. Res., Vol. 16: 579-582.

Tucker, C.J. 1979. Red and photographic infrared linear combination for monitoring vegetation. Remote Sensing of Environment, Vol. 8: 127-150.

U.S.W.C.L. 2001 Thermal crop water stress indices.
http://www.uswcl.ars.ag.gov/epd/remsen/irrweb/thindex.htm
Pp. 1-13. U.S. Water Conservation Laboratory, Phoenix, Arizona.

Van Clooster, M., D. Mallants, J. Vanderborght, J. Diels, J. Van Orshoven, J. Feyen. 1995. Monitoring solute transport in a multi-layered sandy lysimeter using time domain reflectometry. Soil Sci. Soc. Am. J. Vol. 59: 337-344.

Walker, G.K. and J.L. Hatfield. 1983. Stress measurements using foliage temperature. Agronomy Journal, Vol. 75: 623-629.

Wanjura, D.F., C.A. Kelly, C.W. Wendt, J.L. Hatfield. 1984. Canopy temperature and water stress of cotton crops with complete and partial ground cover. Irrigation Science, Vol. 5: 37-46.

Wanjura, D.F., J.L. Hatfield, D.R. Upchurch. 1990. Crop water stress index relationship and crop productivity. Irrigation Science, Vol. 11: 93-99.

Wanjura, D.F., D.R. Upchurch, J.R. Mahan. 1992. Automated irrigation based on threshold canopy temperature. Trans. ASAE. Vol. 35(5): 1411-1417.

Wanjura, D.F. and D.R. Upchurch. 2000. Canopy temperature characterizations of corn and cotton water status. Soil & Water Division of ASAE, Vol. 43(4): 867-875.

Wanjura, D.F. and D.R. Upchurch. 2002. Water status response of corn and cotton to altered irrigation. Irrigation Science, Vol. 21(2): 45-55.

APPENDIX A

Table A.1. Results of calculation CWSI from V8 to R1.

DOY	*186*		*190*		*203*		*204*		*205*		*210*		*212*	
SITES	**GS***	**CWSI**	**GS**	**CWSI**	**GS**	**CWSI**	**GS**	**CWSI**	**GS**	**CWSI**	**GS**	**CWSI**	**GS**	**CWSI**
PLOT 1	V8/9	0.00	V9/10	0.00	V16	0.00	V17	0.00	V17/18	0.00	VT/R1	0.06	R1	0.45
PLOT 2	V8	0.07	V9/10	0.06	V15	0.00	**V15**	**0.01**	**V15**	**0.35**	**VT**	**1.00**	**VT**	**0.98**
PLOT 3	V8	0.11	V9	0.15	**V14**	**1.00**	**V14**	**1.00**	V15	0.64	VT	0.60	VT	0.82
PLOT 4	**V8**	**0.37**	**V9/10**	**1.00**	V14	0.00	V15	0.23	V16	0.00	VT	0.00	VT	0.60
PLOT 5	V8	0.07	V9	0.33	V15	0.00	V15/16	0.23	V16	0.00	VT	0.00	R1	0.54
1	V8	0.29	V9	0.00	V10	n/a	V12	0.00	V14	n/a	V16	n/a	VT/R1	0.00
2	V8/9	0.20	V9/10	0.00	V13	n/a	V14	0.00	V15	n/a	VT	n/a	VT/R1	0.00
3	V8	0.44	V9	0.00	V11	n/a	V13	0.00	V15	n/a	VT	n/a	VT/R1	0.00
4	V9	0.40	V10	0.00	V15	n/a	V15/16	0.00	V16	n/a	VT	n/a	R1	0.00
5	V8/9	0.28	V9/10	0.00	V12	n/a	V13	0.00	V15	n/a	VT	n/a	VT/R1	0.00
6	V8/9	0.30	V9/10	0.00	V15	n/a	V15	0.00	V16	n/a	VT	n/a	R1	0.00
7	V8/9	0.23	V9/10	0.00	V15	n/a	V16	0.00	V17	n/a	VT	n/a	R1	0.00
8	V8	0.42	V9	0.00	V14	n/a	V15	0.00	V15	n/a	VT	n/a	VT/R1	0.00
9	V9	0.14	V10	0.00	V15	n/a	V15	0.00	V16	n/a	VT	n/a	R1	0.00
10	V8	0.17	V9	0.00	V12	n/a	V14	0.00	V16	n/a	VT	n/a	R1	0.00
11	V8	0.35	V9	0.00	V13	n/a	V14	0.00	V16	n/a	VT	n/a	R1	0.00
12	V8	0.33	V9	0.00	V14	n/a	V15	0.00	V16	n/a	VT	n/a	R1	0.00
13	V8	0.14	V9	0.00	V15	n/a	V16	0.00	V17	n/a	VT	n/a	R1	0.00
14	V8	0.35	V9	0.00	V14	n/a	V15	0.00	V16	n/a	VT	n/a	R1	0.00
15	V8	0.30	V9	0.00	V14	n/a	V15	0.00	V16	n/a	VT	n/a	R1	0.00

* Growth Stage (GS): corn growth stage (Ritchie et al., 1989)

Table A.2. Results of calculation CWSI from R1 to R5.

DOY	*213*		*226*		*231*		*233*		*238*		*241*		*263*	
SITES	**GS***	**CWSI**	**GS**	**CWSI**	**GS**	**CWSI**	**GS**	**CWSI**	**GS**	**CWSI**	**GS**	**CWSI**	**GS**	**CWSI**
PLOT 1	R1/R2	0.00	R2	0.00	R3	0.00	R3	0.00	R4	0.07	R4	0.08	R5	0.59
PLOT 2	**VT/R1**	**0.74**	R2	0.00	R2/R3	0.23	R3	0.03	R3	0.20	R4	0.11	R5	0.42
PLOT 3	VT/R1	0.33	R2	0.00	R2/R3	0.15	R3	0.01	R3/R4	0.17	R4	0.12	R5	0.81
PLOT 4	VT	0.14	R2	0.00	R3	0.00	R3	0.00	R3	0.11	R4	0.00	R5	0.35
PLOT 5	R1	0.25	**R2**	**0.00**	**R2/R3**	**0.14**	**R3**	**0.31**	**R3**	**0.83**	R4	0.13	R5	0.49
1	R1	n/a	R2	0.00	R2/R3	0.00	R3	n/a	R3	0.00	R4	n/a	R5	0.00
2	R1	n/a	R2	0.00	R3	0.00	R3	n/a	R3	0.00	R4	n/a	R5	0.00
3	R1	n/a	R2	0.00	R2/R3	0.00	R3	n/a	R3	0.00	R4	n/a	R5	0.00
4	R1	n/a	R2	0.00	R3	0.00	R3	n/a	R3	0.00	R4	n/a	R5	0.00
5	R1	n/a	R2	0.00	R2/R3	0.00	R3	n/a	R3	0.00	R4	n/a	R5	0.07
6	R1	n/a	R2	0.00	R3	0.00	R3	n/a	R3	0.00	R4	n/a	R5	0.00
7	R1	n/a	R2	0.00	R3	0.00	R3	n/a	R3	0.00	R4	n/a	R5	0.00
8	R1	n/a	R2	0.00	R3	0.00	R3	n/a	R3	0.00	R4	n/a	R5	0.00
9	R1	n/a	R2	0.00	R3	0.00	R3	n/a	R3	0.00	R4	n/a	R5	0.00
10	R1	0.00	R2	n/a	R3	n/a	R3	n/a	R3	0.00	R4	n/a	R5	0.00
11	R1	0.14	R2	n/a	R3	0.00	R3	n/a	R3	0.00	R4	n/a	R5	0.00
12	R1	0.00	R2	n/a	R3	0.00	R3	n/a	R3	0.00	R4	n/a	R5	0.00
13	R1	0.00	R2	n/a	R3	0.00	R3	n/a	R3	0.00	R4	n/a	R5	0.00
14	R1	0.00	R2	n/a	R3	0.00	R3	n/a	R3	0.00	R4	n/a	R5	0.00
15	R1	0.00	R2	n/a	R3	0.00	R3	n/a	R3	0.00	R4	n/a	R5	0.00

* Growth Stage (GS): corn growth stage (Ritchie et al., 1989)

Table A.3. Results of calculation WDI from V8 to R1.

DOY	*186*		*190*		*203*		*204*		*205*		*210*		*212*	
SITES	**GS***	**WDI**	**GS**	**WDI**	**GS**	**WDI**	**GS**	**WDI**	**GS**	**WDI**	**GS**	**WDI**	**GS**	**WDI**
PLOT 1	V8/9	0.00	V9/10	0.00	V16	0.00	V17	0.00	V17/18	0.00	VT/R1	0.00	R1	0.00
PLOT 2	V8	0.04	V9/10	0.00	V15	0.14	**V15**	**0.57**	**V15**	**0.52**	**VT**	**1.00**	**VT**	**0.00**
PLOT 3	V8	0.08	V9	0.00	**V14**	**0.53**	**V14**	**0.92**	V15	0.29	VT	0.16	VT	0.00
PLOT 4	**V8**	**0.15**	**V9/10**	**0.34**	V14	0.22	V15	0.30	V16	0.00	VT	0.49	VT	0.00
PLOT 5	V8	0.03	V9	0.00	V15	0.00	V15/16	0.32	V16	0.00	VT	0.00	R1	0.80
1	V8	0.37	V9	0.00	V10	n/a	V12	0.13	V14	n/a	V16	n/a	VT/R1	0.01
2	V8/9	0.22	V9/10	0.00	V13	n/a	V14	0.42	V15	n/a	VT	n/a	VT/R1	0.00
3	V8	0.39	V9	0.00	V11	n/a	V13	0.31	V15	n/a	VT	n/a	VT/R1	0.34
4	V9	0.40	V10	0.00	V15	n/a	V15/16	0.22	V16	n/a	VT	n/a	R1	0.00
5	V8/9	0.24	V9/10	0.00	V12	n/a	V13	0.43	V15	n/a	VT	n/a	VT/R1	0.00
6	V8/9	0.23	V9/10	0.00	V15	n/a	V15	0.09	V16	n/a	VT	n/a	R1	0.00
7	V8/9	0.26	V9/10	0.00	V15	n/a	V16	0.27	V17	n/a	VT	n/a	R1	0.05
8	V8	0.39	V9	0.00	V14	n/a	V15	0.26	V15	n/a	VT	n/a	VT/R1	0.00
9	V9	0.22	V10	0.00	V15	n/a	V15	0.33	V16	n/a	VT	n/a	R1	0.00
10	V8	0.34	V9	0.00	V12	n/a	V14	0.21	V16	n/a	VT	n/a	R1	0.29
11	V8	0.38	V9	0.00	V13	n/a	V14	0.18	V16	n/a	VT	n/a	R1	0.00
12	V8	0.20	V9	0.00	V14	n/a	V15	0.32	V16	n/a	VT	n/a	R1	0.08
13	V8	0.24	V9	0.00	V15	n/a	V16	0.17	V17	n/a	VT	n/a	R1	0.00
14	V8	0.28	V9	0.00	V14	n/a	V15	0.36	V16	n/a	VT	n/a	R1	0.00
15	V8	0.32	V9	0.00	V14	n/a	V15	0.17	V16	n/a	VT	n/a	R1	0.00

* Growth Stage (GS): corn growth stage (Ritchie et al., 1989)

Table A.4. Results of calculation WDI from R1 to R5.

DOY	*213*		*226*		*231*		*233*		*238*		*241*		*263*	
SITES	**GS***	**WDI**	**GS**	**WDI**	**GS**	**WDI**	**GS**	**WDI**	**GS**	**WDI**	**GS**	**WDI**	**GS**	**WDI**
PLOT 1	R1/R2	0.00	R2	0.00	R3	0.00	R3	0.00	R4	0.00	R4	0.00	R5	0.00
PLOT 2	**VT/R1**	**0.82**	R2	0.00	R2/R3	0.66	R3	0.00	R3	0.46	R4	0.00	R5	0.68
PLOT 3	VT/R1	0.34	R2	0.00	R2/R3	0.00	R3	0.00	R3/R4	0.09	R4	0.00	R5	0.23
PLOT 4	VT	0.01	R2	0.00	R3	0.00	R3	0.00	R3	0.44	R4	0.33	R5	0.58
PLOT 5	R1	0.87	**R2**	**0.00**	**R2/R3**	**0.89**	**R3**	**1.00**	**R3**	**1.00**	R4	0.83	R5	0.39
1	R1	n/a	R2	0.00	R2/R3	0.00	R3	n/a	R3	0.01	R4	n/a	R5	0.40
2	R1	n/a	R2	0.00	R3	0.00	R3	n/a	R3	0.38	R4	n/a	R5	0.29
3	R1	n/a	R2	0.00	R2/R3	0.00	R3	n/a	R3	0.22	R4	n/a	R5	0.36
4	R1	n/a	R2	0.00	R3	0.00	R3	n/a	R3	0.59	R4	n/a	R5	0.26
5	R1	n/a	R2	0.00	R2/R3	0.00	R3	n/a	R3	0.44	R4	n/a	R5	0.31
6	R1	n/a	R2	0.00	R3	0.00	R3	n/a	R3	0.48	R4	n/a	R5	0.40
7	R1	n/a	R2	0.00	R3	0.00	R3	n/a	R3	0.46	R4	n/a	R5	0.14
8	R1	n/a	R2	0.00	R3	0.00	R3	n/a	R3	0.38	R4	n/a	R5	0.55
9	R1	n/a	R2	0.00	R3	0.00	R3	n/a	R3	0.23	R4	n/a	R5	0.39
10	R1	0.00	R2	0.00	R3	0.00	R3	n/a	R3	0.27	R4	n/a	R5	0.08
11	R1	0.14	R2	0.00	R3	0.00	R3	n/a	R3	0.25	R4	n/a	R5	0.38
12	R1	0.00	R2	0.00	R3	0.00	R3	n/a	R3	0.33	R4	n/a	R5	0.29
13	R1	0.00	R2	0.00	R3	0.00	R3	n/a	R3	0.11	R4	n/a	R5	0.61
14	R1	0.00	R2	0.00	R3	0.00	R3	n/a	R3	0.38	R4	n/a	R5	0.32
15	R1	0.00	R2	0.00	R3	0.00	R3	n/a	R3	0.43	R4	n/a	R5	0.38

* Growth Stage (GS): corn growth stage (Ritchie et al., 1989)